midas nGen

Analysis Manual

DISCLAIMER

Developers and distributors assume no responsibility for the use of MIDAS Family Program (midas Civil, midas FEA, midas FX+, midas Gen, midas Drawing, midas SDS, midas GTS, SoilWorks, midas NFX, midas Drawing, midas nGen ; here in after referred to as “MIDAS package”) or for the accuracy or validity of any results obtained from the MIDAS package.

Developers and distributors shall not be liable for loss of profit, loss of business, or financial loss which may be caused directly or indirectly by the MIDAS package, when used for any purpose or use, due to any defect or deficiency therein. Accordingly, the user is encouraged to fully understand the bases of the program and become familiar with the users manuals. The user shall also independently verify the results produced by the program.

INDEX

Section 1 Outline

The midas nGen and Foundation programs are designed for developing models and conducting detailed analysis of structural systems. It operates based on finite element analysis code written in C++. The programs provide a variety of analytical capabilities such as static analysis, dynamic analysis, and crane moving analysis (see Table 1.1.1). In order to efficiently conduct such a wide range of analyses, midas nGen includes a diverse and specialized catalog of elements for accurate modeling of structural components.

Table 1.1.1 Analysis capabilities of midas nGen

Analysis Types
Linear static analysis
Nonlinear static analysis
Eigenvalue analysis
Response spectrum analysis
Linear buckling analysis
P-delta analysis
Crane moving load analysis
Linear time history(modal/direct) analysis
Frequency response(modal/direct) analysis
Nonlinear time history analysis

For the purpose of providing the user with the knowledge required to most efficiently make use of the midas nGen or Foundation software programs, this manual provides detailed information regarding the programs' theoretical and technical details.

To improve readability and accessibility, the manual does not include content focused on educating the reader with engineering fundamentals (such concepts are often explained in detail in various other engineering publications) or technical content that is unnecessarily theoretical or esoteric for the average user.

The manual is divided into the following chapters:

- Chapter 2: Nodes and Coordinate Systems
- Chapter 3: Element Modeling
- Chapter 4: Material Models for Detailed Analysis
- Chapter 5: Analysis Algorithms
- Chapter 6: Loads and Boundary Conditions

This manual provides explanations for all capabilities of midas nGen and Foundation, but the available tools may vary depending on the specific version of the software.

Section 2 System of Units

Analysis models require the user to define numerical quantities such as sizes and material properties. Such definitions are based on a particular system of units. Midas nGen allows for easy unit conversion for units of force and length, and the user may also switch unit systems during the model definition process. Before beginning analysis, it is recommended that the model properties be unified by a single system of units—either the English or SI system of units.

Table 1.2.1 Units used in the English/SI systems of units

Quantity	English	SI
Length, position, displacement	Inch	meter
Modulus of Elasticity	lbf/inch2	Newton/meter2
Moment	inch-lbf	Newton-meter
Force	lbf	Newton
Mass	lbf-sec2/inch	kilogram
Time	second	second
Stress	lbf/inch2	Newton/meter2

Although the software conducts analyses using the pre-specified system of units, the analysis results may be converted to a different system in the post-processing stage.

Section 3

File Format and System

Throughout the finite element analysis procedure, the program will create and save several different files. Some temporary files may also appear and disappear depending on the analysis step. The files that will be used and created by the software, along with the respective file type and contents, are shown in Table 1.3.1.

Table 1.3.1 Primary output files of midas nGen

File Name	Type	Contents
ModelName.mpb	Binary	Model
ModelName_AnalysisName.mec	ASCII	Analysis input
ModelName_AnalysisName.log	ASCII	Analysis log
ModelName_AnalysisName.out	ASCII	Analysis results
ModelName_AnalysisName_usr.out	ASCII	Time History analysis results
ModelName_AnalysisName.drct	Binary	Distributed loading information
ModelName_AnalysisName.nfxp	Binary	Analysis results (for post processing)

There are two analysis result file types: .out files, which are ASCII type and .nfxp files, which are binary. Generally speaking, .nfxp files are used for post-processing and interpreting the data thereafter. ASCII .out files may contain the same contents as the .nfxp files. In addition, eigenvalue analysis results (eigenvalues, mass participation factors, etc) are only included in the .out files.

In the case of moving crane analysis, the following files are also created and used by the program.
Except for influence line analysis results, moving crane analysis results are included in .nfxp files (similar to the regular analysis results).

File Name	Type	Contents
ModelName_AnalysisName.CRN	ASCII	Moving analysis input file
ModelName_AnalysisName_#.blk	Binary	Influence line analysis results

ModelName_AnalysisName.CLD	Binary	Crane

Table 1.3.2 shows additional temporary files that are created during the analysis procedure.

Table 1.3.2 Temporary files that are created during analysis

File Name	Usage/Contents
InputName.DASM#.bin	Created for all analysis types, contains FEM-related information
InputName.FACT#.bin#	Created when using the multi-frontal solver, contains matrix information
InputName.EIGS#.bin#	Created when conducting eigenvalue analysis, contains Lanczos iterative methods data
InputName.MSTO#.bin	Internally recorded, contains large matrix and vector data

These temporary files are created in the scratch folder whose default directory is the same as the model file folder.

Section 4 Notation

This manual uses both matrix notation and component notation. Matrix notation is especially convenient for tensors, and thus, if possible, the manual defaults to using matrix notation.

For introducing theory, it is important to clarify the notation for scalars, vectors, second-order tensors or matrices, and fourth-order tensors. The notation to be used in this manual is shown in Table 1.4.1.

Table 1.4.1 Matrix Notation

Quantity	Notation
Scalar	u
Vector	$\mathbf{u}$, $\{*\}$
Second-order Tensor, Matrix	$\mathbf{A}$, $[*]$
Fourth-order Tensor	$\mathbf{C}$

The boldface is used for both vectors and tensors, so the two may be differentiated based on context. Matrix notation is particularly effective for expressing physical meaning or relative physical quantities. However, there are expressions that are either difficult to write in matrix notation or represent component-by-component operations. In such cases, it is more efficient to resort to component notation.

Component notation is based on a specific coordinate system, which is derived from the base vector. The base vector is specified as $\mathbf{e}_i$, $(i=1,2,3)$ in 3-dimensional space, and the base vectors may not be orthogonal to one another. Using the base vector, the vector $\mathbf{u}$ may be expressed as follows:

$$\mathbf{u} = u^1\mathbf{e}_1 + u^2\mathbf{e}_2 + u^3\mathbf{e}_3 \tag{1.4.1}$$

$\mathbf{e}_i$: Base vector

u^i : Component scalar

In component notation, the precise meaning of the subscript i is the covariant base vector or component, and the superscript j refers to the contravariant base vector or component. Generally, for orthonormal coordinate systems, the two are equal and thus do not require differentiation.

When using component notation, it is convenient to use summation convention for summing over multiple indices, as shown below:

$$\mathbf{u} = u^i \mathbf{e}_i \tag{1.4.2}$$

Similarly, the second- and fourth-order tensors may be expressed in component notation as shown below:

$$\mathbf{A} = A^{ij}\mathbf{e}_i\mathbf{e}_j, \quad \mathbf{C} = C^{ijkl}\mathbf{e}_i\mathbf{e}_j\mathbf{e}_k\mathbf{e}_l \tag{1.4.3}$$

This manual uses summation convention, unless otherwise noted.

Section 1

Nodes, DOFs, and Coordinate System

Nodes and elements define the size and shape of a finite element model, and represent the starting point for all analyses. Models defined by nodes and elements are the equivalent of expressing physical phenomena using matrix equations. The unknown variables of such equations are physical quantities such as displacement and rotation, and are called degrees of freedom.

A simple structural analysis example may involve, at each node, three displacement-based and three rotation-based degrees of freedom. These six degrees of freedom are shown in the figure below.

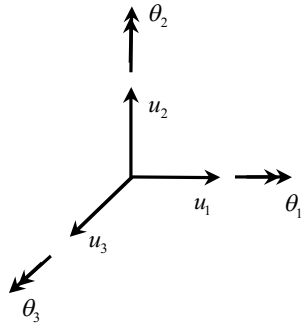

Figure 2.1.1
Displacement and rotational degrees of freedom for an orthogonal coordinate system

Each degree of freedom is typically expressed using the notations shown below:

$$\text{DOF } 1 = T_1 = u_1, \quad \text{DOF } 2 = T_2 = u_2, \quad \text{DOF } 3 = T_3 = u_3$$

$$\text{DOF } 4 = R_1 = \theta_1, \quad \text{DOF } 5 = R_2 = \theta_2, \quad \text{DOF } 6 = R_3 = \theta_3$$

Each node's local coordinate system describes its direction of motion and is defined as the nodal displacement coordinate system. The degrees of freedom mentioned above follow the direction of the coordinate systems assigned to all the nodes. All nodes in a model are programmed to have their directions of motion based on the global coordinate system.

Section 2

Coordinate System

To create a suitable model and conduct proper analyses using FEM techniques for a given problem, access to a diverse range of coordinate systems is essential. For example, a coordinate system is required for the aforementioned case of defining a direction of motion for each node or for defining the axial direction of a structural member. Additionally, a particular coordinate system may be defined for extracting a resulting value. Midas nGen allows for the use of either a rectangular coordinate system or a cylindrical coordinate system.

Figure 2.2.1 Rectangular coordinate system and cylindrical coordinate system

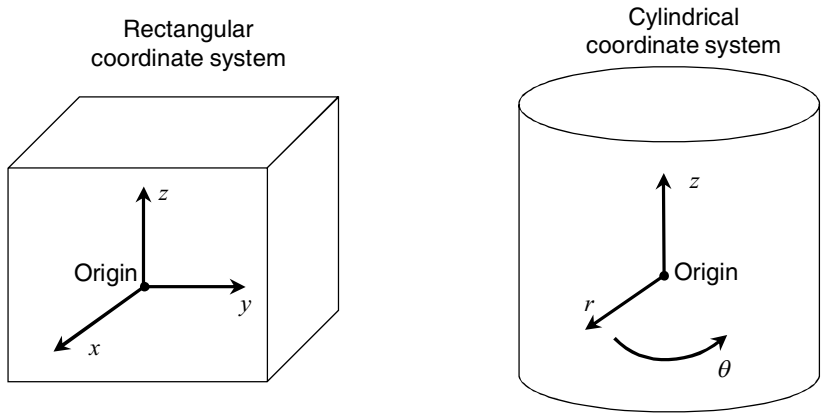

For example, if the direction of motion for a particular node is defined by a cylindrical coordinate system, the degrees of freedom are as follows:

DOF 1 = translation in r −direction
DOF 2 = translation in θ −direction
DOF 3 = translation in z −direction
DOF 4 = rotation in r −direction
DOF 5 = rotation in θ −direction
DOF 6 = rotation in z −direction

The program uses the following coordinate systems for modeling and analysis.

Table 2.2.1 Main coordinate systems used by midas nGen

Coordinate System	Use/Description
GCS : global coordinate system	Unites the entire model, rectangular coordinate system
NDCS : nodal displacement coordinate system	Describes each node's direction of motion, rectangular/cylindrical coordinate system
ECS : element coordinate system	Defined by the node positions of each element, rectangular coordinate system
MCS : material coordinate system	Dictates the material directionality being applied to the elements, rectangular/cylindrical coordinate system
ERCS : element result coordinate system	Used for outputting element analysis results, rectangular/cylindrical coordinate system
EFCS : element formulation coordinate system	Used in finite element formulation, equivalent to the global coordinate system and the element coordinate system

Among these, the element formulation coordinate system is used in the FEM solver, and the material coordinate system is fixed to the global coordinate system. The material coordinate system consequently does not alter the user's experience with midas nGen, but is helpful for understanding the information presented in this manual. In addition, element result coordinate system may influence the interpretation of analysis results. Element, material, and element result coordinate systems are explained with detail in Chapter 3.

Figure 2.2.2 Various coordinate systems used by midas nGen

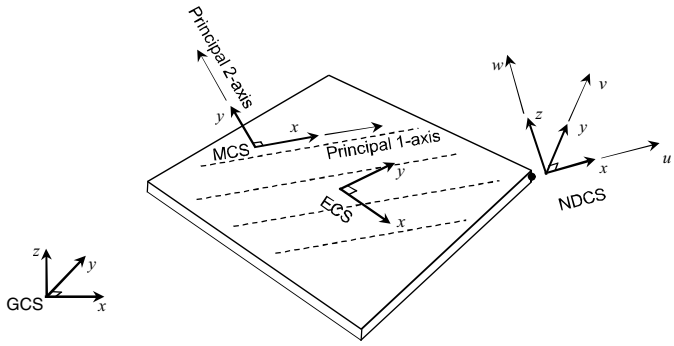
Principal 2-axis
y
x
MCS
Principal 1-axis
y
ECS
x
w
v
z
y
x
u
NDCS
z
y
GCS
x

Section 1 Outline

Midas nGen includes access to a diverse element library that is designed for geometric modeling. Through appropriate use of these elements, users may conduct a wide range of analyses including linear or nonlinear analysis and moving crane analysis. Understanding the characteristics of each element type is crucial for accurate finite element analysis. To aid in this effort, page 3 introduces the theoretical background behind the various finite element techniques that is used in midas nGen.

The following paragraphs introduce the element types available in midas nGen, and their respective shapes, forms, and other characteristics.

Scalar Element

Scalar elements have a single node, and its strain energy and kinetic energy is based on the motion of this node relative to the ground point. These energy quantities may be defined based on two nodes instead, but the quantities do not use the distance between these two nodes or other such geometrical information. Scalar elements include point springs, dampers, and mass. Point springs and dampers are primarily used to incorporate elasticity or damping properties of structural boundaries, whereas point masses are mainly used to incorporate the mass of nonstructural components.

1-Dimensional Form Element

This element is linear and defined by two nodes, and makes use of the distance between the two nodes and other geometrical information. Trusses, beams, and elastic links are elements that are included in this category. Trusses are primarily used for representing braces, and beam elements may represent either beam and column members. Elastic links are nonstructural components and mainly used for representing the rigidity of equipment connections.

2-Dimensional Form Element

This element may be triangular or rectangular, and may consist of three to four nodes. These 2-dimensional form elements may be curved, unlike the linear 1-dimensional form eleements. Shell

elements are an example of 2-dimensional form elements. Shells are often used to model slabs, walls, facades, or pipes.

3-Dimensional Form Element

The shape of a 3-dimensional form element may be a tetrahedron, pentahedron, or hexahedron, and will be defined by four to six nodes. Pentahedronal elements may taken on wedge or pyramid shapes. Solid elements are included in the class of 3-dimensional form elements, and are generally used for modeling components with nonzero volume, such as equipment or foundation.

Rigid link/interpolation Elements

These elements may define rigid body motion between nodes or relative motion via interpolation, and are similar to multi-point constraints. Rigid link elements and interpolation elements are included in this category. Usually these elements are used to define equipment or plant connections.

Section 2

Finite Element Formulation

When the variational form of the stress-strain relationship is applied as a constraint condition to the principle of virtual work originating from stress, the Hu-Washizu variational principle[1, 2] is obtained, and it may be expressed as the equation shown below:

$$\delta G_{ext} = \int_{\Omega} (\nabla \delta \mathbf{u})^T \boldsymbol{\sigma} + \delta \boldsymbol{\varepsilon}^T (\boldsymbol{\sigma}(\boldsymbol{\varepsilon}) - \boldsymbol{\sigma}) + \delta \boldsymbol{\sigma}^T (\nabla \mathbf{u} - \boldsymbol{\varepsilon}) d\Omega \quad (3.2.1)$$

δG_{ext} : Virtual work due to external forc

$\mathbf{u}$: Displacement

$\boldsymbol{\sigma}$: Stress

$\boldsymbol{\varepsilon}$: Strain

$\boldsymbol{\sigma}(\boldsymbol{\varepsilon})$: Stress derived from strain

∇ : Strain-displacement relational operator

The above equation is the most typical expression for simultaneously capturing equilibrium, constitutive relationships, and compatibility conditions. Assuming that the relationship between strain and stress always satisfies the constitutive relationship, the Hellinger-Reissner principle[3, 4] is obtained:

$$\delta G_{ext} = \int_{\Omega} (\nabla \delta \mathbf{u})^T \boldsymbol{\sigma} + \delta \boldsymbol{\sigma}^T (\nabla \mathbf{u} - \boldsymbol{\varepsilon}(\boldsymbol{\sigma})) d\Omega \quad (3.2.2)$$

$\boldsymbol{\varepsilon}(\boldsymbol{\sigma})$: Strain derived from stress

---

[1] Hu, H.C., "On some variational principles in the theory of elasticity and the theory of plasticity," Scintia Sinica, Vol. 4, 1955.

2 Washizu, K., On the Variational Principles of Elasticity, Aeroelastic and Structural Research Laboratory, MIT, Technical Report, 1955.

3 Hellinger, E., "Der allgemeine Ansatz der Mechanik der Kontinua," Encyclopadie der Mathernafischen Wissenschaften, Vol. 4, 1914.

4 Reissner, E., "On a variational theorem in elasticity," Journal of Mathematical Physics, Vol. 29, 1950.

Moreover, with the assumption that the relationship between $\boldsymbol{\varepsilon}$ and $\nabla\mathbf{u}$ always satisfies compatibility conditions, then the general principle of virtual work is obtained:

$$\delta G_{ext} = \int_{\Omega} (\nabla \delta \mathbf{u})^T \boldsymbol{\sigma}(\mathbf{u}) d\Omega \tag{3.2.3}$$

To apply finite element methods to the principle of virtual work, consider the localization of a region of integration as a single element. Within an element, the displacement $\mathbf{u}$ can be interpolated using a shape function as shown below:

$$\mathbf{u}^h = \mathbf{N}\mathbf{d}^e \tag{3.2.4}$$

$\mathbf{N}$: Shape Function

$\mathbf{d}^e$: Element node degree of freedom

Then, by utilizing the displacement-strain relationship $\boldsymbol{\varepsilon}^h = \nabla \mathbf{u}^h = \mathbf{B}\mathbf{d}^e$, the principle of virtual work as applied to the entire element may be expressed as follows:

$$\delta G_{ext} = \delta \mathbf{d}^T \mathbf{F} = \delta \mathbf{d}^T \left[\sum \int_{\Omega_e} \mathbf{B}^T \mathbf{D} \mathbf{B} d\Omega \right] \mathbf{d} = \delta \mathbf{d}^T \mathbf{K} \mathbf{d} \tag{3.2.5}$$

$\mathbf{D}$: Stress-strain relational matrix

In linear analysis, the complete stiffness matrix $\mathbf{K}$ is independent of the vector $\mathbf{d}$ containing all degrees of freedom. The element stiffness matrix $\mathbf{K}^e$ is expressed as:

$$\mathbf{K}^e = \int_{\Omega_e} \mathbf{B}^T \mathbf{D} \mathbf{B} d\Omega \tag{3.2.6}$$

The above equation is appropriate for analysis of elastic structures that experience infinitesimal displacement but, using the same principles, may be applied to nonlinear analysis as well.

Section 3

Shape Functions

The definition of an element is derived from the assumed displacement field derived from shape functions. The indices used in this section do not follow summation convention 1-, 2-, and 3-dimensional shape functions are expressed using the natural coordinate system (ξ, η, ζ).

3.1 1-Dimensional Shapes

2-Node Shape Function

$$N_i = \frac{1 + \xi_i \xi}{2} \ , \ -1 \le \xi \le 1$$

$$\xi_1 = -1, \ \xi_2 = 1$$

2-Node Hermite Shape Function

$N_1 = 1 - 3\xi^2 + 2\xi^3$, $N_2 = l\xi - 2l\xi^2 + l\xi^3$, $N_3 = 3\xi^2 - 2\xi^3$, $N_4 = -l\xi^2 + l\xi^3$, $0 \le \xi \le 1$

l : Element length

3.2 2-Dimensional Shapes

3-Node Triangle

$N_1 = 1 - \xi - \eta$, $N_2 = \xi$, $N_3 = \eta$

Figure 3.3.1 Node locations and natural coordinate system for a triangle

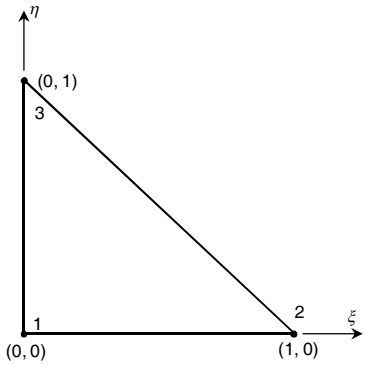

Figure 3.3.2 Node locations and natural coordinate system for a rectangle

4-Node Rectangle

$$N_i = \frac{1}{4}(1+\xi_i\xi)(1+\eta_i\eta)$$

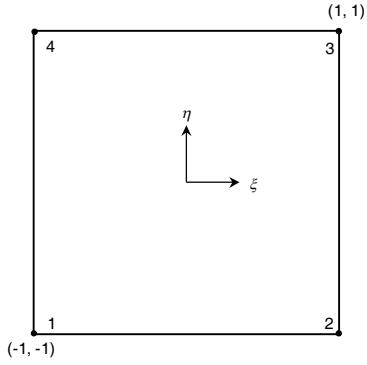

3.3 3-Dimensional Shapes

4-Node Tetrahedron

$$N_1 = 1-\xi-\eta-\zeta \ , \ N_2 = \xi \ , \ N_3 = \eta \ , \ N_3 = \zeta$$

Figure 3.3.3 Node locations and natural coordinate system for a tetrahedron

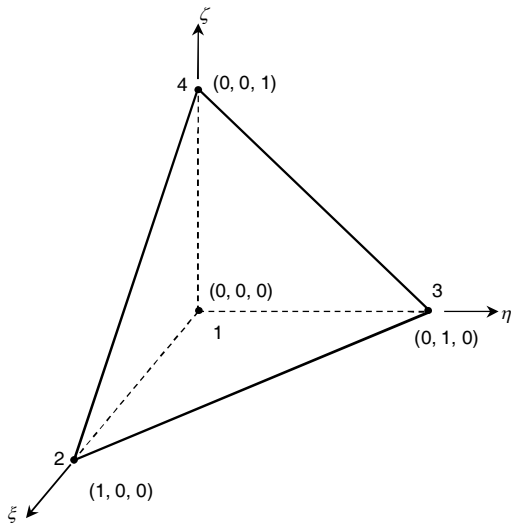

6-Node Pentahedron

$$N_i = \frac{1}{2}(1-\xi-\eta)(1+\zeta_i\zeta)\ ,\ i=1,4$$

$$N_i = \frac{1}{2}\xi(1+\zeta_i\zeta)\ ,\ i=2,5$$

$$N_i = \frac{1}{2}\eta(1+\zeta_i\zeta)\ ,\ i=3,6$$

Figure 3.3.4 Node locations and natural coordinate system for a pentahedron (wedge)

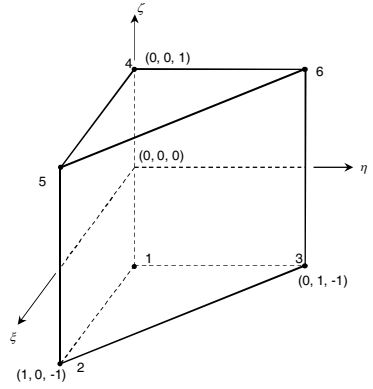

A 5-node pentahedron takes on the shape of a pyramid, and degenerated shape function (derived from the merging of multiple nodes) are widely used. However, because the shape function has numerical integration issues[5], the following alternative is used in midas nGen.

5-Node Pentahedron

$$N_i = \frac{1}{4}\{(1+\xi_i\xi)(1+\eta_i\eta) - \zeta + \xi_i\eta_i\frac{\xi\eta\zeta}{1-\zeta}\}\ ,\ \ i = 1,2,3,4$$

$$N_5 = \zeta$$

Figure 3.3.5 Node locations and natural coordinate system for a pentahedron (pyramid)

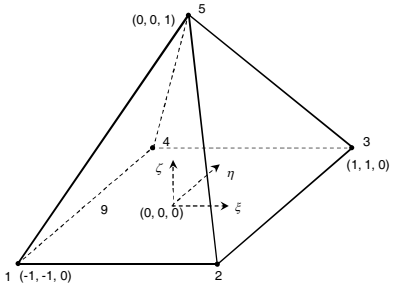

8-Node Hexahedron

$$N_i = \frac{1}{8}(1+\xi_i\xi)(1+\eta_i\eta)(1+\zeta_i\zeta)\ ,\ \ i = 1,2,3,\ldots,8$$

Figure 3.3.6 Node locations and natural coordinate system for a hexahedronal element

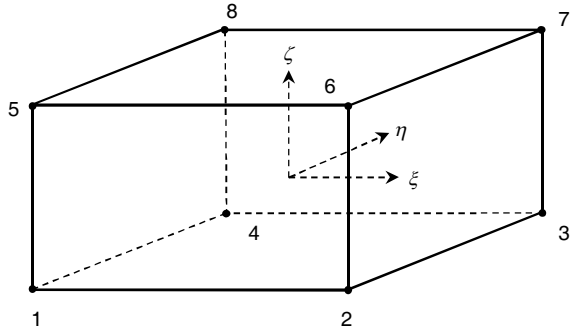

To apply these shape functions in the formulation procedure mentioned in Section 3.1, numerical integration methods are required. Numerical integration is required for calculating the stiffness matrix,

5 Bedrosian, G., "Shape functions and integration formulas for three-dimensional finite element analysis", International Journal for Numerical Methods in Engineering, Vol. 35, 1992

mass matrix, load vector, and internal force, among other quantities. Midas nGen uses two integration methods: Gaussian quadrature integration and Lobatto quadrature integration.

Table 3.3.1 Types and uses of numerical integration methods

Numerical Integration Method	Matrix Type		Applicable Elements
Gaussian quadrature	Stiffness Matrix	Structural elements	All elements that require numerical integration
	Mass Matrix	Consistent mass	All elements
		Lumped mass	All elements that require diagonal scaling6
Lobatto quadrature	Stiffness Matrix	Structural elements	–
	Mass Matrix	Consistent mass	–
		Lumped mass	3-node triangle, 4-node rectangle, 4-node tetrahedron, 6-node pentahedron, 8-node hexahedron

Figure 3.3.8 Points of integration for different numerical integration methods

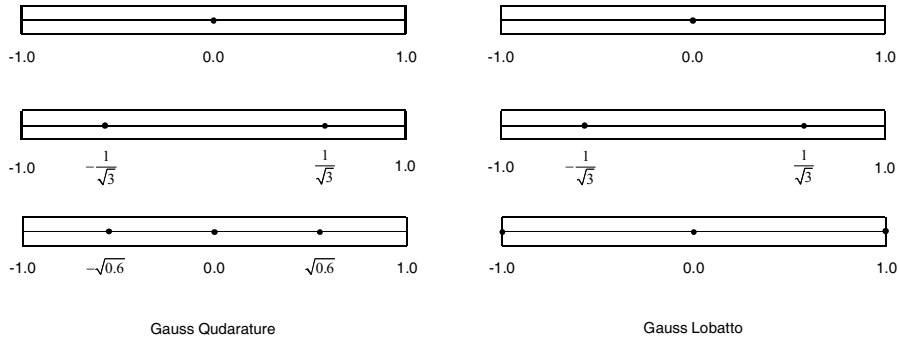

[6] Hinton, E., Tock, T. and Zienkiewicz, O.C., "A Note on mass lumping and related processes in the finite element method," Earthquake Engineering and Structural Dynamics, Vol. 4, 1976

Section 4

Supplementary Information

Regarding Locking Phenomena

Finite elements based on assumed displacement methods are known to yield solutions with very low accuracy. The reason for this is due to locking phenomena. Resolving locking phenomena and thus improving the accuracy of the solution is of utmost importance to a finite element software. Midas nGen improves the precision of each element through the following methods. Each method is not used independently of one another; multiple methods may be combined depending on the element.

4.1 Mixed-hybrid formulation

Mixed-hybrid formulation combines variation theory and displacement, and may be categorized very differently depending on the assumed component. Midas nGen uses the assumed stress method and the mixed-hybrid u-p method.

According to the Hellinger-Reissner principle, displacement and stress may be expressed as unknown variables in the variational equation shown below:

$$\delta G_{ext} = \int_{\Omega} (\nabla \delta \mathbf{u})^T \boldsymbol{\sigma} + \delta \boldsymbol{\sigma}^T (\nabla \mathbf{u} - \mathbf{D}^{-1} \boldsymbol{\sigma}) d\Omega \tag{3.4.1}$$

For the shape function for a random element, the displacement may be assumed to be of the form $\mathbf{u}^h = \mathbf{N}\mathbf{d}^e$ and the stress may be assumed to be of the form $\boldsymbol{\sigma} = \mathbf{P}\boldsymbol{\beta}^e$. With these substitutions, the above equation's right hand side may be written as:

$$\delta \mathbf{d}^{eT} \bar{\mathbf{Q}}^T \boldsymbol{\beta}^e + \delta \boldsymbol{\beta}^{eT} (\bar{\mathbf{Q}} \mathbf{d}^e - \bar{\mathbf{P}} \boldsymbol{\beta}^e) \tag{3.4.2}$$

Here,

$$\bar{\mathbf{Q}} = \int_{\Omega_e} \mathbf{P}^T \mathbf{B} d\Omega_e \tag{3.4.3}$$

$$\bar{\mathbf{P}} = \int_{\Omega_e} \mathbf{P}^T \mathbf{D}^{-1} \mathbf{P} d\Omega_e \tag{3.4.4}$$

$\boldsymbol{\beta}^e$ is not assumed to be continuous between elements, and thus may be eliminated within elements as shown below:

$$\boldsymbol{\beta}^e = \bar{\mathbf{P}}^{-1} \bar{\mathbf{Q}} \mathbf{d}^e \tag{3.4.5}$$

If the above is substituted into Equation 3.4.2, then the element stiffness is as follows:

$$\mathbf{K}^e = \bar{\mathbf{Q}}^T \bar{\mathbf{P}}^{-1} \bar{\mathbf{Q}} \tag{3.4.6}$$

The function $\mathbf{P}$ presumes the stress of an element, and thus the appropriate selection of $\mathbf{P}$ is the most important decision in determining the performance of an element. For example, a shell element's in-plane stress[7] is assumed to be as follows:

$$\boldsymbol{\sigma} = \begin{Bmatrix} \sigma_{xx} \\ \sigma_{yy} \\ \tau_{xy} \end{Bmatrix} = \mathbf{P}\boldsymbol{\beta} = \mathbf{T}\hat{\mathbf{P}}\boldsymbol{\beta} = \mathbf{T} \begin{bmatrix} 1 & 0 & 0 & \eta & 0 \\ 0 & 1 & 0 & 0 & \xi \\ 0 & 0 & 1 & 0 & 0 \end{bmatrix} \boldsymbol{\beta} \tag{3.4.7}$$

Here, $\mathbf{T}$ is the coordinate transformation matrix of the contravariant of the stress component:

$$\boldsymbol{\sigma} = \mathbf{T}\hat{\boldsymbol{\sigma}} = \begin{bmatrix} j_{11}^2 & j_{21}^2 & 2j_{11}j_{21} \\ j_{12}^2 & j_{22}^2 & 2j_{12}j_{22} \\ j_{11}j_{12} & j_{21}j_{22} & j_{11}j_{22} + j_{12}j_{21} \end{bmatrix} \begin{Bmatrix} \sigma_{\xi\xi} \\ \sigma_{\eta\eta} \\ \tau_{\xi\eta} \end{Bmatrix} \tag{3.4.8}$$

7 Pian, T.H.H. and Sumihara, K., "Rational approach for assumed stress finite elements," International Journal for Numerical Methods in Engineering, Vol. 20, 1984

Each component of the transformation matrix is calculated using the Jacobian, and typically uses the values at the middle of the element.

$$\mathbf{J} = \begin{bmatrix} \frac{\partial x}{\partial \xi} & \frac{\partial y}{\partial \xi} \\ \frac{\partial x}{\partial \eta} & \frac{\partial y}{\partial \eta} \end{bmatrix} = \begin{bmatrix} j_{11} & j_{12} \\ j_{21} & j_{22} \end{bmatrix} \tag{3.4.9}$$

Hybrid u-p method assumes all components of stress $\boldsymbol{\sigma}$, but only for hydrostatic stress or pressure p; therefore, it has traditionaly been applied to locking phenomena due to incompressible materials. The stress tensor is decomposed into the deviatoric stress and pressure, and applies the Hu-Washizu variational principle.

$$\begin{aligned} \boldsymbol{\sigma} &= \boldsymbol{\sigma}_{dev} - p\mathbf{I} \\ p &= Ktr(\boldsymbol{\varepsilon}) \end{aligned} \tag{3.4.10}$$

$\boldsymbol{\sigma}_{dev}$: Deviatoric Stress
K : Bulk Modulus
$tr(\boldsymbol{\varepsilon})$: Trace of Strain

4.2 ANS: Assumed Natural Strain

Assumed natural strain method does not stray too far from classical displacement assumption method and thus is widely known as a method that can be easily applied in practice. In particular, this method is applied frequently to shell element analysis[8, 9, 10]. In principle, Hu-Washizu principle serves as its base, but when being applied to finite element methods it may best be categorized as a type of B-bar method[11].

[8] MacNeal, R.H., "Derivation of element stiffness matrices by assumed strain distribution," Nuclear Engineering and Design, Vol. 70, 1982

[9] Hughes, T.J.R. and Tezduyar, T.E., "Finite elements based upon Mindlin plate theory with particular reference to the four-node bilinear isoparametric element," Journal of Applied Mechanics, Vol. 48, 1981

[10] Bathe, K.J. and Dvorkin, E.N., "A formulation of general shell elements-The use of mixed interpolation of tensorial components," International Journal for Numerical Methods in Engineering, Vol. 22, 1986

[11] Hughe, T. J. R., The Finite Element Method, Prentice Hall Inc., Englewood Cliffs, NJ, 1987

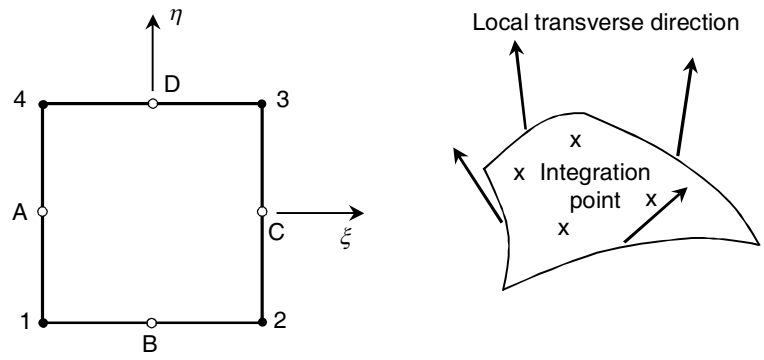

Figure 3.4.1 Assumed lateral shear strain

For example, consider the application of the assumed natural strain method to the the lateral shear strain of the four-node shell element shown above. Of the natural coordinate system components, $\gamma_{\xi z}$ is known at locations B and D, and $\gamma_{\eta z}$ is known at locations A and C. Using these values, the strain at the points of integration may be interpolated as follows:

$$\gamma_{\xi z} = \frac{1}{2}(1-\eta)\gamma_{\xi z}^{B} + \frac{1}{2}(1+\eta)\gamma_{\xi z}^{D} \tag{3.4.11}$$

$$\gamma_{\eta z} = \frac{1}{2}(1-\xi)\gamma_{\eta z}^{A} + \frac{1}{2}(1+\xi)\gamma_{\eta z}^{C} \tag{3.4.12}$$

Strain in the natural coordinate system may be transformed into space coordinates by using the following transformations:

$$\boldsymbol{\gamma} = \begin{Bmatrix} \gamma_{xz} \\ \gamma_{yz} \end{Bmatrix} = \mathbf{T}^{-T} \begin{Bmatrix} \gamma_{\xi z} \\ \gamma_{\eta z} \end{Bmatrix} \tag{3.4.13}$$

Here, $\mathbf{T}$ is a coordinate transformation matrix of the covariant component, as shown below:

$$\mathbf{T} = \begin{bmatrix} j_{11} & j_{21} \\ j_{12} & j_{22} \end{bmatrix} \tag{3.4.14}$$

Each component of the transformation matrix is calculated using the Jacobian. The assumed natural strain method only modifies the strain by using equations 3.4.11-13. Essentially, it is the equivalent of modifying the $\mathbf{B}$ matrix in the assumed displacement method, as shown below.

$$\boldsymbol{\varepsilon} = \nabla \mathbf{u} = \overline{\mathbf{B}}\mathbf{d}^e \tag{3.4.15}$$

4.3 EAS: Enhanced assumed strain

The enhanced assumed strain method is very similar to the incompatible modes[12] method (and also yields the same results), but in contrast its theoretical base is the Hu-Washizu principle and begins from the assumed strains instead of assumed displacements. The following Hu-Washizu variational equation assumes three unknown varialbes: displacement, strain, stress:

$$\delta G_{ext} = \int_\Omega (\nabla^T \delta \mathbf{u})\boldsymbol{\sigma} + \delta \boldsymbol{\varepsilon}^T (\mathbf{D}\boldsymbol{\varepsilon} - \boldsymbol{\sigma}) + \delta \boldsymbol{\sigma}^T (\nabla \mathbf{u} - \boldsymbol{\varepsilon}) d\Omega \tag{3.4.16}$$

Strain $\boldsymbol{\varepsilon}$ is taken to be the sum of compatible strain (calculated from displacement) and incompatible strain (enhanced assumed strain).

$$\boldsymbol{\varepsilon} = \nabla \mathbf{u} + \overline{\boldsymbol{\varepsilon}} \tag{3.4.17}$$

If the above is substituted into Equation 3.4.16 and rearranged, the result is as follows:

$$\delta G_{ext} = \int_\Omega (\nabla^T \delta \mathbf{u})\mathbf{D}(\nabla \mathbf{u} + \overline{\boldsymbol{\varepsilon}}) + \delta \overline{\boldsymbol{\varepsilon}}^T (\mathbf{D}\nabla \mathbf{u} + \mathbf{D}\overline{\boldsymbol{\varepsilon}} - \boldsymbol{\sigma}) - \delta \boldsymbol{\sigma}^T \overline{\boldsymbol{\varepsilon}} d\Omega \tag{3.4.18}$$

With the assumption that stress distribution and incompatible strains are orthogonal within the element, then the equation may be modified to become a function of only displacement and enhanced assumed strain, as shown below:

$$\delta G_{ext} = \int_\Omega \nabla^T \delta \mathbf{u}\mathbf{D}(\nabla \mathbf{u} + \overline{\boldsymbol{\varepsilon}}) + \delta \overline{\boldsymbol{\varepsilon}}^T (\mathbf{D}\nabla \mathbf{u} + \mathbf{D}\overline{\boldsymbol{\varepsilon}}) d\Omega \tag{3.4.19}$$

For the shape function of a random element, if the displacement is substituted with $\mathbf{u}^h = \mathbf{N}\mathbf{d}^e$ and the enhanced strain is assumed to be of the form $\overline{\boldsymbol{\varepsilon}} = \mathbf{G}\boldsymbol{\alpha}^e$, the right hand side of the above equation can be written as follows:

[12] Taylor, R.L., Beresford, P.J. and Wilson, E.L., "A non-conforming element for stress analysis," International Journal for Numerical Methods in Engineering, Vol. 10, 1976

$$\delta \mathbf{d}^{eT} \mathbf{K}_{dd}^{e} \mathbf{d}^{e} + \delta \mathbf{d}^{eT} \mathbf{K}_{d\alpha}^{e} \boldsymbol{\alpha}^{e} + \delta \boldsymbol{\alpha}^{eT} \mathbf{K}_{\alpha d}^{e} \mathbf{d}^{e} + \delta \boldsymbol{\alpha}^{eT} \mathbf{K}_{\alpha\alpha}^{e} \boldsymbol{\alpha}^{e} \tag{3.4.20}$$

Here, $\mathbf{K}_{dd}^{e}$ is the classical element stiffness matrix based on assumed displacement, and $\mathbf{K}_{d\alpha}^{e}$ and $\mathbf{K}_{\alpha\alpha}^{e}$ may be written as:

$$\mathbf{K}_{d\alpha}^{e} = \int_{\Omega_e} \mathbf{B}^{T} \mathbf{D} \mathbf{G} d\Omega_e \tag{3.4.21}$$

$$\mathbf{K}_{\alpha\alpha}^{e} = \int_{\Omega_e} \mathbf{G}^{T} \mathbf{D} \mathbf{G} d\Omega_e \tag{3.4.22}$$

$\boldsymbol{\alpha}^{e}$ is assumed to be discontinuous between elements and there is no external work towards $\delta \boldsymbol{\alpha}^{e}$. Thus, within the element, it may be elimited as:

$$\boldsymbol{\alpha}^{e} = -\mathbf{K}_{\alpha\alpha}^{e-1} \mathbf{K}_{\alpha d}^{e} \mathbf{d}^{e} \tag{3.4.23}$$

If the above is substituted into equation 3.4.20, then the element stiffness matrix is:

$$\mathbf{K}^{e} = \mathbf{K}_{dd}^{e} - \mathbf{K}_{d\alpha}^{e} \mathbf{K}_{\alpha\alpha}^{e-1} \mathbf{K}_{\alpha d}^{e} \tag{3.4.24}$$

Appropriate selection of $\mathbf{G}$, which assumes enhanced strain values, is the most important factor in determining element performance.

4.4 Reduced Integration Methods

Strain that is calculated at points of integration with low orders of integration is known to be more precise relative to those at other locations. Moreover, the locking phenomena in elements typically occurs due to unnecessary orders of integration for strain calculations, and can be resolved through reduced integration methods. However, depending on the case, reduced integration can worsen the numerical properties of the stiffness matrices and may trigger spurious zero energy modes or hourglass modes.

4.5 Stabilization Technique for Reduced Integration

Generally, 3-dimensional low order element strain may be approximated as follows:

$$\boldsymbol{\varepsilon} = \nabla \mathbf{u} \approx (\mathbf{B}_0 + \mathbf{B}_1(\xi, \eta, \zeta))\mathbf{d}^e \tag{3.4.25}$$

Resolving locking phenomena by using reduced integration is the equivalent of exclusively using $\mathbf{B}_0$, which is equal to evaluating the strain at the element's midpoint. However, when using the strain at the midpoint of the element, problems occur when failing the patch test (which connects equal strain values). Thus, to resolve this issue, it is normal to substitute $\mathbf{B}_0$ with $\bar{\mathbf{B}}_0$ [13]. $\bar{\mathbf{B}}_0$, which corresponds to average strain, satisfies the following equation:

$$\bar{\mathbf{B}}_0 = \frac{1}{V_e}\int_{\Omega_e} \mathbf{B} d\Omega_e \tag{3.4.26}$$

Here, V_e represents element volume. If $\bar{\mathbf{B}}_0$ is exclusively used, because it corresponds to average strain the strain energy from the spurious zero energy mode is not considered. For low order elements, this phenomenon is quite severe and requires stabilization.

Within the class of "hourglass control" stabilization methods there are various options. Midas nGen uses the physical stabilization method suggested by Puso[14]. As an example, for stable strain calculations of an 8-node hexahedron element, $\mathbf{B}_1$ is extressed in natural coordinates as shown below:

$$\tilde{\mathbf{B}}_1 = \xi\tilde{\mathbf{B}}_\xi + \eta\tilde{\mathbf{B}}_\eta + \zeta\tilde{\mathbf{B}}_\zeta + \xi\eta\tilde{\mathbf{B}}_{\xi\eta} + \eta\zeta\tilde{\mathbf{B}}_{\eta\zeta} + \zeta\xi\tilde{\mathbf{B}}_{\zeta\xi} \tag{3.4.27}$$

If all strain values in the above equation are used, the effects due to reduced integration disappear. As a result, a portion of shear strain terms are excluded.

The application of average strain and stabilization techniques not only gives the equivalent effect of selective reduced integration, but the numerical integration procedure is also replaced with the following equation and thus there is a huge benefit in computing speed.

---

[13] Flanagan, D.P. and Belytschko, T., "A uniform strain hexahedron and quadrilateral with orthogonal hourglass control," International Journal for Numerical Methods in Engineering, Vol. 17, 1981

[14] Puso, M.A., "A highly efficient enhanced assumed strain physically stabilized hexahedral element," International Journal for Numerical Methods in Engineering, Vol. 49, 2000

$$\int_{\Omega_e}[]d\Omega_e = \frac{V_e}{8}\iiint[]d\xi d\eta d\zeta \tag{3.4.28}$$

4.6 Non-conforming element

Non-conforming elements use strain decomposition methods to satisfy compatilibty conditions in integration form. The aforementioned EAS method is a kind of non-conforming element. In general, compatibility conditions between elements can be expressed in integration form as:

$$\int_{\Omega_e} u^*_{i,j}d\Omega = \int_{\partial\Omega_e}\bar{u}_i n_j dS \tag{3.4.29}$$

u^* : displacement assumed within the element

$\bar{u}$: displacement assumed on the outer surface of the element

n_j : direction cosine orthogonal to the outer surface the element

j : differentiation in the j direction

Displacement assumed within the element is composed of the typical shape function and an additional portion:

$$\mathbf{u}^* = \mathbf{N}\mathbf{d}^e + \mathbf{P}\boldsymbol{\lambda} \tag{3.4.30}$$

Similarly, displacement assumed on the outer surface of the element is composed of the typical shape function and an additional portion. However, the assumed displacement is expressed as an interpolation of the nodal point.

$$\bar{\mathbf{u}} = \mathbf{N}\mathbf{d}^e + \alpha\mathbf{M}\mathbf{d}^e \tag{3.4.31}$$

$\mathbf{M}$: Additional shape function ($\neq \mathbf{N}$)

In the above equation, α is a random coefficient, and an appropriate value is selected based on the convergence of the element or accuracy of the value. If equations 3.4.30 and 3.4.31 are substituted in 3.4.29, $\boldsymbol{\lambda}$ may be calculated using $\mathbf{d}^e$. Applying the resulting value for $\boldsymbol{\lambda}$, the element strain can be written as shown below:

$$\boldsymbol{\varepsilon} = \mathbf{B}\mathbf{d}^e + (\nabla\mathbf{P})\boldsymbol{\lambda} \tag{3.4.32}$$

Using a non-conforming element is the equivalent of modifying the **B** matrix as shown below when using the assumed displacement method:

$$\boldsymbol{\varepsilon} = \nabla \mathbf{u} = \bar{\mathbf{B}}\mathbf{d}^{e} \tag{3.4.33}$$

Section 5

Continuum Elements

Continuum elements are used to model elements with volume, such as foundations or equipment. In 3-dimensional analysis, continuum elements belong to the class of solid elements.

5.1 Solid elements

Solid elements are mainly used for modeling structural components with volume, such as foundation. Midas nGen provides the user with the option to choose between tetrahedrons, pentahedrons, or hexahedrons, and the elements may have 4, 5, 6, or 8 nodes. Pentahedrons may be wedge or pyramid shaped.

Coordinate System

A tetrahedronal element's ECS is the equivalent of applying a plane stress element's ECS to the triangular shape formed by nodes 1, 2, and 3.
A pentagonal wedge-shaped element's ECS is the equivalent of applying a plane stress element's ECS to the triangular shapes formed by the midpoints of nodes 1 and 4, 2 and 5, and 3 and 6.
A pentagonal pyramid-shaped element's ECS is the equivalent of applying a plane stress element's ECS to the quadrangular shape formed by nodes 1 2, 3, and 4.
In the case of a hexagonal element, vectors whose roles resemble those of typical ECS vectors are defined as follows:

- **r** : Vector connecting the midpoint of nodes 1, 5, 8, 4 to the midpoint of nodes 2, 6, 7, 3
- **s** : Vector connecting the midpoint of nodes 1, 2, 6, 5 to the midpoint of nodes 4, 3, 7, 8
- **t** : Vector connecting the midpoint of nodes 1, 2, 3, 4 to the midpoint of nodes 5, 6, 7, 8

The orthogonal coordinate system that is most adjacent to the above three vectors become the hexagonal element's ECS.

Figure 3.5.1 Coordinate system for a solid element

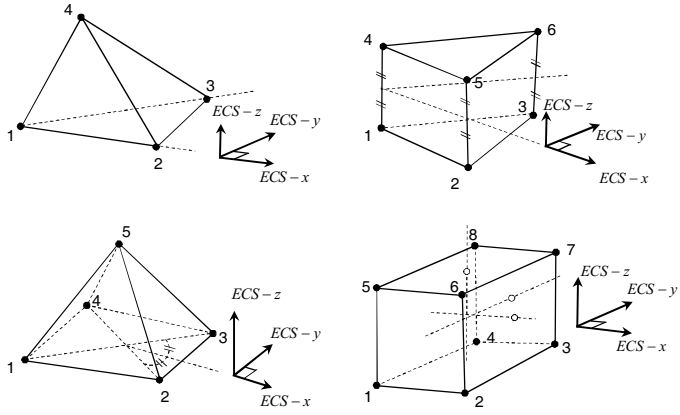

Degrees of Freedom

A solid element has degrees of freedom defined about the x, y, and z axes of the GCS.

$$\mathbf{u}_i = \{u_i \quad v_i \quad w_i\}^T \tag{3.5.1}$$

Stress and Strain

A solid element's stress and strain is defined by the GCS and the components are as follows:

$$\boldsymbol{\sigma} = \begin{Bmatrix} \sigma_{xx} \\ \sigma_{yy} \\ \sigma_{zz} \\ \tau_{xy} \\ \tau_{yz} \\ \tau_{zx} \end{Bmatrix}, \quad \boldsymbol{\varepsilon} = \begin{Bmatrix} \varepsilon_{xx} \\ \varepsilon_{yy} \\ \varepsilon_{zz} \\ \gamma_{xy} \\ \gamma_{yz} \\ \gamma_{zx} \end{Bmatrix} \tag{3.5.2}$$

(3-Dimensional Stress and Strain)

Figure 3.5.2 A solid element's stress and strain

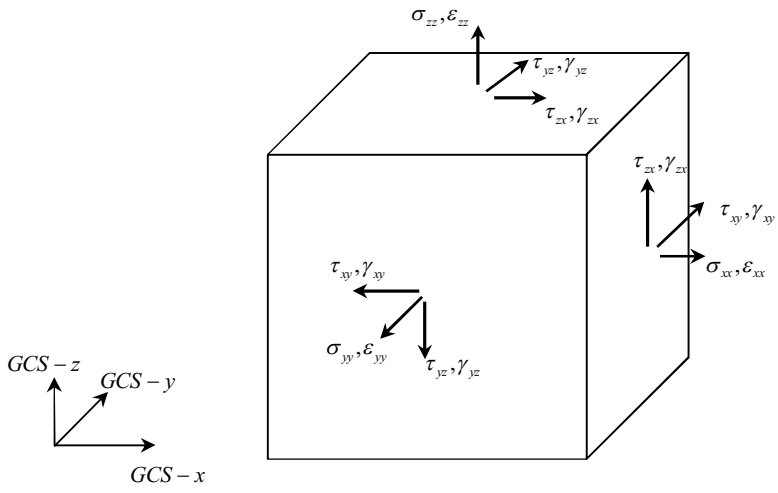

Loads

A solid element may be subject to the following loads.

Table 3.5.1 Loads that are applicable to a solid element

Load Type	Description
Self-weight due to gravity	Applied based on material density
Pressure load	Distributed loading applied to the element surface
Element temperature load	Element temperature that may cause volume changes

Element Result

In midas nGen, a solid element's results are output using the default coordinate system specified by the user. The element result coordinate system (ERCS) that the user may select is the member's element coordinate system (defined by the element units).

Table 3.5.2 List of results for a solid element

Result		Description
Stress	Stress component	Location: vertex/element midpoint σ_{xx} , σ_{yy} , σ_{zz} , τ_{xy} , τ_{yz} , τ_{zx}
	Principal stress	Location: vertex/element midpoint P_1 , P_2 , P_3 , in the direction of principal stress
	Von-Mises stress	Location: vertex/ element midpoint σ_v
	Max shear stress	Location : vertex/ element midpoint $\tau_{\max}$
	Octahedral stress	Location : vertex/ element midpoint τ_o
	Mean pressure	Location : vertex/ element midpoint p_0

Selection of Elements

Midas nGen has a wide range of solid elements for the user to select from, that may improve computational efficiency. The following shows the commonly used names in the midas nGen software

and the related finite element technique and integration methods. The shaded sections are the default values.

Table 3.5.3 Various techniques that may be applied to a solid element

Shape	Number of nodes	Name	Element technique	Stiffness matrix numerical integration	Lumped mass calculation method
Tetrahedron	4	Full integration	Assumed displacement method	1 points	Lobatto
		Enhanced	EAS, u-p hybrid method	4 points	Lobatto
Wedge	6	Full integration	Assumed displacement method	3X2 points	Lobatto
		Reduced integration (stabilized)	Reduced integration method (stabilized)	1X1 points	Lobatto
		Hybrid	Hybrid method	3X2 points	Lobatto
Pyramid	5	Full integration	Assumed displacement method	4X 2points	Diagonal scaling
		Reduced integration	Reduced integration method	1X1 points	Diagonal scaling
		Hybrid	Hybrid method	4X2 points	Diagonal scaling
Hexahedron	8	Full integration	Assumed displacement method	2X2X2 points	Lobatto
		Reduced integration (stabilized)	Reduced integration (stabilized)	1X1X1 points	Lobatto
		Hybrid	Hybrid method	2X2X2points	Lobatto

Each element's characteristics are outlined below.

► 4-node element : The displacement result does not depend on technique, but stress is most accurate when using EAS and u-p hybrid method.
► 6-node element : Performance is particularly outstanding when applying the hybrid method for thin structural elements.
► 8-node element : Performance is particularly outstanding when applying the hybrid method for flexural structural elements or the reduced integration method.

Nonlinear analysis

P-delta effects cannot be considered for a solid element, and midas nGen only supports linear elastic materials for solid elements. Even in nonlinear analysis, these elements are still considered to be linear elements.

Section 6

Structural Elements

Structural elements are elements that most efficiently express certain loading conditions, and include truss, beam, and shell elements. When modeling, it is important to verify whether the loading and strain conditions are compatible with the element.

6.1 Truss element

Truss elements are a 1-dimensional element defined by two nodes. These elements are usually used for modeling elements whose lengths are large relative to their cross section and thus whose flexural behaviors are neglected in analysis. A space truss or diagonal brace are examples of such cases.

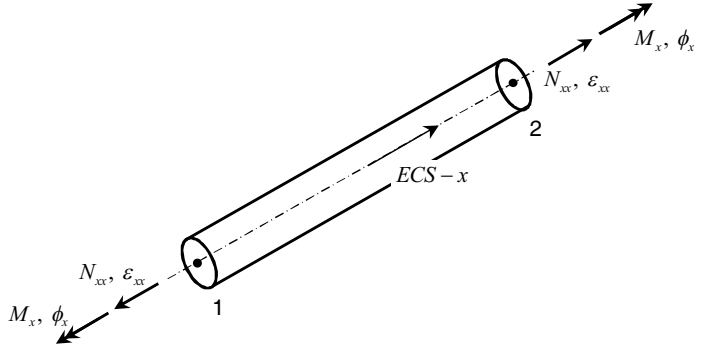

Figure 3.6.1 Cooridnate system, stress, and strain for a truss element

Coordinate System

In the truss element's ECS, the x-axis direction represents the direction from node 1 to node 2. Finite element formulation uses the ECS as the basis.

Degrees of Freedom

A truss element has displacement and rotation degrees of freedom in the x-axis direction of its ECS.

$$\mathbf{u}_i = \{u_i\}\ ,\ \boldsymbol{\theta}_i = \{\theta_{xi}\} \tag{3.6.1}$$

Stress and Strain

As shown in Figure 3.6.1, a truss element's axial and torsional strain are defined with respect to the axis defined in its ECS.

$$\mathbf{N} = \{N_{xx}\}\ ,\ \boldsymbol{\varepsilon} = \{\varepsilon_{xx}\} \tag{3.6.2}$$

(Axial force and strain)

$$\mathbf{T} = \{M_x\}\ ,\ \boldsymbol{\varphi} = \{\phi_x\} \tag{3.6.3}$$

(Torsional moment and rotation)

Loads

A truss element may be subject to the following loads.

Table 3.6.1 Loads that may be applied to a truss element

Load Type	Description
Self-weight due to gravity	Applied based on material density
Element temperature load	Element temperature that may trigger an axial length change

Element Results

The following table shows the element results generated when using a truss element. The basis coordinate system is always the ECS.

Table 3.6.2 List of truss element results

Result		Description
Stress	Axial stress	Location: Element midpoint, σ_{xx}
	Torsional stress	Location: Element midpoint Torsional stress is calculated based on c ($\tau = Tc/J$)
Force /Moment	Axial force	Location: Element midpoint, N_{xx}
	Torsional Moment	Location: Element midpoint, M_x

Nonlinear Analysis

Truss elements can incorporate geometric nonlinearity for the output of linear buckling analysis and P-delta analysis. These elements may be specified as compression- or tension-only elements, and these settings will be applied as a material property. In the case of compression- or tension-only elements, nonlinear analysis is conducted automatically for typical static loads. For nonlinear loading combinations, compressive or tensile properties are determined depending on the case. The software will also output the contribution from each load case.

6.2 Beam Element

Beam elements are 1-dimensional linear elements defined by two nodes, and are used to model elements with long lengths (compared to their cross-sectional areas) that experience flexural deformations. If the ratio of the cross-sectional height or width to the length exceeds 1/5, effects of shear deformations may dominate. In such cases, it is recommended that the user resort to shell or solid elements in place of the beam element.

Coordinate System

The ECS of a beam element is automatically decided based on its location in space. Finite element formulation for a beam element is based on its ECS. The ECS is defined using the following process.

ECS-x: ECS-x is defined to be in the direction in which the GCS-X component is positive based on the constructured 1-dimensional member vector. In the case in which the 1-dimensional member's x-axis vector component is zero, the direction in which the GCS-Y component is positive is used. In the case in which both the x-axis and y-axis vector components are zero, the direction in which the GCS-Z component is positive is used.

ECS-z: ECS-z is defined after determining the ECS-x axis. The GCS-z axis is projected onto the plane perpendicular to ECS-x, and the ECS-z is defined to be in the positive direction of the projection of the GCS z-axis.
If the ECS-x and GCS-z axes are equal, the ECS-z cannot be defined following the procedure outlined above. Thus, the GCS-y axis is projected onto the plane perpendicular to ECS-x, and the ECS-y is determined to be in the positive direction of the projection of the GCS y-axis.

Figure 3.6.2 The development of a beam element's ECS based on its location in space

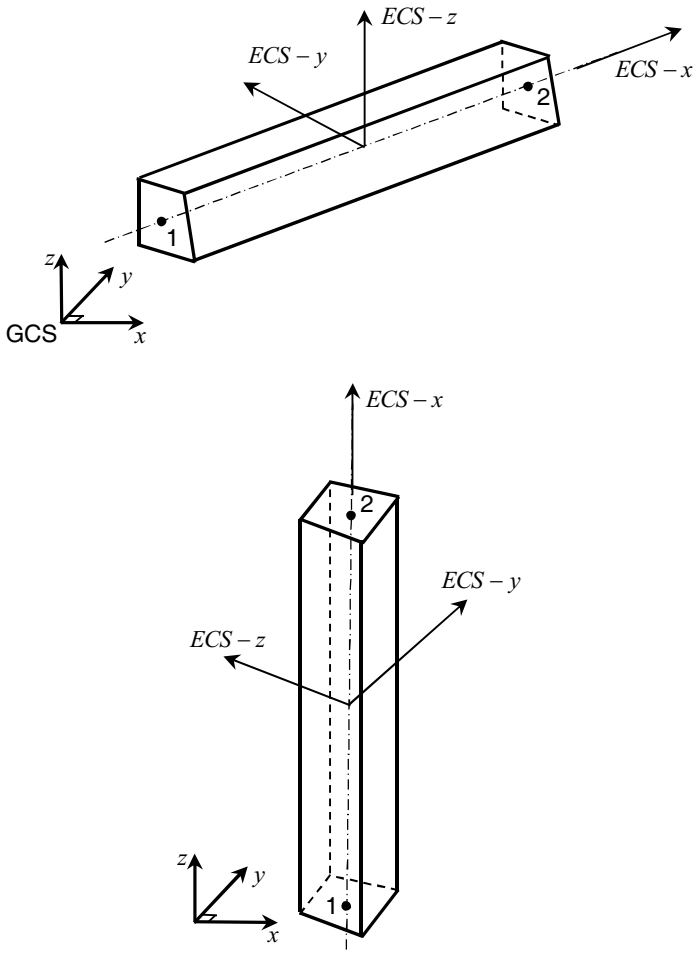

Degrees of freedom

A beam element has displacement and rotation degrees of freedom in all axes directions of its ECS.

$$\mathbf{u}_i = \{u_i \quad v_i \quad w_i\}^T, \ \boldsymbol{\theta}_i = \{\theta_{xi} \quad \theta_{yi} \quad \theta_{zi}\}^T \tag{3.6.4}$$

Stress and strain

As shown in Figure 3.6.3, a beam element will experience axial, flexural, torsional, and shear strains. When neglecting shear strains (by applying Euler's principle), shear area should be set to zero.

$$\mathbf{N} = \{N_{xx}\}\ ,\ \boldsymbol{\varepsilon} = \{\varepsilon_{xx}\} \tag{3.6.5}$$

(Axial force and strain)

$$\mathbf{M} = \begin{Bmatrix} M_y \\ M_z \end{Bmatrix},\ \boldsymbol{\kappa} = \begin{Bmatrix} \kappa_y \\ \kappa_z \end{Bmatrix} \tag{3.6.6}$$

(Flexural moment and curvature)

$$\mathbf{T} = \{M_x\}\ ,\ \boldsymbol{\varphi} = \{\phi_x\} \tag{3.6.7}$$

(Torsional moment and rotation)

$$\mathbf{Q} = \begin{Bmatrix} Q_y \\ Q_z \end{Bmatrix},\ \boldsymbol{\gamma} = \begin{Bmatrix} \gamma_{xy} \\ \gamma_{zx} \end{Bmatrix} \tag{3.6.8}$$

(Shear force and strain)

Figure 3.6.3 Coordinate system, stress, and strain for a beam element

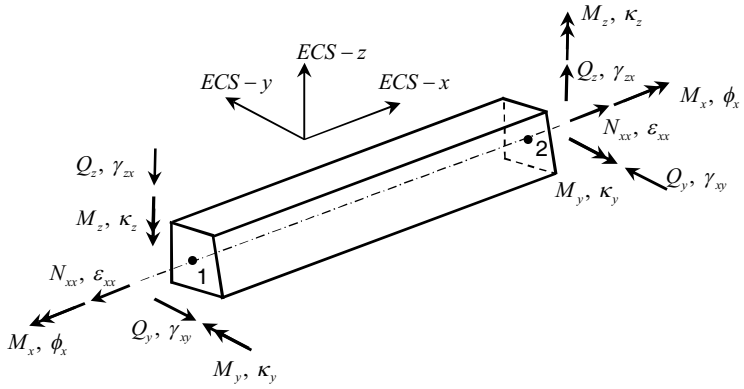

Loads

A beam element may be subject to the following loads.

Table 3.6.3 Loads that may be applied to a beam element

Load Type	Description
Self-weight due to gravity	Applied based on material density

Beam element load	Distributed loading applied to an arbitrary portion of the distance between the two element nodes, or a concentrated load applied to an arbitrary location between the two element nodes
Beam element temperature load	Average cross-sectional temperature load that may cause an axial length change Cross-sectional temperature gradient that may cause a differential curvature

Beam element loading can be expressed as a distributed or concentrated loading as shown in Figure 3.6.4, and the direction can be defined based on either the ECS or the GCS. If the distributed loading is defined based on the GCS, the load should be defined in such a way that incorporates the angle between the GCS and ECS. This way, the load will be effectively applied based on the length of the segment perpendicular to the loading direction.

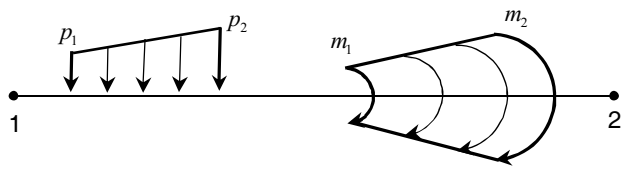

Figure 3.6.4 Examples of loading on the beam element

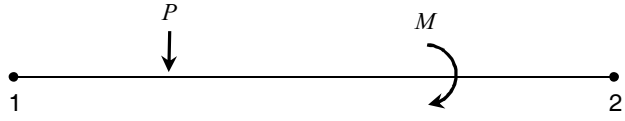

Figure 3.6.5 Load angle adjustments based on the loading direction for a beam element

Distributed beam load on original segment

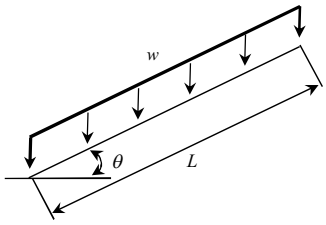

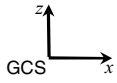

Distributed beam load on projected segment

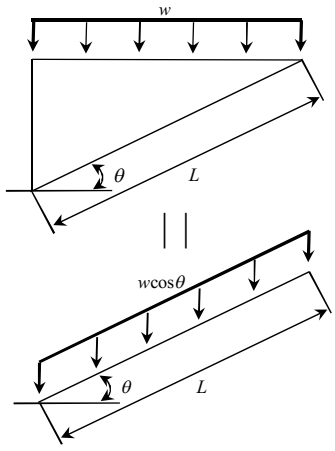

Element Results

It is important to be able to view the results at not only the endpoints of a beam element but also at internal points along the length of the beam. Thus, each element is partitioned into four output segments of equal length. Beam elments may be viewed at the endpoints (A-B) of each output segment, and the results are shown in the list below. The basis coordinate system for stress and force is always the ECS. For internal displacement, which is used in calculating the member's greatest relative deflection, the basis coordinate system is always the GCS.

Table 3.6.4 List of element results for a beam element

Result		Description
Stress	Axial stress	Location: Points A-B of each segment σ_{xx}
	Torsional stress	Location: Points A-B of each segment Torsional stress is calculated from c ($\tau = Tc / J$)
	Combined stress	Location: Points A-B of each segment, σ_{xx} due to axial force and flexure at user-specified locations (1,2,3,4)
	Combined stress-Max	Location: Points A-B of each segment The absolute maximum value of the sums of axial stress and point stress at locations 1~4
	Bending stress	Location: Points A-B of each segment The absolute maximum of the bending stress in each direction σ_{xx} at locations 1~4
	Torsional stress	Location: Points A-B of each segment Calculated at the location at which the ratio of the 1st moment of area to the product of the cross-sectional width and area moment of inertia is maximized
	Shear stress	Location: Points A-B of each segment $\tau_{xy} = Q_y / (S_{ky} A)$, $\tau_{xz} = Q_z / (S_{kz} A)$
	Von-mises stress	Location: Points A-B of each segment $\sigma_v = \sqrt{\sigma_{xx}^2 + 3\left(\tau_{xy}^2 + \tau_{xz}^2 + \tau_{xx}^2\right)}$
Force /Moment	Axial force	Location: Points A-B of each segment N_{xx}
	Bending moment	Location: Points A-B of each segment

		M_y, M_z
	Torsional moment	Location: Points A-B of each segment M_x
	Shear force	Location: Points A-B of each segment Q_y, Q_z
Internal displacement	Translation	T_X, T_Y, T_Z

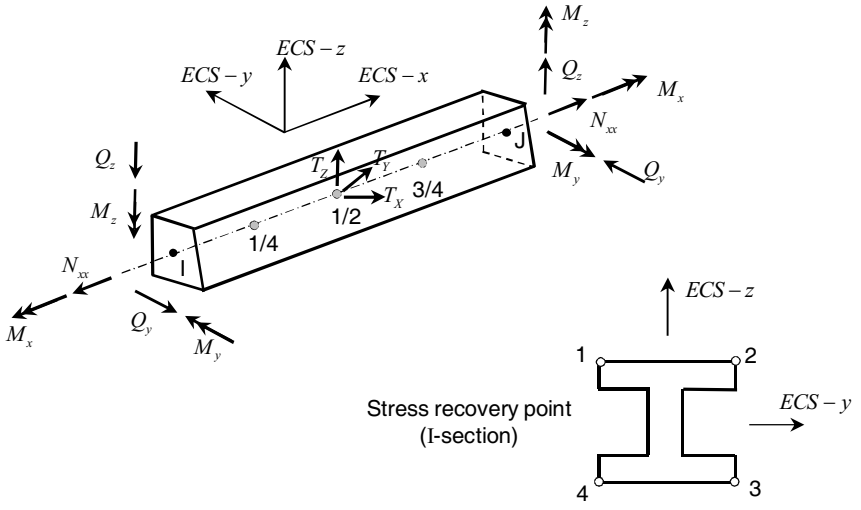

Figure 3.6.6 Beam element result locations and directions

Internal Displacement

In each output segment, the displacement is calculated based on linear beam theory, which takes into account shear strains. The calculated displacement reflects all loading cases and offset information that may be applied in midas nGen. Therefore, the result is equal to the value obtained by subdividing the element and accurate displacement may be achieved even with a few elements. However, because the results are based on linear assumptions, the values do not reflect nonlinear effects such as P-delta effects.

End release

End releases are used when, for both ends of a structural member (such as in the case of pin connection), mutual restraints for motion in a specific direction do not occur. End releases are applied

in the ECS, so users defining conditions in the GCS should be aware of the relationship between the two coordinate systems. Moreover, nodes at which end releases have been applied will attain new degrees of freedom for unrestrained motions. Thus, the entire structure to which these nodes connect may become unstable. Therefore, a comprehensive consideration of the structure's stability—including the end releases—is necessary.

Figure 3.6.7 Examples of applying end releases

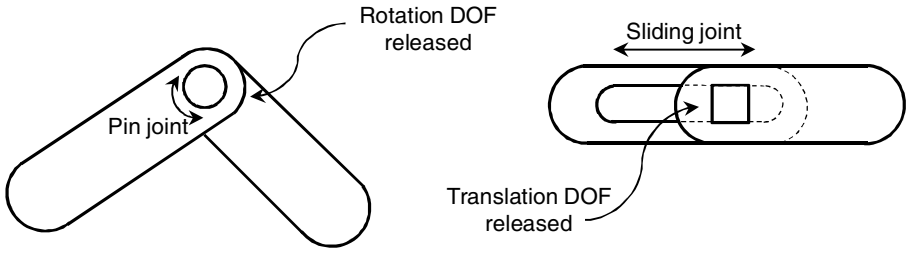

Offsets

Offsets may be used on beam elements when the neutral axis is isolated from the nodes or if the neutral axes of connecting elements do not match. Offsets are defined based on the beam element nodes' NCS. When the offset is set up in the axial direction of the element, it is interpreted as a change in element length.

Figure 3.6.8 Examples of applying offsets

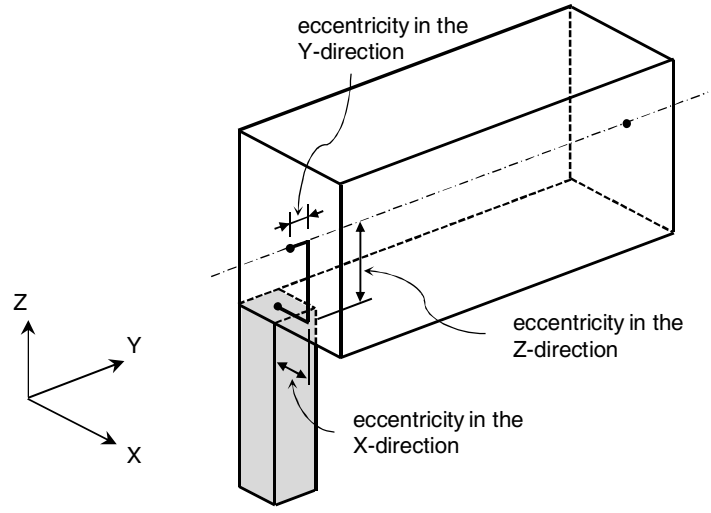

Rigid End Offsets

A structure composed of frame members will be analyzed by taking the length of its members to be the distances between the intersections of element neutral axes. As a result, a rather large displacement—as well as end and center moment—may be calculated. To resolve this issue, beam and column connections or rigid end zones may be considered.

If it is assumed that there is neither flexural nor shear deformation at the connections, the effective length for flexural and shear deflection may be expressed as the difference between the distance between the intersection of each members' neutral axes (both end points) and the rigid end offset length:

$$L' = L - ZF\left(R_i + R_j\right) \tag{3.6.9}$$

L' : Effective length

L : Distance between the intersection of neutral axes

R_i, R_j : Rigid end lengths of the end points

ZF : Rigid end modification factor ($0 \le ZF \le 1$)

If the element length is only considered to be a function of the effective length, a small error may occur with computation of the deformation occurring at the connection. The error may be controlled by using

the rigid end modification factor. This factor does not affect axial or torsional deformation, because, when calculating the axial and torsional deformations, the entire length of the element (L) is used.
The rigid end offset may be used by incorporating the panel zone effects or by manually setting the rigid end lengths. In the latter instance, the rigid end modification factor is essentially 1.0.

The user must be cautious of the following details when using rigid end offsets.

▶Calculation of element stiffness : When calculating element stiffness, the distance between the elements is used to calculate axial and torsional stiffness. When calculating shear or flexural stiffness, the effective length (after incorporating the rigid end modification factor) is used.
▶Calculation of distributed loading or self-weight: the distributed loading that is placed between the element nodes and rigid end offsets are only considered at the nodes as a shearing force, and the distributed loading on the remaining lengths are replaced as an equivalent shearing force and moment.
▸ When incorporating end releases: Rigid end offsets should be considered at the connections of column or girder members, in the case where either or both end connections have end releases due to a pinned connection.

Figure 3.6.9 Rigid end offsets built into a beam column connection

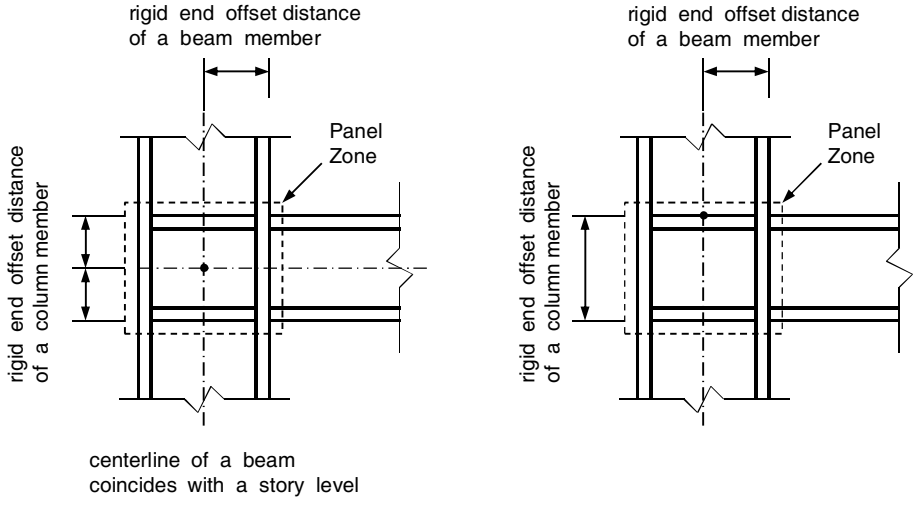

Tapered Section

Changes in the cross section of a beam element are defined based on the ECS. In the case of a quadrilateral cross section whose y-axis experiences linear changes along the length and the z-axis is constant, the cross-sectional area undergoes first-order changes and the moment of inertia undergoes third-order changes. The following list shows the degree of changes that area and moment of inertia (for each axis) undergo for different tapered sections.

Table 3.6.5 Degree of cross section changes in a beam element with a tapered section

y-axis	z-axis	A	$I_{xx}(=J)$	I_{yy}	I_{zz}
constant	constant	1	1	1	1
constant	linear	1	1	3	1
linear	constant	1	1	1	3
linear	linear	2	2	4	4

$$A(x)=\left\{\sqrt[m]{A_1}+\left(\sqrt[m]{A_2}-\sqrt[m]{A_1}\right)\left(\frac{x}{L}\right)\right\}^m,\ m=1,2 \tag{3.6.10}$$

$$I(x)=\left\{\sqrt[n]{I_1}+\left(\sqrt[n]{I_2}-\sqrt[n]{I_1}\right)\left(\frac{x}{L}\right)\right\}^n,\ n=1,3,4 \tag{3.6.11}$$

Here, the subscripts attached to the cross-sectional area and moment of inertia signify the ends of the element.

Geometric stiffness calculations use the effective cross section properties instead, as shown below.

$$A_{eff}=\begin{cases}\dfrac{A_1+A_2}{2} & ,m=1\\ \dfrac{A_2+\sqrt{A_1A_2}+A_2}{3} & ,m=2\end{cases} \tag{3.6.12}$$

$$I=\frac{I_1+\sqrt[4]{I_1^{\,3}I_2}+\sqrt{I_1I_2}+\sqrt[4]{I_1I_2^{\,3}}+I_2}{5} \tag{3.6.13}$$

Nonlinear Analysis

Beam elements can only incorporate geometric nonlinearities, and cannot take on nonlinear or inelastic material properties.

Crane Moving Analysis

With beam elements, concurrent force/moment may be verified through crane moving analysis results. Like typical analysis results, outputs may be viewed at both ends of each segment. Additional selection criteria exist to ensure that load conditions for which the maximum and minimum values are equivalent tend to be less preferred.

Table 3.6.6 Selection criteria for crane moving analysis results of a beam element

Maximum/minimum selection criteria component		Additional selection criteria 1	Additional selection criteria 2
Concurrent force/moment	N_{xx}	$\sqrt{M_y^2 + M_z^2}$	$\sqrt{Q_y^2 + Q_z^2}$
	Q_y	N_{xx}	$\lvert Q_z \rvert$
	Q_z	N_{xx}	$\lvert Q_y \rvert$
	M_x	$\sqrt{Q_y^2 + Q_z^2}$	$\sqrt{M_y^2 + M_z^2}$
	M_y	$\lvert M_z \rvert$	$\lvert N_{xx} \rvert$
	M_z	$\lvert M_y \rvert$	$\lvert N_{xx} \rvert$

6.3 Shell Elements

Shell elements are triangular or quadrilateral elements that are defined by three or four nodes on a curved surface. These elements are often used to model walls, pipes with large diameters, or other elements with small thickness subject to flexural strains. Shell elements take into account 2-dimensional stress conditions and flexural or shear strains.

Coordinate System

Oftentimes, shell elements are defined as curved surfaces and the element nodes may not all exist on the same plane. This is reflected in the definition of the ECS. The x-axis of the ECS is defined to be in the direction of the vector connecting node 1 to node 2. The z-axis is defined to be in the cross product of the vector connecting node 1 to node 2 and the vector connecting node 1 to node 3. In the case of a quadrilateral shell element, the ECS x-axis is defined as the vector bisecting the angle between the diagonal connecting nodes 1 to 3 and the diagonal connecting nodes 4 to 2. The cross product of these two diagonals is defined as the ECS z-axis. The finite element formulation for a shell element is based on the ECS.

Figure 3.6.10 Coordinate systems of a shell element

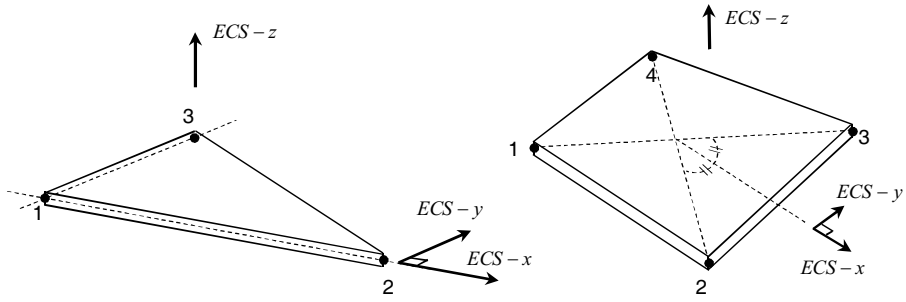

To define the material directionality (for constructing the MCS), the user may either specify an angle relative to the vector connecting nodes 1 and 2, or define an arbitrary coordinate system.

Curved surface modeling

The shell element in midas nGen assumes an inherent normal vector for each node, which is called the director. Strain is expressed as a function of this vector's motion. The direction of the rotational degree of freedom for each element node is also defined based on the director, and, thus, there is no moment about the director within the element. This vector may be normal to the element surface, but this is not the case for shell elements modeling a curved surface.

Figure 3.6.11 Angle between elements when modeling a curved surface

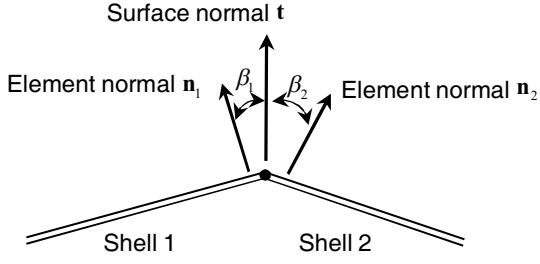

For example, consider Figure 3.6.11. There is a refraction angle between adjacent angles, and in such cases the surface normal vector may be calculated as follows:

$$\mathbf{t} = \frac{\sum \mathbf{n}_i}{\left\| \sum \mathbf{n}_i \right\|} \tag{3.6.14}$$

$\mathbf{t}$: Surface normal vector (normal to the curved surface)

$\mathbf{n}_i$: Vectors normal to the element surface

Here, if the angle β between $\mathbf{t}$ and $\mathbf{n}_i$ exceeds the allowable value, then the member is considered as an angled member and a surface normal vector is not defined. At nodes where a curved surface normal vector is not defined, the director becomes the vector normal to the element surface.

Expressing geometric characteristics by creating a surface normal vector can greatly improve accuracy of results, but it is important to be cautious of using this method when using symmetry conditions to model a half circle or quarter circle. Because the shell 2 in Figure 3.6.11 does not exist for models with symmetry conditions, it is impossible to attain a surface normal vector that is geometrically accurate. In such cases, it is in fact better to not create a surface normal vector.

Degrees of freedom

The ECS of a shell element has displacement degrees of freedom for x, y, and z axes.

$$\mathbf{u}_i = \{u_i \quad v_i \quad w_i\}^T \tag{3.6.15}$$

The rotational degrees of freedom are defined by the two directions orthogonal to the director:

$$\boldsymbol{\theta}_i = \{\theta_{\bar{x}i} \quad \theta_{\bar{y}i}\} \tag{3.6.16}$$

As previously explained, the director is a curved surface normal vector or the element normal vector.

Stress and strain

As shown in Figure 3.6.12, a shell element can experience 2-dimensional stress conditions, flexural strains, and shear strains defined based on the ECS. The shell element used in midas nGen always considers shear strains.

$$\mathbf{N} = \begin{Bmatrix} N_{xx} \\ N_{yy} \\ N_{xy} \end{Bmatrix}, \quad \boldsymbol{\varepsilon} = \begin{Bmatrix} \varepsilon_{xx} \\ \varepsilon_{yy} \\ \gamma_{xy} \end{Bmatrix} \tag{3.6.17}$$

(In-plane stress and strain)

$$\mathbf{M} = \begin{Bmatrix} M_{xx} \\ M_{yy} \\ M_{xy} \end{Bmatrix}, \ \boldsymbol{\kappa} = \begin{Bmatrix} \kappa_{xx} \\ \kappa_{yy} \\ \kappa_{xy} \end{Bmatrix} \tag{3.6.18}$$

(Flexural moment and curvature)

$$\mathbf{Q} = \begin{Bmatrix} Q_{zx} \\ Q_{yz} \end{Bmatrix}, \ \boldsymbol{\gamma} = \begin{Bmatrix} \gamma_{zx} \\ \gamma_{yz} \end{Bmatrix} \tag{3.6.19}$$

(Shear force and strain)

Figure 3.6.12 Stress and strain for a shell element

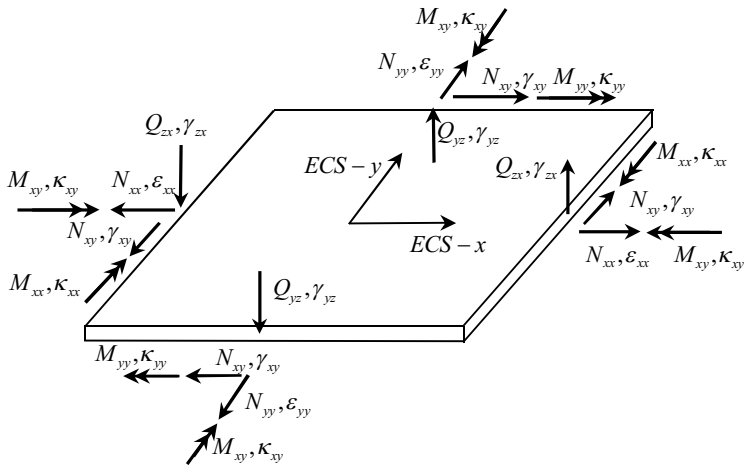

Loads

A shell element may be subject to the following loads.

Table 3.6.7 Loads that may be applied to a shell element

Load Type	Description
Self-weight due to gravity	Applied based on material density
Pressure load	Distributed loading that may be applied to the element surface or side
Element temperature load	Temperature load that may cause an axial deformation Temperature gradient that may trigger a rotational strain

Element Results

In midas nGen, shell element results are provided at two locations: the upper and lower surfaces in the direction of the element thickness. The following shows the element results for a shell element. The basis coordinate system is the element coordinate system (ECS).

Table 3.6.8 List of element results for a shell element

Result		Description
Stress	In-plane stress	Location: Upper/lower, vertex/element center σ_{xx} , σ_{yy} , τ_{xy}
	Principal stress	Location: Upper/lower, vertex/element center P_1 , P_2 , 주응력 방향
	Von-Mises stress	Location: Upper/lower, vertex/element center σ_v
	Max shear stress	Location: Upper/lower, vertex/element center $\tau_{\max}$
	Maximum values	Location: vertex/element center The maximum value between upper/lower surfaces, (P_1 , P_2 , σ_v , $\tau_{\max}$)
Force/ Moment	In-plane force	Location: vertex/element center N_{xx} , N_{yy} , N_{xy}
	Bending moment	Location: vertex/element center M_{xx} , M_{yy} , M_{xy}
	Shear force	Location: vertex/element center Q_{zx} , Q_{zy}
	Principal in-plane force	Location: vertex/element center N_1 , N_2
	Principal bending moment	Location: vertex/element center M_1 , M_2
	Max shear force	Location: vertex/element center $Q_{\max}$

Figure 3.6.13 Shell element result directions

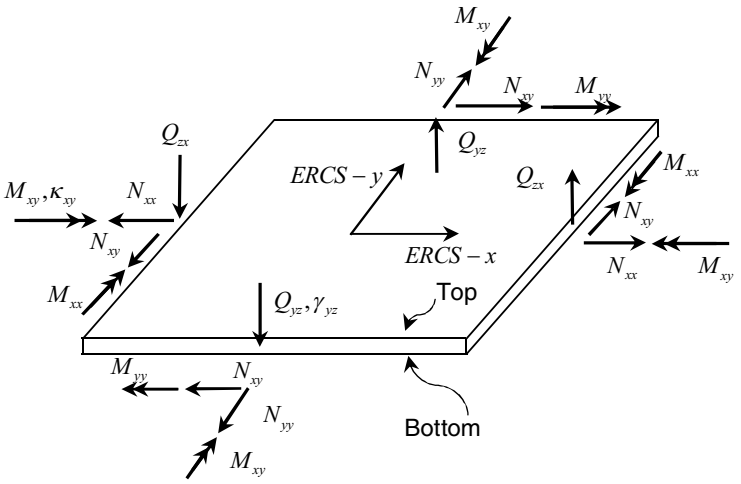

Offsets

When the shell element's neutral plane is separated from the element nodes, or when the neutral planes of connecting elements do not match, offsets may be used. Offsets within a shell element may take on constant values in the direction of the element director.

End releases

End releases are used in situations in which, for element nodes, mutual restraints do not occur in a specific direction of motion, such as in the case of pin connections. Unlike beam elements, the end releases for shell elements are applied based on the NCS. If the user wishes to input conditions based on the ECS, then the relationship between the NCS and ECS should be accounted for. Moreover, nodes at which end releases have been applied will attain new degrees of freedom for those unrestrained motions, and thus the entire structure that is connected to these nodes may become unstable. Therefore, a comprehensive consideration of the structure's stability—including the end releases—is necessary.

Selection of Elements

Midas nGen has a wide range of shell elements for the user to select from. In particular, depending on the direction in which strains may develop in a shell element (for example, depending on the in-plane and lateral directions), techniques and methods that can be used will vary widely. The following shows

the commonly used names in the midas nGen software and the related finite element technique and integration methods. The hybrid method is the default method.

Table 3.7.9 Various techniques that may be applied to a shell element

Shape	Number of nodes	Number of degrees of freedom per node	Name	Element Technique (In-plane/Lateral)	Stiffness matrix numerical integration	Lumped mass calculation method
Triangular	3	5	Full integration	Assumed displacement method/ANS	1 points	Lobatto
			Hybrid	Hybrid method/ANS+Hybrid method	3 points	Lobatto
Quadrilateral	4	5	Full integration	Assumed displacement method/ANS	2X2 points	Lobatto
			Reduced integration (stabilized)	Reduced integration /ANS (stabilized)	1x1 points	Lobatto
			Hybrid	Hybrid method/ANS+Hybrid method	2X2 points	Lobatto

Nonlinear Analysis

Shell elements cannot incorporate P-delta effects. In midas nGen, shell elements may only take on linear elastic material properties. In nonlinear analyses, the shell elements are still considered to behave linearly.

Section 7

Special Use Elements

7.1 Point Spring/Damper Element

Point spring/damper elements are used in a variety of situations. They may be used to incorporate elastic stiffnesses of adjacent structures or foundation/ground boundary conditions that lie at the boundary zones of a model. They may also be used to prevent singular errors that occur due to trusses that may lack sufficient degrees of freedom. Furthermore, they may be used to incorporate not only elastic stiffness but also damping constants into modeling ground viscosity boundary conditions. Nodal damping is not applied in static analyses and only applied in dynamic analyses.

Coordinate System

Point spring/damper elements do not define their own coordinate systems and refer to the GCS.

Degrees of Freedom

Point spring/damper elements have displacement and rotational degrees of freedom about all three axes.

$$\mathbf{u}_i = \{u_i \quad v_i \quad w_i\}^T, \ \boldsymbol{\theta}_i = \{\theta_{xi} \quad \theta_{yi} \quad \theta_{zi}\}^T \tag{3.7.1}$$

Element Force

Point spring/damper elements may experience force and moment in the three axial directions.

$$\mathbf{N} = \begin{Bmatrix} N_{xx} \\ N_{xx} \\ N_{zz} \end{Bmatrix}, \ \mathbf{M} = \begin{Bmatrix} M_{xx} \\ M_{yy} \\ M_{zz} \end{Bmatrix} \tag{3.7.2}$$

(Axial force and moment)

Loads

Point spring/damper elements do not take on material properties and are defined by their stiffnesses. Consequently, only concentrated loads or moments may be applied.

Element Results

In midas nGen, the point spring/damper element results are calculated and output based on the GCS.

Table 3.7.1 List of results for point spring/damper elements

Result		Description
Force	Force	Location: Element center N_{xx} , N_{yy} , N_{zz}
Moment	Bending moment	Location: Element center M_{xx} , M_{yy} , M_{zz}

7.2 Elastic Link Element

Elastic link elements connect two nodes with a user-defined stiffness and thus, like point spring elements, do not have any other structural properties other than stiffness. Typical elastic link elements have translational and rotational stiffness properties defined with respect to each of the three axes. In addition, tension-only and compression-only properties may be assigned, but in such a case, stiffnesses may only be set in the ECS-x direction. Elastic links can be applied to elastomeric bearings or ground boundary conditions that have compression-only characteristics.

Coordinate System/Degrees of Freedom

Elastic link element coordinate systems and degrees of freedom are defined in the same way as those of beam elements.

Element Force

Like point spring elements, elastic link elements may experience force and moment in all three axial directions.

Load

Like point spring elements, element link elements may not be subject to loads other than concentrated forces and moments.

Element Results

Element results for an elastic link element are the same as those of a point spring element, but the basis coordinate system is always the ECS.

7.3 Rigid Link/Interpolation Element

Rigid link and interpolation elements restrain relative movement between element nodes. Here, the principal agents of the restraint are called the independent node or independent DOF. The node or DOF that receives restraint is referred to as the dependent node or dependent DOF, respectively.

Rigid link elements restrain the relative geometric motion of various nodes caused by a single node. In other words, various dependent nodes are connected to an independent node. The relationship between independent and dependent nodes is as follows:

$$\begin{aligned}\mathbf{u}^D &= \mathbf{u}^I + \mathbf{r}\times\boldsymbol{\theta}^I = \mathbf{u}^I + (\Delta\mathbf{x})\times\boldsymbol{\theta}^I \\ \boldsymbol{\theta}^D &= \boldsymbol{\theta}^I\end{aligned} \tag{3.7.3}$$

$\mathbf{u}^D, \boldsymbol{\theta}^D$: Displacement and rotation of a dependent node

$\mathbf{u}^I, \boldsymbol{\theta}^I$: Displacement and rotation of an independent node

$\Delta\mathbf{x}$: Vector pointing from a dependent node to an independent node ($\mathbf{x}^I - \mathbf{x}^D$)

To define the degree of freedom which responds to the restraint on the independent node, the user may select from the six degrees of freedom belonging to the dependent node. With this, the user may define a rigid link element that is defined in a specific direction.

The following shows an example of inducing rigid body motion in the x-y plane.

$$u^D = u^I - \theta_z^I \Delta y\ ,\ v^D = v^I + \theta_z^I \Delta x\ ,\ \theta_z^D = \theta_z^I \tag{3.7.4}$$

Figure 3.7.1 Example of in-plane rigid body motion

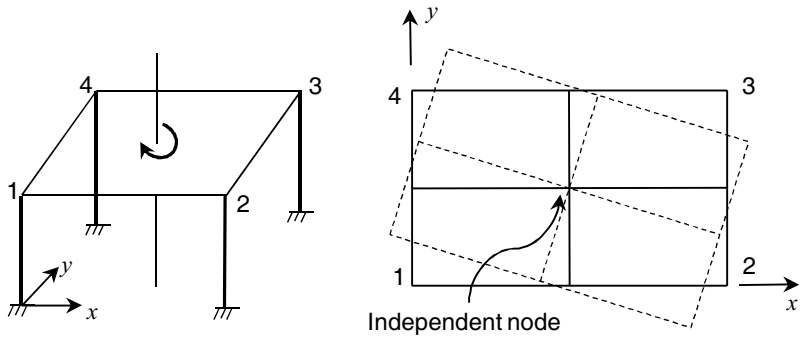

An interpolation element allows for the definition of a single node's motion based on the motion of other selected nodes. Thus, various independent nodes are connected to a single dependent node. Interpolation elements are used to distribute loads due to equipment across various nodes, and are used internally within the software. Consequently, interpolaton elements restrain fewer nodes compared to rigid link elements, and thus have a reduced restraining ability. The following example shows how force is distributed, in order to demonstrate the displacement relationship between the independent and dependent nodes, on a two-dimensional x-y plane.

Figure 3.7.2 Relationship between the center of mass of the independent node and the force exerted on the dependent node

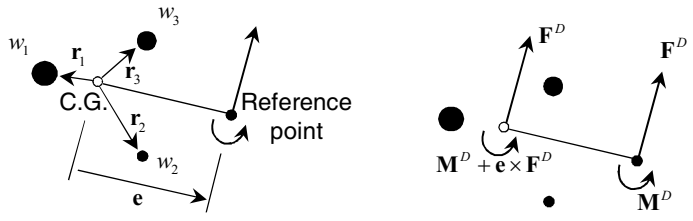

Figure 3.7.2 shows independent nodes that is subjected to distributed loading to weight w_i. The dependent node is located at a distance of e from the center of mass of these nodes. Then, the force F^D and moment M^D exerted on the dependent node may be expressed as a moment ($M^D + e \times F^D$) with respect to the center of mass. The force and moment exerted on the center of mass due to the dependent node may be dispersed to each independent node as a weighted average force, as shown below:

$$\mathbf{F}_i \overset{\text{def}}{=} \hat{w}_i \left(\mathbf{F}^D + \mathbf{T}^{-1} \left(\mathbf{M}^D + \mathbf{e} \times \mathbf{F}^D \right) \times \mathbf{r}_i \right) \tag{3.7.5}$$

Here, $\hat{w}_i$ is a weight normalized by the sum of the weights. $\mathbf{T}$ is an intertia tensor that represents the average based on the center of mass of the dependent nodes.

$$\hat{w}_i = \frac{w_i}{\sum w_i} \tag{3.7.6}$$

$$\mathbf{T} = \sum_i \hat{w}_i \left[\left(\mathbf{r}_i^{\mathrm{T}} \mathbf{r}_i \right) \mathbf{I} - \mathbf{r}_i \mathbf{r}_i^{\mathrm{T}} \right] \tag{3.7.7}$$

The force relationship may then be transformed into displacement and rotation relationships.

$$\mathbf{u}^D = \sum_i \hat{w}_i \mathbf{u}^I + \left(\mathbf{T}^{-1} \sum_i \hat{w}_i \left(\mathbf{r}_i \times \mathbf{u}^I \right) \right) \times \mathbf{e} \tag{3.7.8}$$

$$\theta^D = \mathbf{T}^{-1} \sum_i \hat{w}_i \left(\mathbf{r}_i \times \mathbf{u}^I \right) \tag{3.7.9}$$

Eventually, the relationship defines how the average motion of the independent nodes determines the motion of the dependent nodes. As a result of this characteristic, relative to the rigid link element, the interpolation element restrains fewer degrees of freedom.

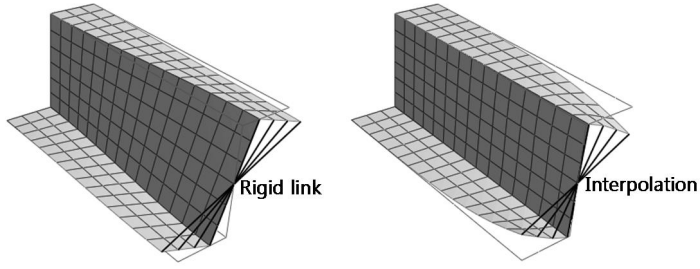

Figure 3.7.3 Comparison of the motion of rigid link elements and interpolation elements

Section 8

Geometric Stiffness

Geometric or stress stiffnesses are stiffnesses that occur due to a change in internal force caused by geometric changes in a structure with nonzero resistance to force. Geometric stiffnersses are used in linear buckling analyses and P-delta analyses. The following shows a list of elements that incorporate geometric stiffness.

Table 3.8.1 Element types that incorporate geometric stiffness

Element Type	Force component	Degree of Freedom component	
		P-delta Analysis	Linear Buckling Analysis
Truss	Axial force N_{xx}	Axial force N_{xx}	Axial force N_{xx}
Elastic Link	Axial force N_{xx}	Axial force N_{xx}	Axial force N_{xx}
Beam	Axial force N_{xx}	Axial force N_{xx}	Axial force N_{xx}
Shell	In-plane resultant force N_{xx}, N_{yy}, N_{xy} Flexural Moment M_{xx}, M_{yy}, M_{xy} Shear force Q_{zx}, Q_{yz}	-	Axial force N_{xx}
Solid	Stress Components σ_{xx}, σ_{yy}, σ_{zz}, τ_{xy}, τ_{yz}, τ_{zx}	-	u, v, w

8.1 Calculation of geometric stiffness

Midas nGen calculates geometric stiffness using the updated Lagrangian formulation, which assumes the objective stress rate to be the Jaumann stress rate. For example, the internal force of a solid element may be calculated as a function of stress and assumed strain, as shown below:

$$\delta u_i f_i = \int \sigma_{ij} \delta D_{ij} dV \tag{3.8.1}$$

δD_{ij} : assumed strain $\frac{1}{2}(\frac{\partial \delta u_i}{\partial x_j}+\frac{\partial \delta u_j}{\partial x_i})$

The tangent slope of the internal force is a stiffness, and if we take the variation of the previous equation, the integrand becomes:

$$d\sigma_{ij}\delta D_{ij}+\sigma_{ij}d\delta D_{ij} \tag{3.8.2}$$

In the above equation, variation was neglected for the region of integration. A solid element's EFCS is the GCS, so it is fixed regardless of strain in the structure. Thus, $d\delta D_{ij}=0$. The stress increment due to the objective stress rate in the first equation is as follows:

$$d\sigma_{ij}=dw_{ik}\sigma_{kj}+\sigma_{ij}dw_{jk}+C_{ijkl}dD_{kl} \tag{3.8.3}$$

δw_{ij} : Incremental spin $\frac{1}{2}(\frac{\partial \delta u_i}{\partial x_j}-\frac{\partial \delta u_j}{\partial x_i})$

If equations 3.8.2 and 3.8.3 are substituted into equation 3.8.1 and then rearranged, the tangent stiffness may be obtained as follows:

$$\delta u_i K_{ij} du_j=\int \delta D_{ij}C_{ijkl}dD_{kl}+\sigma_{ij}(\delta L_{ki}dL_{kj}-2\delta D_{ik}dD_{kj})dV \tag{3.8.4}$$

δL_{ij} : Incremental displacement gradient, $\delta D_{ij}+\delta w_{ij}$

In the integrand, the first term is the material stiffness and the second term is the geometric stiffness.

Section 9

Element Examples

1) Twisted Beam

REFERENCE	MacNeal et al.[1]
ELEMENTS	Shell elements, solid elements
MODEL FILENAME	Element01.mpb

The figure below shows a beam model whose cross-section is rotated by 90 degrees at the free end. The left end is restrained as a fixed end. The problem is to verify the performance of the element using the displacement at point A, caused by the element's in-plane and out-of-plane motions due to the uniform distributed loads at the right end.

Figure 9.1.1
Twisted beam model

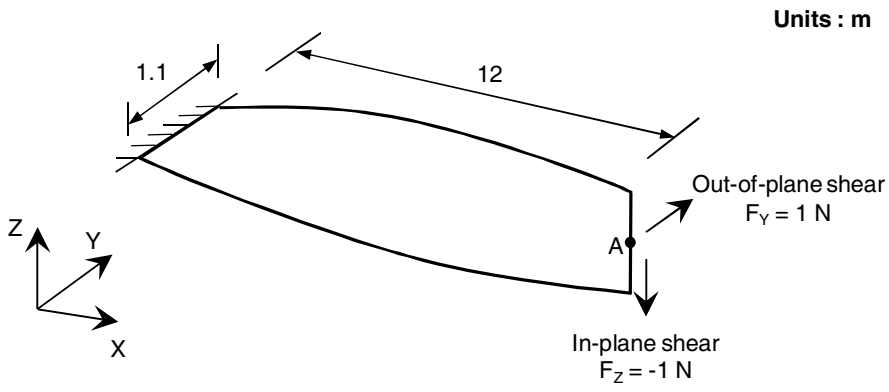

Material data	Elastic modulus	*E = 29 MPa*
	Poisson's ratio	*ν = 0.22*
Section property	Thickness	*t = 0.32 m*

Table 9.1.1 Displacements u_Y and u_Z at the point A - shell elements

Load		u_Z^A [m] in-plane shear F_Z	u_Y^A [m] out-of-plane shear F_Y
Reference		*5.424×10^{-3}*	*1.754×10^{-3}*
Element type	Number of elements		
TRIA-3	2×(12×2)	*5.322×10^{-3}*	*1.463×10^{-3}*
QUAD-4	2×12	*5.405×10^{-3}*	*1.733×10^{-3}*

Table 9.1.2 Displacements u_Y and u_Z at the point A - solid elements

Load		u_Z^A [m] in-plane shear F_Z	u_Y^A [m] out-of-plane shear F_Y
Reference		5.424×10^{-3}	*1.754×10^{-3}*
Element type	Number of elements		
TETRA-4	144	*0.384×10^{-3}*	*0.267×10^{-3}*
PENTA-6	48×1	*2.344×10^{-3}*	*0.743×10^{-3}*
HEXA-8	2×12×1	*5.411×10^{-3}*	*1.738×10^{-3}*

2) Curved Cantilever Beam

REFERENCE	MacNeal et al.[1]
ELEMENTS	Beam elements, shell elements, solid elements
MODEL FILENAME	Element02.mpb

The figure below shows a curved cantilever beam with a fixed right end. In-plane and out-of-plane shear distributed loads are applied to the left end. The problem is to verify the element performance (specifically in-plane and out-of-plane motion) through the displacement at point A.

Figure 9.2.1
Curved cantilevered beam model

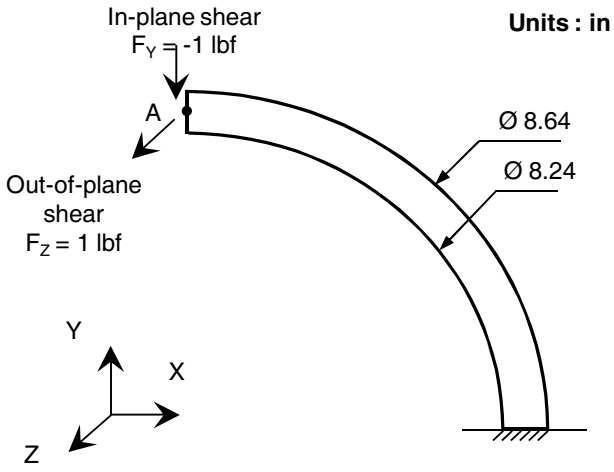

Material data	Elastic modulus	*E = 10 Mpsi*
	Poisson's ratio	$\nu = 0.25$
Section property	Thickness	*t = 0.1 in*

Table 9.2.1 Displacements u_Y and u_Z at the point A - beam elements

Load		u_Y^A [*in*] in-plane shear F_Y	u_Z^A [*in*] out-of-plane shear F_Z
Reference		*-8.734×10^{-2}*	*5.022×10^{-1}*
Element type	Number of elements		
BEAM-2	6	*-8.735x10^{-2}*	*4.968x10^{-1}*

Table 9.2.2 Displacements u_Y and u_Z at the point A - shell elements

Load		u_Y^A [*in*] in-plane shear F_Y	u_Z^A [*in*] out-of-plane shear F_Z
Reference		*-8.734×10^{-2}*	*5.022×10^{-1}*
Element type	Number of elements		
TRIA-3	1x(6x2)	*-0.222x10^{-2}*	*4.347x10^{-1}*
QUAD-4	1x6	*-8.543x10^{-2}*	*4.739x10^{-1}*

Table 9.2.3 Displacements u_Y and u_Z at the point A - solid elements

Load		u_Y^A [*in*] in-plane shear F_Y	u_Z^A [*in*] out-of-plane shear F_Z
Reference		*-8.734×10^{-2}*	*5.022×10^{-1}*
Element type	Number of elements		
TETRA-4	76	*-0.236x10^{-2}*	*0.043x10^{-1}*
PENTA-6	1 x (6 x 2) x 1	*-0.221x10^{-2}*	*0.347x10^{-1}*
HEXA-8	1 x 6 x 1	*-8.534x10^{-2}*	*4.415x10^{-1}*

3) Cantilever Beam

REFERENCE	MacNeal et al.[1]
ELEMENTS	Shell elements, solid elements
MODEL FILENAME	Element03.mpb

The figure below shows a linear cantilever beam whose left end is fixed. The problem is to verify how the element results change as a function of the mesh, when there is a concentrated load and torque load in three different directions at node A. Element performance may be verified by checking the displacement components at point A. Here, the angle of rotation refers to the calculated relative angle of rotation due to the displacements of points B and C.

Figure 9.3.1
Cantilever beam model

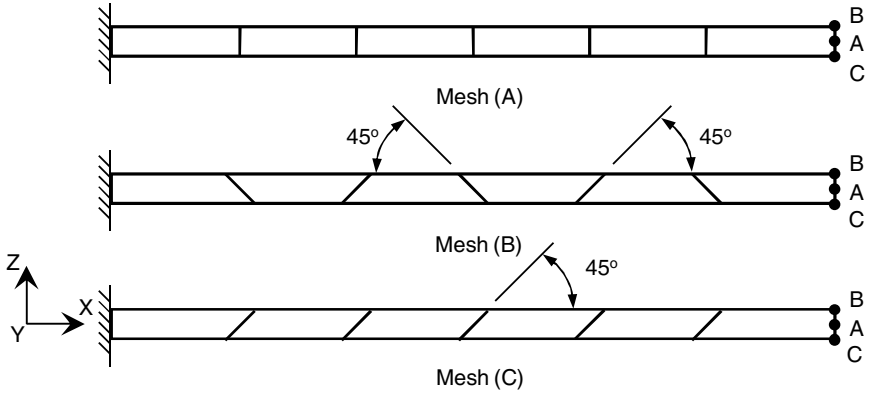

Material data	Elastic modulus	*E = 10 Mpsi*
	Poisson's ratio	$\nu = 0.3$
Section property	Thickness	*t = 0.1 in*

Table 9.3.1 Displacements and rotation at the point A - shell elements, mesh (A)

Load		u_X^A [*in*] extension F_X	u_Y^A [*in*] out-of-plane F_Y	u_Z^A [*in*] in-plane F_Z	θ_X^A [*rad*] twist M_X
Reference		3.000×10^{-5}	4.321×10^{-1}	1.081×10^{-1}	3.408×10^{-2}
Element type	Number of elements				
TRIA-3	2×(12×2)	3.000×10^{-5}	4.199×10^{-1}	0.034×10^{-1}	2.979×10^{-2}
QUAD-4	2×12	3.000×10^{-5}	4.238×10^{-1}	1.073×10^{-1}	3.019×10^{-2}

Table 9.3.2 Displacements and rotation at the point A - shell elements, mesh (B)

Load		u_X^A [*in*] extension F_X	u_Y^A [*in*] out-of-plane F_Y	u_Z^A [*in*] in-plane F_Z	θ_X^A [*rad*] twist M_X
Reference		3.000×10^{-5}	4.321×10^{-1}	1.081×10^{-1}	3.408×10^{-2}
Element type	Number of elements				
TRIA-3	2×(12×2)	3.000×10^{-5}	4.177×10^{-1}	0.016×10^{-1}	3.137×10^{-2}
QUAD-4	2×12	3.000×10^{-5}	4.171×10^{-1}	0.240×10^{-1}	3.020×10^{-2}

Table 9.3.3 Displacements and rotation at the point A - shell elements, mesh (C)

Load		u_X^A [*in*] extension F_X	u_Y^A [*in*] out-of-plane F_Y	u_Z^A [*in*] in-plane F_Z	θ_X^A [*rad*] twist M_X
Reference		3.000×10^{-5}	4.321×10^{-1}	1.081×10^{-1}	3.408×10^{-2}
Element type	Number of elements				
TRIA-3	2×(12×2)	3.000×10^{-5}	4.201×10^{-1}	0.024×10^{-1}	3.508×10^{-2}
QUAD-4	2×12	3.000×10^{-5}	4.238×10^{-1}	0.086×10^{-1}	3.022×10^{-2}

Table 9.3.4 Displacements and rotation at the point A - solid elements, mesh (A)

Load		u_X^A [*in*] extension F_X	u_Y^A [*in*] out-of-plane F_Y	u_Z^A [*in*] in-plane F_Z	θ_X^A [*rad*] twist M_X
Reference		3.000×10^{-5}	4.321×10^{-1}	1.081×10^{-1}	3.408×10^{-2}
Element type	Number of elements				
TETRA-4	222	3.000×10^{-5}	$0.031x10^{-1}$	$0.023x10^{-1}$	$0.029x10^{-2}$
PENTA-6	1x(6x2)x1	3.000×10^{-5}	$0.509x10^{-1}$	$0.034x10^{-1}$	$0.077x10^{-2}$
HEXA-8	1x6x1	3.000×10^{-5}	$4.249x10^{-1}$	$1.072x10^{-1}$	$2.931x10^{-2}$

4) Pinched Hemispherical Shell with Hole

REFERENCE	MacNeal et al.[1], Simo et al.[2]
ELEMENTS	Shell elements, solid elements
MODEL FILENAME	Linearstatic04.mpb

The figure below shows a pinched hemispherical shell with a 18˚ hole at the top. Using symmetry conditions, only ¼ of the hemisphere was modeled. Concentrated loads are applied at at point A (pointing outwards) and at point B (pointing inwards). The problem is to verify the element model using the displacement at point A.

Figure 9.4.1
Pinched hemispherical shell with hole

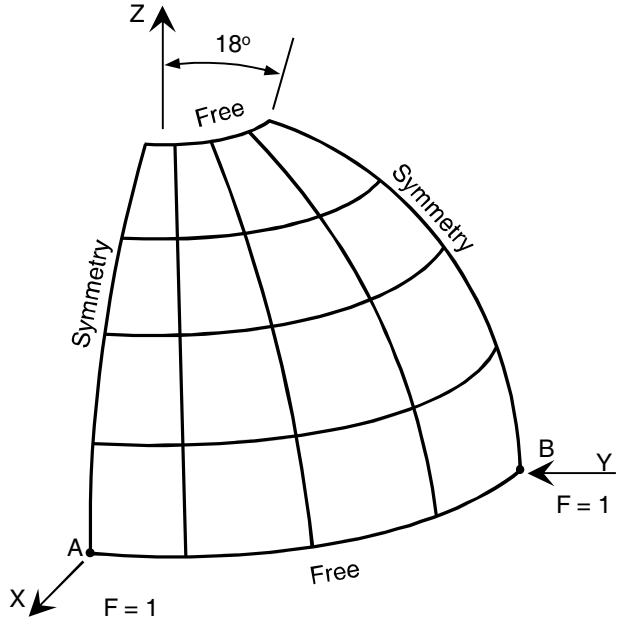

Material data	Elastic modulus	$E = 6.825x10^7$ *psi*
	Poisson's ratio	$\nu = 0.3$
Section property	Thickness	$t = 0.04$ *in*

Table 2.4.1 Displacement u_X at the point A - shell elements

		u_X^A [in]		
Reference		*9.4x10^{-2} (Ref. 1), 9.3x10^{-2}(Ref. 2)*		
Number of elements per side		*4*	*8*	*12*
Element type	TRIA-3	*9.799x10^{-2}*	*9.439 x10^{-2}*	*9.343 x10^{-2}*
	QUAD-4	*9.701x10^{-2}*	*9.445 x10^{-2}*	*9.373 x10^{-2}*

Table 2.4.2 Displacement u_X at the point A - solid elements

		u_X^A [in]		
Reference		*9.4x10^{-2} (Ref. 1), 9.3x10^{-2}(Ref. 2)*		
Number of elements per side		*4*	*8*	*12*
Element type	PENTA-6	*0.004 x10^{-2}*	*0.015 x10^{-2}*	*0.033 x10^{-2}*
	HEXA-8	*1.016 x10^{-2}*	*7.404 x10^{-2}*	*8.872 x10^{-2}*

5) In-plane Truss

REFERENCE	McCormac[3]
ELEMENTS	Truss elements
MODEL FILENAME	Element05.mpb

The figure below shows a 2-dimensional in-plane truss made of elements with various cross-sectional profiles. Vertical loads are applied to points A, B, and C. The problem is to verify the vertical displacement at point A under these loading conditions.

Figure 9.5.1
Truss model

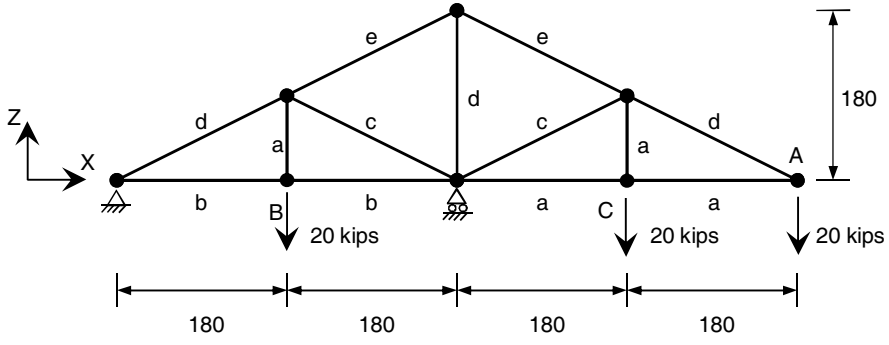

Units : in

Material data	Elastic modulus	$E = 3.0x10^4$ *psi*
Section property	Area	$A = 1.0\ in^2$ (element-a) $A = 2.0\ in^2$ (element-b) $A = 1.5\ in^2$ (element-c) $A = 3.0\ in^2$ (element-d) $A = 4.0\ in^2$ (element-e)

Table 9.5.1 Displacement u_Z at the point A

		u_Z^A [*in*]
Reference		*-2.63*
TRUSS-2	13-elements	*-2.63*

6) Diamond-Shaped Plate

REFERENCE	NAFEMS[4]
KEYWORDS	Shell elements, solid elements
MODEL FILENAME	Element06.mpb

The figure below shows a diamond-shaped plate model with obtuse angles of 150 degrees. It is subject to a uniform load of 700 Pa. Element performance is verified using the principal stress of the center of the plate (point E) on the bottom plane.

Figure 9.6.1
Skewed plate model

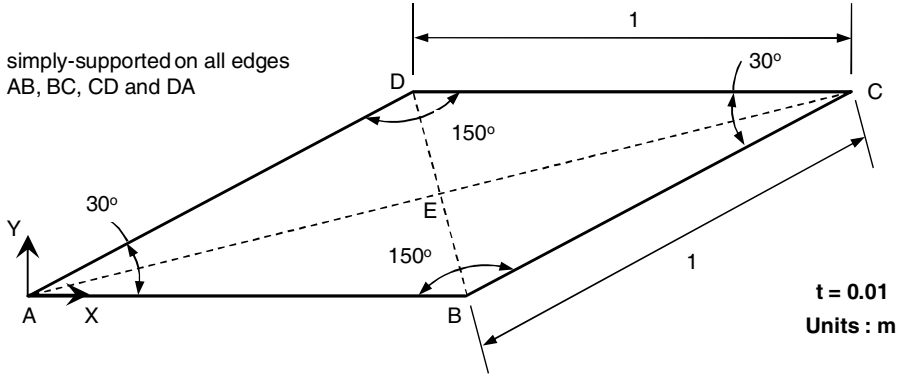

Material data	Elastic modulus	*E = 210 GPa*
	Poisson's ratio	$\nu = 0.3$
Section property	Thickness	*t = 0.01 m*

Table 9.6.1 Maximum principal stress at bottom surface σ_{P1} - shell elements

		σ_{P1}^{E} [*MPa*]		
Reference		*0.802*		
Number of elements per side		2	4	8
Element type	TRIA-3	*0.804*	*0.783*	*0.804*
	QUAD-4	*0.666*	*0.799*	*0.799*

Table 9.6.2 Maximum principal stress at bottom surface σ_{P1} - solid elements

		σ_{P1}^{E} [*MPa*]		
Reference		*0.802*		
Number of elements per side		2	4	8
Element type	PENTA-6	*0.329*	*0.087*	*0.251*
	HEXA-8	*0.336*	*0.675*	*0.736*

7) Thick Plate

REFERENCE	NAFEMS[4]
ELEMENTS	Solid elements
MODEL FILENAME	Element07.mpb

The figure below shows a thick plate with an elliptical inner length and a circular outer length. The outer length is fixed in the direction of the plate thickness. The plate experiences a uniform pressure of 1MPa on its top surface, and using symmetry conditions, only a quarter of the plate was modeled. Element performance may be verified based on the the y-axis vertical stress (σ_{YY}^{D}) at node D.

Figure 9.7.1
Thick plate model

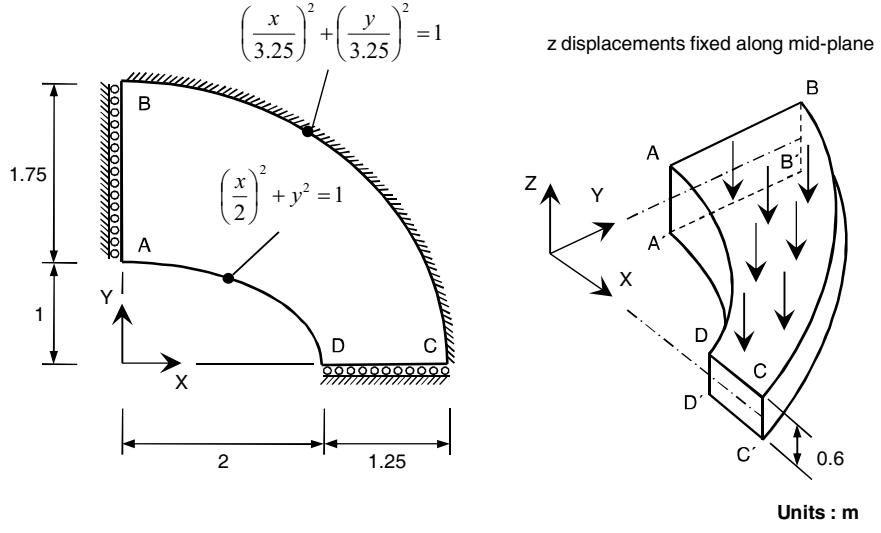

Material data	Elastic modulus	*E = 210 GPa*
	Poisson's ratio	ν *= 0.3*
Section property	Thickness	*t = 0.6 m*

Table 9.7.1 Stress σ_{YY} at the point D

		σ_{YY}^{D} [*MPa*]	
Reference		*5.38*	
Number of elements per side		3x2	6x4
Element type	PENTA-6	*4.878*	*5.751*
	HEXA-8	*5.321*	*5.577*

8) Cantilever with Variable Thickness

REFERENCE	Young et al[5]
ELEMENTS	Beam elements, solid elements
MODEL FILENAME	Element08.mpb

The figure below shows a cantilever beam whose cross section changes linearly along its length. Tension, lateral displacement, and concentrated moment are applied to its right end. Element performance may be verified using the vertical displacement.

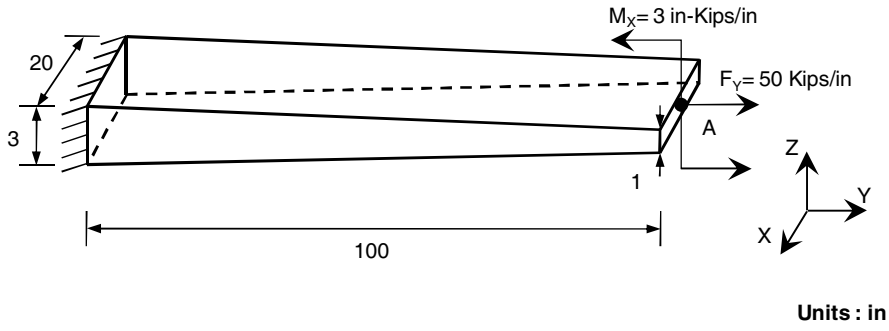

Figure 9.8.1
Cantilever model with variable thickness

Units : in

Material data	Elastic modulus	$E = 1.0x10^3$ *ksi*
	Poisson's ratio	$\nu = 0.3$

Table 9.8.1 Displacement u_Z subjected to end moment, and u_Y subjected to end tension at the point A - beam elements

Load		u_Z^A [*in*] End moment	u_Y^A [*in*] End tension
Reference		*20.0*	*2.7465*
Element type	Number of elements		
BEAM-2	1	*20*	*2.7465*

Table 9.8.2 Displacement u_Z subjected to end moment, and u_Y subjected to end tension at the point A - solid elements

Load		u_Z^A [*in*] End moment	u_Y^A [*in*] End tension
Reference		*20.0*	*2.7465*
Element type	Number of elements		
TETRA-4	60	*0.27*	*2.6930*
PYRAM-5	30	*0.50*	*2.6931*
PENTA-6	(5x3)x1	*6.09*	*2.7031*
HEXA-8	5x1	*19.95*	*2.7026*

9) Cylindrical roof

REFERENCE	MacNeal[1], Simo et al.[2]
ELEMENTS	Shell elements, solid elements
MODEL FILENAME	Element09.mpb

The figure below shows a single-span cylindrical roof (Scordelis-Lo roof). Using symmetry conditions, only ¼ of the roof is modeled. Self-weight of 360 lbf/ft^3 is applied. The problem is to verify element performance by solving for the vertical displacement of point A (the midpoint in the direction of element thickness, at the center of the free end).

Figure 9.9.1
Scordelis-Lo barrel vault model

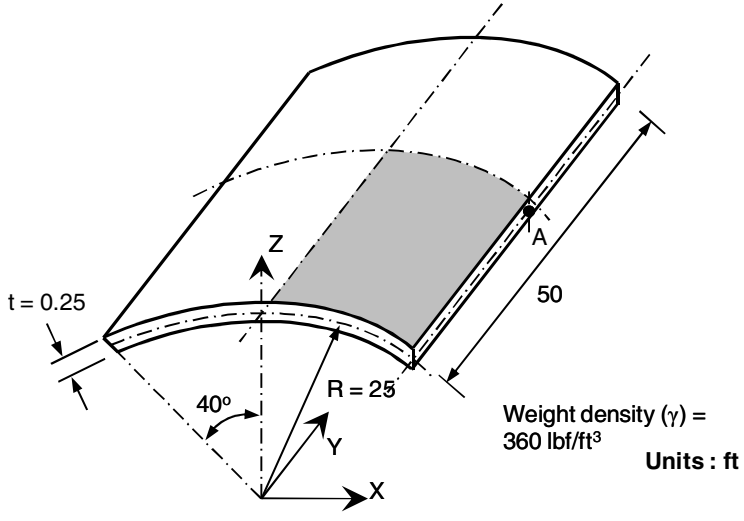

Material data	Elastic modulus	$E = 4.32x10^8$ lbf/ft^2
	Poisson's ratio	$\nu = 0$

Table 9.9.1 Vertical displacement u_Z at the point A - shell elements

		u_Z^A [*ft*]		
Reference		*-0.3024*		
Number of elements per side		*4*	*6*	*8*
Element type	TRIA-3	*-0.2019*	*-0.2381*	*-0.2603*
	QUAD-4	*-03195*	*-0.3080*	*-0.3058*

Table 9.9.2 Vertical displacement u_Z at the point A - solid elements

		u_Z^A [*ft*]		
Reference		*-0.3024*		
Number of elements per side		*4*	*6*	*8*
Element type	PENTA-6	*-0.0163*	*-0.0228*	*-0.1326*
	HEXA-8	*-0.3118*	*-0.3061*	*-0.3046*

10) Z-Section Cantilever

REFERENCE	NAFEMS[4]
ELEMENTS	Shell elements
MODEL FILENAME	Element10.mpb

The figure below shows a z-section cantilever model. The left end is fixed, and and the flange of the right end is subject to a uniform vertical load in its shear direction (S = 0.6 MN). There is a total torque of 1.2 MN-m exerted. Element performance may be verified using the axial stress (σ_{XX}) at point A.

Figure 9.10.1
Z-section cantilever model

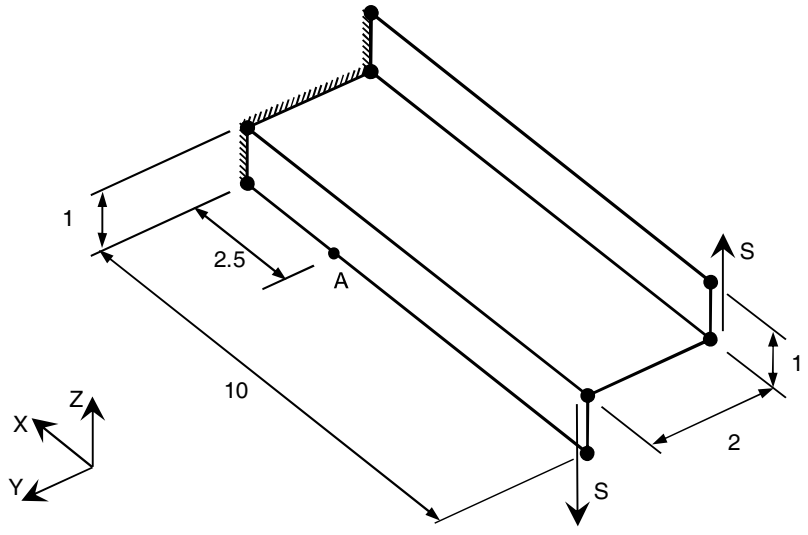

Units : m

Material data	Elastic modulus	*E = 210 GPa*
	Poisson's ratio	*ν = 0.3*
Section property	Thickness	*t = 0.1 m*

Table 9.10.1 Stress σ_{XX} at the point A

		σ_{XX}^{A} [*MPa*]
Reference		*-108*
Element type	Number of elements	
TRIA-3	48	*-30.789*
QUAD-4	24	*-110.231*

11) Hemisphere under point loads

REFERENCE	NAFEM[4]
ELEMENTS	Shell elements, solid elements
MODEL FILENAME	Element11.mpb

The figure below shows how symmetry conditions may be used to model a quarter of a hemisphere. There are concentrated loads at points A and B. Element performance may be verified by verifying the radial component of displacement at point A.

Figure 9.11.1
Hemisphere quadrant model

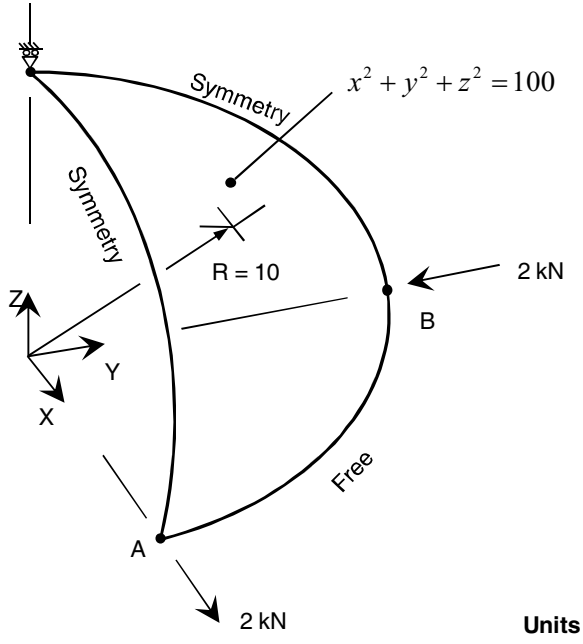

Material data	Elastic modulus	*E = 68.25 Gpa*
	Poisson's ratio	$\nu = 0.3$
Section property	Thickness	*t = 0.04 m*

Table 9.11.1 Displacement u_X at the point A obtained using shell elements

		u_X^A [m]	
Reference		1.850×10^{-1}	
Number of elements per side		4	8
Element type	TRIA-3	1.844×10^{-1}	1.851×10^{-1}
	QUAD-4	1.048×10^{-1}	1.809×10^{-1}

Table 9.11.2 Displacement u_X at the point A obtained using solid elements

		u_X^A [m]	
Reference		1.850×10^{-1}	
Number of elements per side		4	8
Element type	PENTA-6	9.422×10^{-5}	3.533×10^{-4}
	HEXA-8	9.995×10^{-3}	1.192×10^{-1}

12) Square Plate

REFERENCE	Zienkiewicz et al[6]
ELEMENTS	Shell elements, solid elements
MODEL FILENAME	Element12_thick.mpb, Element12_thin.mpb

The figure below shows a square plate whose four sides have been fixed. There is a uniform pressure of 1Pa being exerted on the plate. Element performance may be verified using the displacement at point A (element center). Results should be checked with two different thicknesses: 0.001m and 0.1m. Using symmetry conditions, only a quarter of the entire structure was modeled.

Figure 9.12.1
Hemisphere quadrant model

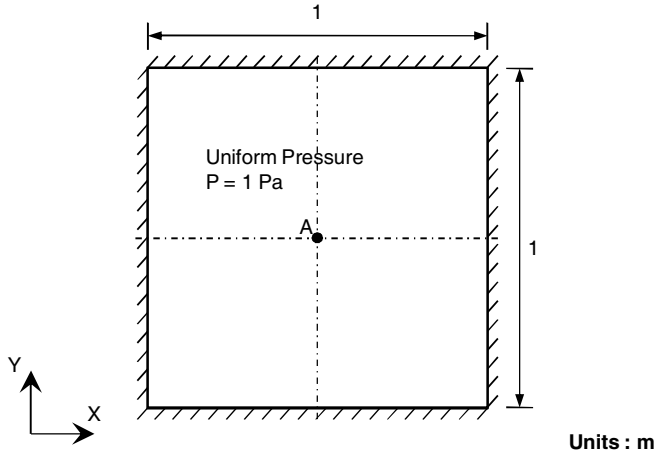

Material data	Elastic modulus	*E = 29.0 kPa (Model A)* *E = 29.0 GPa (Model B)*
	Poisson's ratio	$\nu = 0.3$
Section property	Thickness	*t = 0.1 m (Model A)* *t = 0.001 m (Model B)*

Table 9.12.1 Displacement u_Z obtained at the point A -shell elements, t=0.1m

		u_Z^A [m]		
Reference		$5.645x10^{-4}$		
Number of elements		2x2	4x4	8x8
Element type	TRIA-3	$5.548x10^{-4}$	$5.675x10^{-4}$	$5.670x10^{-4}$
	QUAD-4	$6.145x10^{-4}$	$5.815x10^{-4}$	$5.704x10^{-4}$

Table 9.12.2 Displacement u_Z obtained at the point A - solid elements, t=0.1m

		u_Z^A [m]		
Reference		$5.645x10^{-4}$		
Number of elements		2x2x1	4x4x1	8x8x1
Element type	PENTA-6	$2.752x10^{-4}$	$4.358x10^{-4}$	$5.169x10^{-4}$
	HEXA-8	$5.355x10^{-4}$	$5.488x10^{-4}$	$5.516x10^{-4}$

Table 9.12.3 Displacement u_Z obtained at the point A - shell elements, t=0.001m

		u_Z^A [m]		
Reference		$4.763x10^{-4}$		
Number of elements		2x2	4x4	8x8
Element type	TRIA-3	$4.533x10^{-4}$	$4.725x10^{-4}$	$4.759x10^{-4}$
	QUAD-4	$4.562x10^{-4}$	$4.714x10^{-4}$	$4.765x10^{-4}$

Table 9.12.4 Displacement u_Z obtained at the point A - solid elements, t=0.001m

		u_Z^A [m]		
Reference		4.763×10^{-4}		
Finite element mesh		2x2x1	4x4x1	8x8x1
Element type	PENTA-6	0.005×10^{-5}	0.021×10^{-5}	0.080×10^{-5}
	HEXA-8	4.667×10^{-4}	4.735×10^{-4}	4.757×10^{-4}

13) Cylindrical shell patch test

REFERENCE	NAFEMS[4]
ELEMENTS	Shell elements
MODEL FILENAME	Element13.mpb

The figure below shows a cylindrical plate model used for an element patch test. There is a distributed moment of 1kN-m/m exerted on length DC, and a distributed pressure of 0.6MPa being applied in the outwards direction across the entire surface. Element performance may be verified using the outward tangential stress at point E.

Figure 9.13.1
Cylindrical shell patch test

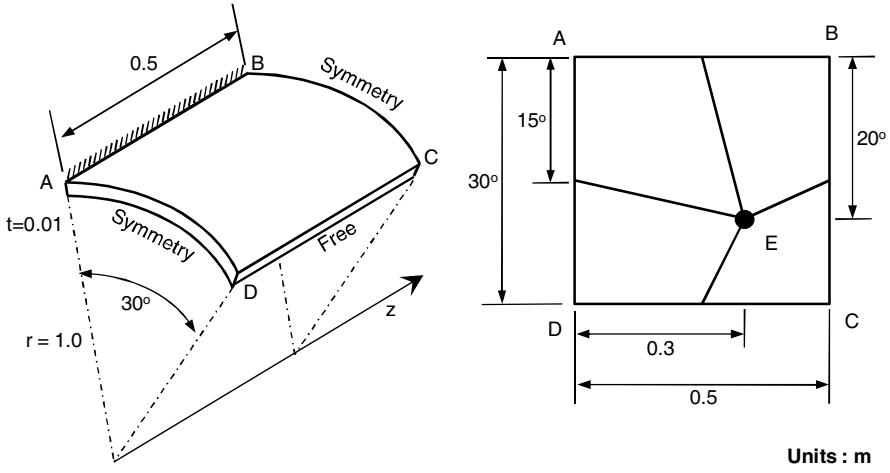

Material data	Elastic modulus	*E = 210 Gpa*
	Poisson's ratio	$\nu = 0.3$
Section property	Thickness	*t = 0.01 m*

Table 9.13.1 Tangential stress $\sigma_{\theta\theta}$ at the point E for load cases 1 and 2

		$\sigma_{\theta\theta}^{E}$ [*MPa*]	
Reference		*60*	
Load Case		Edge moment (Case 1)	Outward pressure (Case 2)
Element type	Number of elements		
TRIA-3	(4x2)	*43.903*	*41.083*
QUAD-4	4	*52.908*	*68.487*

14) Statically Indeterminate Column

REFERENCE	Timoshenko[1]
ELEMENTS	Beam elements, truss elements
MODEL FILENAME	Element14.mpb

The figure below shows a statically indeterminate column with both ends fixed. The two internal nodes are subject to vertical loads. Element performance may be verified through the reaction forces caused by the vertical loading. Both beam and truss elements were used in the model.

Figure 9.14.1
Column model with fixed ends

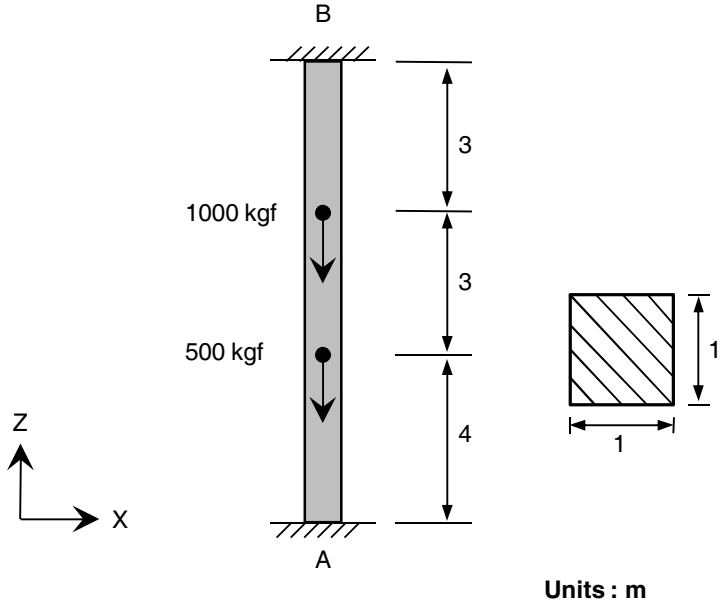

Material data	Elastic modulus	$E = 3.0x10^7\ kgf/m^2$
	Poisson's ratio	$\nu = 0.0$
Section property	Area	$A = 1.0\ m^2$

Table 9.14.1 Reaction forces F_Z at the at the supports

Reaction		F_Z^A [*kgf*]	F_Z^B [*kgf*]
Reference		*600*	*900*
Element type	Number of elements		
TRUSS-2	3	*600.000*	*900.000*
BEAM-2	3	*600.000*	*900.000*

15) 2-span Continuous Beam

REFERENCE	Lausen et al.[8]
ELEMENTS	Beam elements
MODEL FILENAME	Element15.mpb

The figure below shows a two-span continuous beam fixed on both ends and hinged between the two ends. The left beam is subject to a distributed load, and the right beam is subject to a concentrated load at its center. Element performance may be verified using the moments at the supports.

Figure 9.15.1
Continuous beam

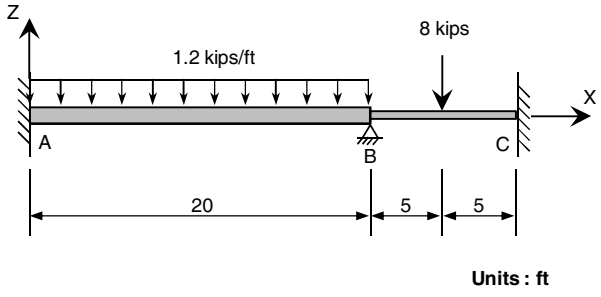

Material data	Elastic modullus	$E = 4.32x10^6$ *kips/ft*^{2}
	Poisson's ratio	$\nu = 0.0$
Section property	Moment of inertia	*AB* : $I_x = 0.0201$ *ft*^{4} *BC* : $I_x = 0.0067$ *ft*^{4}

Table 9.15.1 Bending moment M_Y at the supports

Bending moment		M_Y^A [*kips-ft*]	M_Y^A [*kips-ft*]	M_Y^A [*kips-ft*]
Reference		*-49.0*	*-22.0*	*-4.00*
Element type	Number of elements			
BEAM-2	2	*-49.0*	*-22.0*	*-4.00*

16) Overhanging Beam

REFERENCE	Timoshenko[7]
ELEMENTS	Beam elements
MODEL FILENAME	Element16.mpb

The figure below shows a beam with overhanging ends and bilateral symmetry. Using the bilateral symmetry, the model can only include the beam from its center to the right end. There is a distributed load acting on both overhanging ends. Element performance may be verified through the displacement caused by the distributed load.

Figure 9.16.1
Overhanging beam model

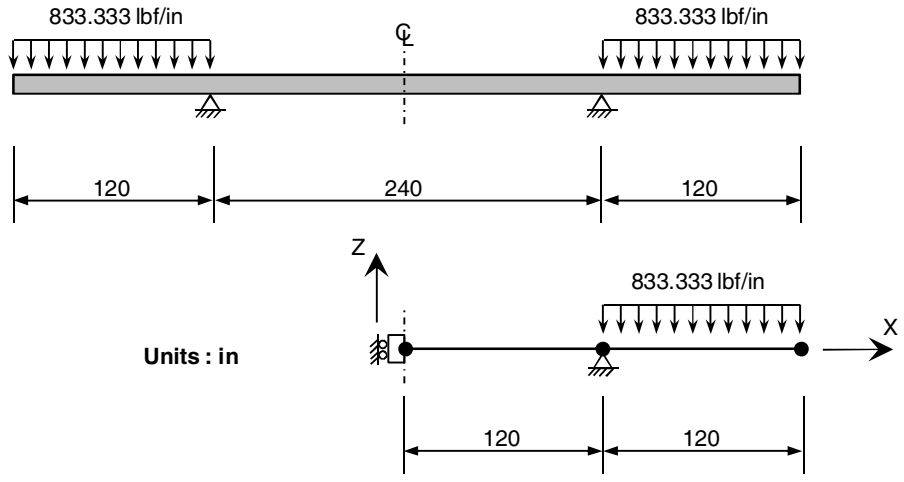

Material data	Elastic modullus	$E = 3.0x10^7$ *psi*
	Poisson's ratio	$\nu = 0.0$
Section property	Moment of inertia	$I_x = 7892.0$ *in*^{4}

Table 9.16.1 Displaccement u_z at the at center

		u_z [*in*]
Reference		*0.182*
Element type	Number of elements	
BEAM-2	2	*0.182*

17) 2-span Frame

REFERENCE	AISC[9]
ELEMENTS	Beam elements
MODEL FILENAME	Element17.mpb

The figure below shows an in-plane 2-span frame in which the frame members are hinge-connected. There are two loading cases on the beam, as shown below. Model performance may be verified using the left beam (beam A)'s shear force and moment.

Figure 9.17.1
Plane frame model

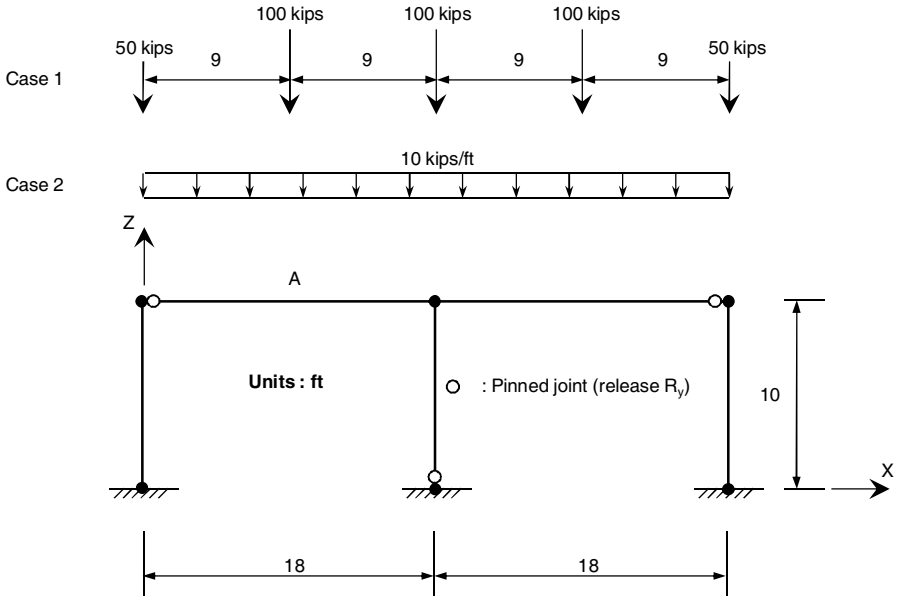

Material data	Elastic modulus	$E = 3.0x10^3$ kips/in^2
	Poisson's ratio	$\nu = 0.0$
Section property	Area	$A = 1.0\ x10^7$ in^2
	Moment of inertial (Columns)	$I_x = 1.3824\ x10^4$ in^4
	Moment of inertial (Beams)	$I_x = 2.7000\ x10^4$ in^4

Table 9.17.1 Bending moment M_Y and Shear forces Q_Z of element A for Case 1

	Location	M_Y [*kip-in*]	Q_Z [*kip*]
Reference	*0.00L*	*0.00*	*-31.25*
	0.25L	*1687.50*	*-31.25*
	0.50L	*3375.00*	*68.75*
	0.75L	*-337.50*	*68.75*
	1.00L	*-4050.00*	*68.75*
Element type			
BEAM-2	*0.00L*	*0.00*	*-31.25*
	0.25L	*1687.50*	*-31.25*
	0.50L	*3375.00*	*68.75*
	0.75L	*-337.50*	*68.75*
	1.00L	*-4050.00*	*68.75*

Table 9.17.2 Bending moment M_Y and Shear forces Q_Z of element A for Case 2

	Location	M_Y [*kip-in*]	Q_Z [*kip*]
Reference	*0.00L*	*0.00*	*-67.50*
	0.25L	*2430.00*	*-22.50*
	0.50L	*2430.00*	*22.50*
	0.75L	*0.00*	*67.50*
	1.00L	*-4860.00*	*112.50*
Element type			
BEAM-2	*0.00L*	*0.00*	*-67.50*
	0.25L	*2430.00*	*-22.50*
	0.50L	*2430.00*	*22.50*
	0.75L	*0.00*	*67.50*
	1.00L	*-4860.00*	*112.50*

18) Elastic Supports

REFERENCE	Beaufait. W., et al.[10]
ELEMENTS	Beam elements
MODEL FILENAME	Element18.mpb

The figure below shows an in-plane frame model with elastic support conditions. There are concentrated loads exerted on both the column and beam. The column is connected to the beam with a pinned joint. Model performance may be verified with the displacement and rotation at each of the beam's nodes (A, B, and C).

Figure 9.18.1
Beam with elastic supports model

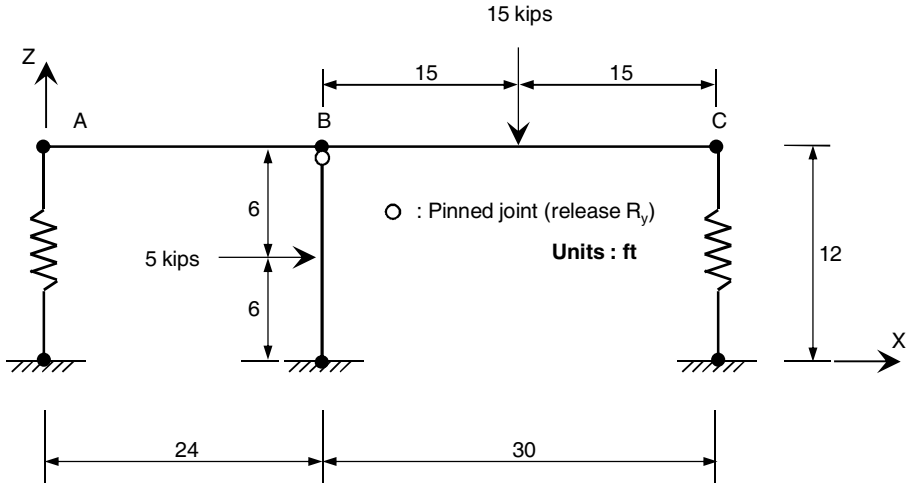

Material data	Elastic modullus	$E = 4.32x10^6$ *kips/ft*^{2}
	Poisson's ratio	$\nu = 0.0$
Section property	Area (Beam)	$A = 0.125$ *ft*^{2}
	Area (Column)	$A = 0.175$ *ft*^{2}
	Moment of inertia (Beam)	$I_x = 0.263$ *ft*^{4}
	Moment of inertia (Column)	$I_x = 0.193$ *ft*^{4}
	Spring constant	$K = 1200$ *kips/ft*

Table 9.18.1 Displacement u_X at the points (A, B, C)

Displacement	u_X^A [ft]	u_X^B [ft]	u_X^C [ft]
Reference	1.079 x10^{-3}	1.079 x10^{-3}	1.079 x10^{-3}
Element type			
BEAM-2	1.079 x10^{-3}	1.079 x10^{-3}	1.079 x10^{-3}

Table 9.18.2 Displacement u_Z at the points (A, B, C)

Displacement	u_Z^A [ft]	u_Z^B [ft]	u_Z^C [ft]
Reference	1.787 x10^{-3}	-0.180 x10^{-3}	-4.820 x10^{-3}
Element type			
BEAM-2	1.787 x10^{-3}	-0.180 x10^{-3}	-4.820 x10^{-3}

Table 9.18.3 Rotation θ_Y at the points (A, B, C)

Rotation	θ_Y^A [rad]	θ_Y^B [rad]	θ_Y^C [rad]
Reference	-0.099 x10^{-3}	0.444 x10^{-3}	-0.361 x10^{-3}
Element type			
BEAM-2	-0.099 x10^{-3}	0.444 x10^{-3}	-0.361 x10^{-3}

References

[1] MacNeal, R.H., and Harder, R.L., “A Proposed Standard Set of Problems to Test Finite Element Accuracy,” Finite Element Analysis and Design, Vol. 1, pp. 3-20, 1985

[2] Simo, J.C., Fox, D.D., and Rifai, M.S., “On a Stress Resultant Geometrically Exact Shell Model. Part II: The Linear Theory,” Computer Methods in Applied Mechanics and Engineering, Vol. 73, pp. 53-92, 1989

[3] McCormac, J.C., “Structural Analysis”, International Textbook Company, Scranton, PA, 1965

[4] NAFEMS, “The Standard NAFEMS Benchmarks, Rev. 3”, NAFEMS, Glasgow, 1990

[5] Young, W.C., and Budynas, R.G., “Roark’s Formulas for Stress and Strain, 7th Edition”, McGraw-Hill, New York, 2002

[6] Zienkiewicz, O., and XU, Z., “Linked Interpolation for Reisner-Midlin Plate Elements: Part I-A simple quadrilateral,” International Journal for Numerical Methods in Engineering, Vol. 36, pp. 3043-3056, 1993

[7] Timoshenko, S., “Strength of Materials, Parts I, Elementary Theory and Problems,” 3rd Edition, D.Van Nostrand Co., Inc., New York, 1956

[8] Lausen, Harold I., “Structural Analysis,” McGraw Hill Book Co. Inc., New York, 1969

[9] American Institute of Steel Construction, “Manual of Steel Construction – Allowable Stress Design,” Chicago, Illinois, 1989

[10] Beaufait F.W.,et al., “Computer Methods of Structural Analysis,” Prentice-Hall, Inc., New Jersey, 1970

Section 1

Properties of Elastic Materials

Elastic materials return to their original shape (i.e. without residual displacement) after external loads are removed. Midas nGen allows for the use of either linear elastic material models or nonlinear elastic material models. An explanation of each model follows. Table 4.1.1 summarizes the material types that may be applied to the different elements in Midas nGen.

Table 4.1.1 Elastic material types that may be applied to different elements

Material Type	요소 종류			
	Truss/Elastic Link/Spring	Beam	Shell	Solid
Linear Elastic Isotropic	v	v	v	v
Nonlinear Elastic (1D)	v			

1.1 Isotropic Materials

Isotropic materials maintain the same properties along an arbitrary direction. Linear elastic isotropic materials, whose properties are based on Hooke's law, may be applied to all element types in midas nGen (except for a few exceptions). Stress-strain relationships of an isotropic material that maintains equal properties in all three directions may be expressed in terms of elastic moudulus E , Poission ratio ν , and coefficient of thermal expansion α . This relationship is shown below.

$$\begin{Bmatrix} \sigma_{xx} \\ \sigma_{yy} \\ \sigma_{zz} \\ \tau_{xy} \\ \tau_{yz} \\ \tau_{zx} \end{Bmatrix} = \begin{bmatrix} \frac{E(1-\nu)}{(1+\nu)(1-2\nu)} & \frac{\nu E(1-\nu)}{(1+\nu)(1-2\nu)} & \frac{\nu E(1-\nu)}{(1+\nu)(1-2\nu)} & 0 & 0 & 0 \\ & \frac{E(1-\nu)}{(1+\nu)(1-2\nu)} & \frac{\nu E(1-\nu)}{(1+\nu)(1-2\nu)} & 0 & 0 & 0 \\ & & \frac{E(1-\nu)}{(1+\nu)(1-2\nu)} & 0 & 0 & 0 \\ & symmetric & & \frac{E}{2(1+\nu)} & 0 & 0 \\ & & & & \frac{E}{2(1+\nu)} & 0 \\ & & & & & \frac{E}{2(1+\nu)} \end{bmatrix} \begin{Bmatrix} \varepsilon_{xx} - \alpha\Delta T \\ \varepsilon_{yy} - \alpha\Delta T \\ \varepsilon_{zz} - \alpha\Delta T \\ \gamma_{xy} \\ \gamma_{yz} \\ \gamma_{zx} \end{Bmatrix} \quad (4.1.1)$$

For 2-dimensional analysis, $\tau_{yz} = \tau_{zx} = \gamma_{yz} = \gamma_{zx} = 0$, and for plane strain analyses, $\varepsilon_{zz} = 0$. Incorporating these properties, 2-dimensional stress-train relationship may be expressed as the following:

$$\begin{Bmatrix} \sigma_{xx} \\ \sigma_{yy} \\ \tau_{xy} \end{Bmatrix} = \begin{bmatrix} \frac{E}{1-\nu^2} & \frac{\nu E}{1-\nu^2} & 0 \\ \frac{\nu E}{1-\nu^2} & \frac{E}{1-\nu^2} & 0 \\ 0 & 0 & \frac{E}{2(1+\nu)} \end{bmatrix} \begin{Bmatrix} \varepsilon_{xx} - \alpha\Delta T \\ \varepsilon_{yy} - \alpha\Delta T \\ \gamma_{xy} \end{Bmatrix} \quad (4.1.2)$$

The stress-strain relationship for lateral shear is as follows.

$$\begin{Bmatrix} \tau_{zx} \\ \tau_{zy} \end{Bmatrix} = \begin{bmatrix} G & 0 \\ 0 & G \end{bmatrix} \begin{Bmatrix} \gamma_{zx} \\ \gamma_{zy} \end{Bmatrix} \quad (4.1.3)$$

Isotropic materials may be defined by two material constants. The two may be selected from E, G , ν . The third is defined based on the relationship shown below.

$$G = \frac{E}{2(1+\nu)} \quad (4.1.4)$$

To ensure physical stability of isotropic materials, the Poisson ratio must defined to be within the boundaries shown below:

$$-1.0<\nu<0.5 \tag{4.1.5}$$

1.2 Nonlinear elastic behavior of truss elements

Midas nGen provides the following nonlinear elastic behavior models for truss elements, for the convenience of the user.

- Compression-only behavior
- Gap behavior
- Tension-only behavior
- Hook behavior

Figure 4.1.1 Nonlinear elastic models for truss elements

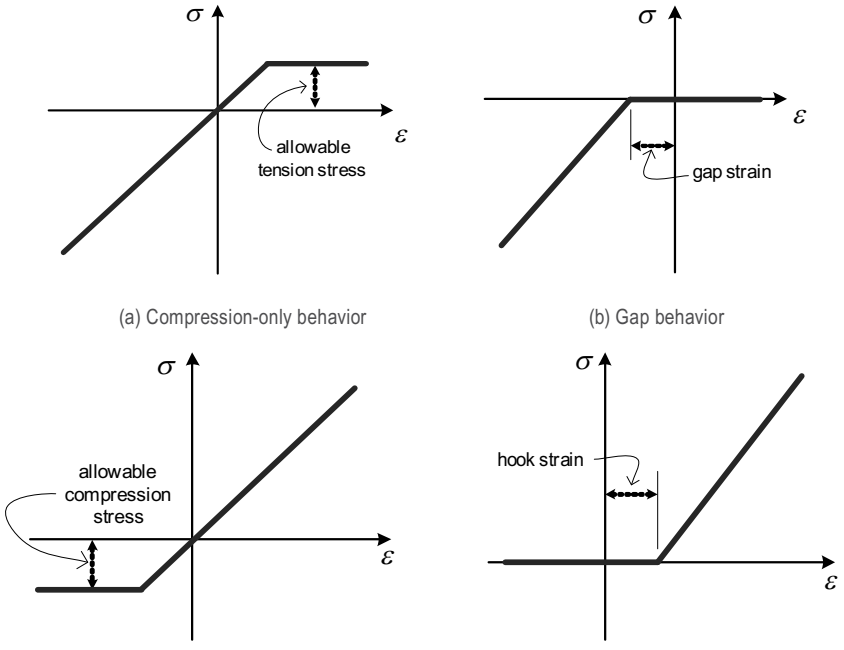

(a) Compression-only behavior

(b) Gap behavior

(c) Tension-only behavior (d) Hook behavior

Gap and hook models are defined by units of length. Gap strains and hook strains are calculated based on the element's initial length.

1.3 Nonlinear elastic behavior of elastic link/spring elements

Midas nGen provides the following models for elastic link/spring elements:

- General behavior
- Tension only behavior
- Compression only behavior

Tension and compression only behavior models are defined similar to the nonlinear material behaviors defined for truss elements in Section 1.2. Truss element behaviors are expressed as a function of stress and strain, but elastic link and spring elements do not have cross section properties. Thus, the behaviors are expressed as a function of force and displacement, as shown below in Figure 4.1.2.

Figure 4.1.2 Compression only and tension only behavior for elastic link

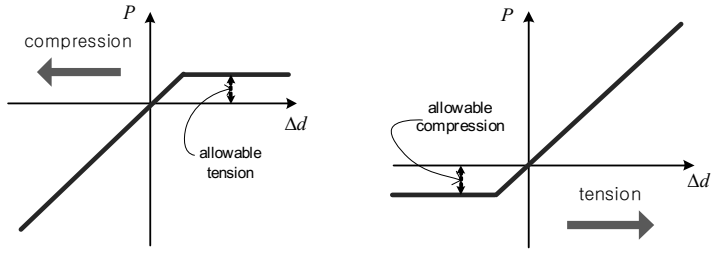

(a) Compression-only (b)Tension-only

In figure 4.1.2, $_{\Delta d}$ refers to the relative displacement between the nodes, and P represents the internal force of the member. Resistance in compression-only and tension-only behavior models may only applied to spring elements.

Section 2

Material Examples

1) Axial Motion of an Elastic Link Element

REFERENCE	Gere[1]
ELEMENTS	Elastic link element, Beam elements
MODEL FILENAME	Material1.mpb

The figure below shows an elastic link connecting two fixed-end beams. The right end of the elastic link is subject to a force of 100N. The model and material setup may be verified by the reaction at point A, using either tension only or compression only material properties.

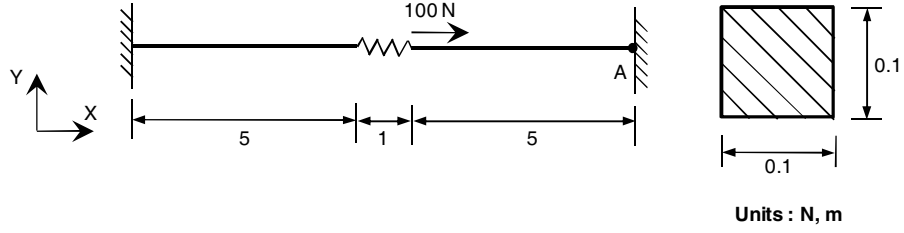

Figure 2.1.1
Axial beam with elastic link

Material data	Young's modulus	*E = 10.0 GPA*
Link property	Stiffness	*2.00x10^7 N/m^2*

Table 2.1.1 X directional reaction at the prescribed point A

	Reaction [N]	
Link Type	Result	Reference
Tension Only	*-66.667*	*-66.667*
Compression Only	*-100.000*	*-100.000*

2) Behavior of a Truss Structure with Brace

REFERENCE	None
ELEMENTS	Truss element, Beam elements
MODEL FILENAME	Material2.mpb

The figure below shows truss structures with and without a brace. There is a nodal load exerted on the structure, in the leftward direction. The truss-element forming the brace exhibits compression-only behavior. Model setup may be verified by comparing the x-displacement at point A, for both the structure with and without the brace. In this loading case, the brace experiences tension. Thus, using a compression-only brace in the structure should yield the same results as the structure without a brace.

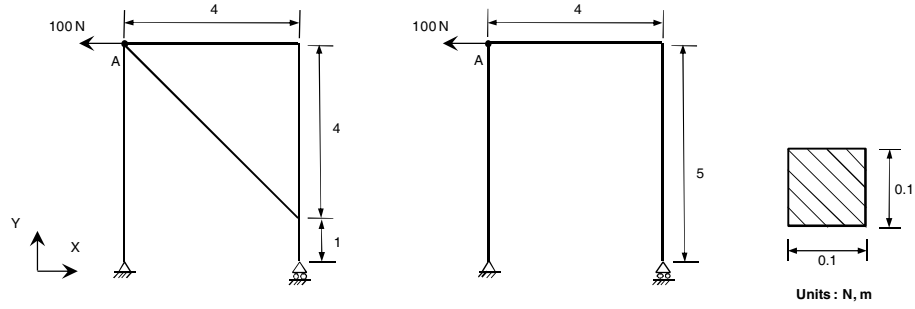

Figure 2.2.1
Truss structure with or without brace

Material data	Young's modulus	*E = 210.0 GPA*

Table 2.2.1 x-displacement at the prescribed point A

	Displacement	
Truss Type	With Brace	Without Brace
	-1.31278E-005	*-1.31278E-005*

3) Behavior of a Point Spring Element

REFERENCE	Gere[1]
ELEMENTS	Beam element, Point spring
MODEL FILENAME	Material3.mpb

The figure below shows a beam with a fixed right end. On its left is a compression-only point spring that allows for some tension. The beam's left end is subject to an external force of 100N. Model setup may be verified using the axial force of the beam and spring elements.

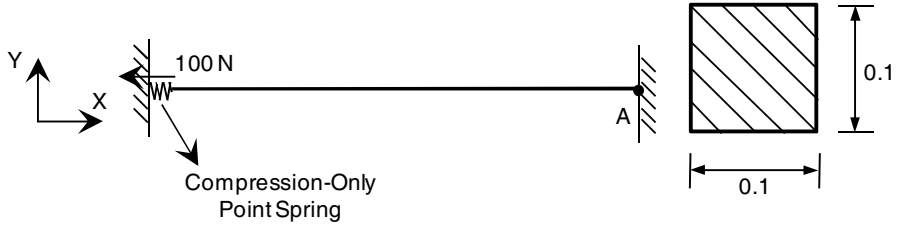

Figure 2.3.1
Beam element with point spring

Material data	Young's modulus	*E = 10.0 GPA*
Spring Property	Stiffness	*$1.0x10^7$ N/m^2*
	Allowable tension	*30N*

Table 2.3.1 Axial forces of the beam and spring elements

	Displacement	
Element Type	Result	Reference
Spring element	*30N*	*30N*
Beam element	*70N*	*70N*

References

[1] James M. Gere, Barry J. Goodno, Mechanics of Materials, 2012

Section 1

System of Equations Solver

The System of Equations Solver finds the solution $\mathbf{u}$ to matrix problems of the form shown in Equation 5.1.1:

$$\mathbf{Ku} = \mathbf{p} \tag{5.1.1}$$

The Solver is not only used in linear static analysis, but also other analysis methods including but not limited to eigenvalue analysis, dynamic analysis, and nonlinear anslysis. The Solver includes the typical Gaussian Elimination method for solving the system of simultaneous equations. Additionally, it includes an iterative solver that minimizes error through a direct solver based on LU decomposition.

Direct solvers are not influenced by the numerical irregularities of the matrix and can arrive at a stable solution. Thus, they are used frequently in structural analysis. However, if the matrix becomes too large, then the number of iterations and the computational time per iteration can increase exponentially. Consequently, for such matrix, the use of an iterative solver that relies on relatively less memory is recommended. One must also remain cautious of possible numerical irregularities in structural analysis problems. Such irregularities may not allow one to arrive at a desired solution through an iterative solver, or the number of iterations required to arrive at such a solution may become too large. Midas nGen allows for automated selection of direct and iterative solvers based on the nature and size of the problem.

In the direct solver, a solution to a system of simultaneous equations is found through two steps. The first step is matrix decomposition, and the second step is forward-backward substitution (FBS). LU

decomposition—usually applied to asymmetrical matrices—can be modified for the symmetric stiffness matrix $\mathbf{K}$ that forms the basis of finite element analyses:

$$\mathbf{L}\mathbf{L}^T\mathbf{u} = \mathbf{p} \quad \text{or} \quad \mathbf{L}\mathbf{D}\mathbf{L}^T\mathbf{u} = \mathbf{p} \tag{5.1.2}$$

$\mathbf{L}$: Lower Triangular Matrix

$\mathbf{D}$: Diagonal Matrix

Typically, matrix decomposition methods that involve $\mathbf{D}$ are required in which the stiffness matrix is not positive definite. In midas nGen, linear static analyses rely on $\mathbf{L}\mathbf{L}^T$ -type matrix decomposition (Cholesky decomposition method). For eigenvalue or nonlinear analyses, the positive definiteness of the stiffness matrix is not guaranteed and thus $\mathbf{L}\mathbf{D}\mathbf{L}^T$ -type decomposition methods are used instead.

When direct solvers are applied, it is important to be cognizant of matrix sparsity. Typically, the stiffness matrix $\mathbf{K}$ that arises from finite element analysis includes many zeros and is thus a sparse matrix. This characteristic is an important one, as the different ways that solvers utilize matrix sparsity can cause a noticeable difference in required memory and computational complexity. As a result, midas nGen does not simply rely on direct solvers that are often used for dense matrices (and thus do not manipulate matrix sparsity). Instead, the default solver is a multi-frontal solver that utilizes matrix sparsity to optimize computational complexity and required memory space.

In multi-frontal solvers, the minimization of problem complexity and memory through manipulation of matrix sparsity requires reordering of the degrees of freedom. The reordered DOFs are then decomposed and used in various frontal solvers. Equation 5.1.1 is a schematic representation of efficient calculation processes via rectangular component networks formed by DOF reordering. DOF reordering is realized through an algorithm called recursive bisection; the forward substitute sequence is the same as matrix decomposition, and backwards substitution is done in the reverse order.

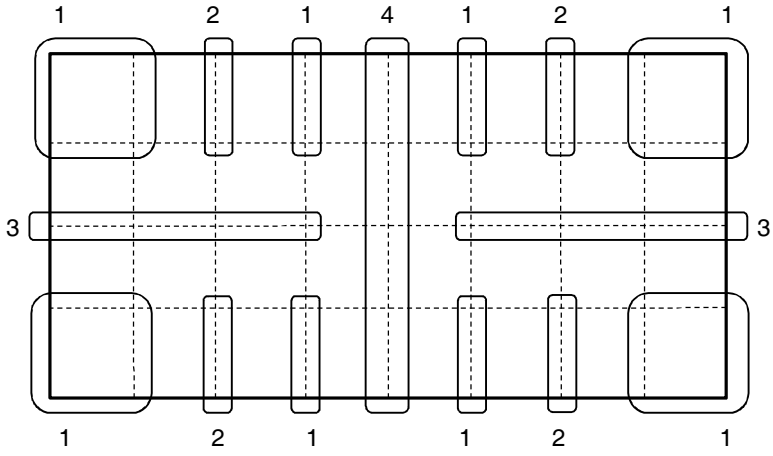

Figure 5.1.1 Example sequence for matrix decomposition used in multi-

The multi-frontal solver used in midas nGen does not build and save the complete stiffness matrix, and as a result uses less memory compared to typical multi-frontal solvers. For larger problems where more memory may be needed, the out-of-core analysis capability allows the software to automatically use additional hard disk memory to complete the computations.

Moreover, for the purpose of realizing the multi-frontal solver method, midas nGen takes full advantages of the computational abilities of the graphics processing unit (GPU). Recently there has been increased demand in large problems and thus an increased focus on the importance of th efficiency of finite element methods, which serves as the centerpiece of structural analysis. GPU's are made of many core units, and thus provide improved computational abilities compared to CPU's.

Iterative solvers reduce the error in the approximate solution through multiple iterations, and thus it is important to induce convergence and reduce error using the smallest number of iterations and lowest computation time. Typically, the number of iterations is defined by the preconditioning technique. In

midas nGen, one of two stable preconditioning techniques are used regardless of the element. They are the SA (smoothed aggregation) and AMG (algebraic multi-grid) [1] methods.

The AMG method uses multi-grids, so the number of iterations is not largely affected by the number of degrees of freedom. It shows stable convergence even for elements where each node has translational and rotational degrees of freedom (e.g. shell elements). Iterative solvers that use the AMG method automatically define multi-grids, which are created based on the set of adjacent nodes and the degrees of freedom that represent the said set of nodes. Figure 5.1.2 shows a sample set of nodes that define a multi-grid.

Figure 5.1.2 A set of nodes that define a multi-grid

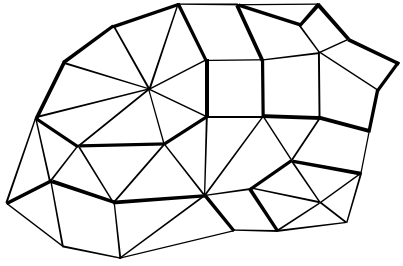

As previously explained, the performance of direct and iterative solvers depends on the size of the problem, and to help on this end, midas nGen offers the capability to automatically decide between the two. For small-sized problems, the direct solver is used as it relies on dense matrices. Moderately-sized problems use the multi-frontal solver and large problems use the AMG iterative solver.

The automated selection criteria consider the following:

▸ In cases where conditions are known from experience: Automation is based on the number of elements/nodes input by the user

[1] Vanek, P., Mandel, J. and Bresina, M.,"Algebraic Multigrid by Smoothed Aggregation for Second and Fourth order Elliptic Problems," Computing, Vol. 56, 1996

► In cases where conditions are not known from experienced: Automation is based on the number of degrees of freedom in the model and system memory size

Section 2 Eigenvalue Extraction

2.1 Eigenvalue Extraction Methods

Eigenvalue extraction is the core algorithm of all normal mode analysis and buckling analysis. Eigenvalue extraction takes the form of the equation shown below:

$$\mathbf{K}\phi_i - \lambda_i \mathbf{B}\phi_i = \mathbf{0} \ \text{(no summation)} \tag{5.2.1}$$

$\mathbf{K}$: Stiffness matrix

: All analyses – Mass matrix ($\mathbf{M}$)

$\mathbf{B}$: Buckling analysis – Geometric stiffness matrix ($\mathbf{K}_g$)

The buckling analysis mode of midas nGen software allows for the use of a steady stiffness matrix and/or geometric stiffness matrix. Thus, eigenvalue extraction is divided into loading sets:

$$\left(\mathbf{K} + \sum \alpha^n \mathbf{K}_g^n\right)\phi_i - \lambda_i \left(\sum \alpha^m \mathbf{K}_g^m\right)\phi_i = \mathbf{0} \ \text{(no summation for } i\text{)} \tag{5.2.2}$$

α^n : Loading set geometric stiffness contribution factor that is added to the steady stiffness matrix

α^m : Loading set geometric stiffness contribution factor that increases as a function of the buckling coefficient

In midas nGen, the eigenvalue extraction method is linked to and changes based on the method of solving simultaneous equations. The default method for the simultaneous equation solver uses the Lanczos iterative method. If a dense matrix method is selected, then eigenvalue extraction also uses a direct approach using dense matrices. Each method has the following characteristics.

• Lanczos Iterative Method

► Appropriate for large problems

► Some eigenvalues may be omitted, so it is recommended that the Sturm sequence check option is used.

• Direct approach using dense matrices

► If the number of degrees of freedom is on the order of 10^3 , then performance may worsen significantly. Thus, this method is appropriate for small problems.

► Eigenvalues are not omitted.

The Lanczos iterative method[2] calculates approximate eigenvalues using the tridiagonal matrix that is created in the process of defining the Krylov subspace $span(\mathbf{V}_1, \mathbf{V}_2, ..., \mathbf{V}_k)$. Block tridiagonal matrices are used for effective eigenvalue analysis, and the standard of the number of eigenvalues are similar kept to the size of the tridiagonal matrix. Thus, this method takes little computational time and is appropriate for large problems. However, some eigenvalues may be omitted and thus it is recommended that the user select an option that checks for missing eigenvalues.

The direct approach using dense matrices undergoes matrix decomposition, definition of tridiagonal matrices, and eigenvalue calculation procedures. Eigenvalue computation and tridiagonal matrix creation is based on the complete model matrix. Thus, this approach does not omit eigenvalues but is not appropriate for large problems.

Calculation Range for Eigenvalues

Typically, in modal analysis, the number of eigenvalues and range can be defined based on the modal participation factor (Equation 5.3.1) or modal effective mass (Equation 5.3.3). It may also be defined

[2] Hughes, T.J.R., The Finite Element Method, Prentice-Hall International, Inc., New Jersey, 1987

based on the frequency range of interest. If the number of eigenvalues and the range is defined based on these factors, then they may follow the user input options shown in the table below.

Table 5.2.1 Number of eigenvalues and definition of the range for calculation

Definition of Variables (v_1 , v_2 , N Input or no input)	Range of Eigenvalues	Number of Eigenvalues
v_1 , v_2 , N	$v_1 < v < v_2$	At most N eigenvalues
v_1 , no input, N	$v_1 < v$	At most N eigenvalues
No input, v_2 , N	$v < v_2$	At most N eigenvalues
No input, no input, N	$-\infty < v < \infty$	At most N eigenvalues
v_1 , v_2 , no input	$v_1 < v < v_2$	All eigenvalues
v_1 , no input, no input	$v_1 < v$	All eigenvalues
No input, v_2 , no input	$v < v_2$	All eigenvalues
No input, no input, no input	$-\infty < v < \infty$	All eigenvalues

For the inputs shown above, v_1 , v_2 are frequencies in Hz.

Eigenvalue Calculation Result

Eigenvector, which is the result of eigenvalue analysis, satisfies Equation 5.2.1 regardless of any changes in size.

$$a(\mathbf{K}\phi_i - \lambda_i \mathbf{B}\phi_i) = \mathbf{K}\varphi_i - \lambda_i \mathbf{B}\varphi_i = \mathbf{0}$$
$$\varphi_i = a\phi_i \tag{5.2.3}$$

Therefore, it is necessary to express the size of the calculated eigenvector in a consistent manner. Midas nGen applies eigenvector normalization in the following form, which must be satisfied for all different analysis types:

$$\phi_i^T \mathbf{M} \phi_i = 1 \tag{5.2.4}$$

Even when solution is based on the direct approach using dense matrices, the eigenvalue calculation algorithm only returns approximate values and thus the accuracy cannot be guaranteed. Midas nGen adopts the following eigenvalue results to check the accuracy of the calculated eigenvalues and eigenvectors.

Table 5.2.2 Results of numerical results other than eigenvalues and eigenvectors

Result	Calculation
Generalized mass	$b_i = \phi_i^T \mathbf{B} \phi_i$
Generalized stiffness	$k_i = \phi_i^T \mathbf{K} \phi_i$
Orthogonality loss	$\delta_i = \max(\frac{\phi_{i-1}^T \mathbf{K} \phi_i}{k_i}, \frac{\phi_{i-1}^T \mathbf{B} \phi_i}{b_i})$
Error measure	$e_i = \frac{\left\|\mathbf{K}\phi_i - \lambda_i \mathbf{B}\phi_i\right\|}{\left\|\mathbf{K}\phi_i\right\|}$

2.2 Automatic Extraction

In all analysis, the number of extracted eigenvalues may be decided based on how many eigenvalues are required to satisfy a specified mass participation factor (typically 80-90%, internally set at 90%). Midas nGen offers the ability to automatically minimize the number of eigenvalues to satisfy the mass participation factor of the selected degrees of freedom (for more information on mass participation factors, please refer to Section 3) by incrementally adding to the number of eigenvalues. Additional eigenvalues are solved by recycling the decomposed stiffness matrix and can be more efficient that manual repetition. The default number of eigenvalues is set at the user-specified number of modes. Using the ratio of the number of additional eigenvalues that were computed to the incremental increase in the mass participation factor, the number of modes is increased and computation is repeated until the mass participation factor tolerance is satisfied.

$$\Delta N_{i+1} = \frac{\Delta P_i}{\Delta N_i} \tag{5.2.5}$$

ΔN_{i+1} : Number of additional eigenvalues that were computed

ΔN_i : Number of additional eigenvalues that were computed in the previous computation

ΔP_i : The incremental increase in the mass participation factor (in the direction of the selected degree of freedom) in the previous computation

When using this method, eigenvalues are found in iterated calculations, so there are no additional calculations for computing omitted eigenvalues. The default number of eigenvalues is the user-specified number of modes. In the case in which the default value is too low, the software then finds additional eigenvalues. If the default number of modes is selected with consideration of the number of degrees of freedom, model size, and other characteristics, then the eigenvalue extraction process would proceed in a much more efficient manner.

Additional Items

1. When the dense matrix solver method is being used, then all possible modes are computed at once, and the minimum number of eigenvalues required to satisfy mass participation factors are computed.
2. The limit on the mass participation factor, which serves as a base for seismic analysis, does not include restrained masses.
3. If the target mass participation factor is too close to the mass participation factor when using all modes, then the calculation may become too inefficient. Thus, midas nGen provides a warning message and automatically reduce the target mass participation factor before proceeding with further computations.

2.3
Modal Analysis Examples

1) Pin-ended cross model

REFERENCE	NAFEMS[1]
ELEMENTS	Beam elements
MODEL FILENAME	Eigen01.mpb

The figure below shows four beams crossing one another. The ends of these beams are pinned.

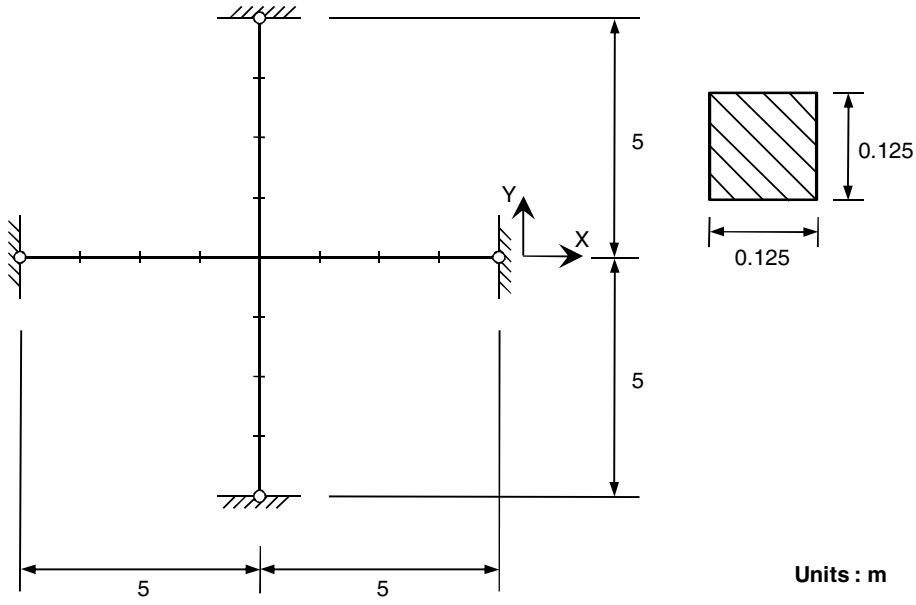

Figure 2.3.1.1
Pin-ended cross model

Material data	Elastic modulus Mass density	*E = 200 GPa* ρ*= 8000 kg/m*^{3}
Section property	Square cross-section	*0.125 m x 0.125 m*
Mass option		*Coupled mass*

Figure 2.3.1.2
Vibration mode shapes

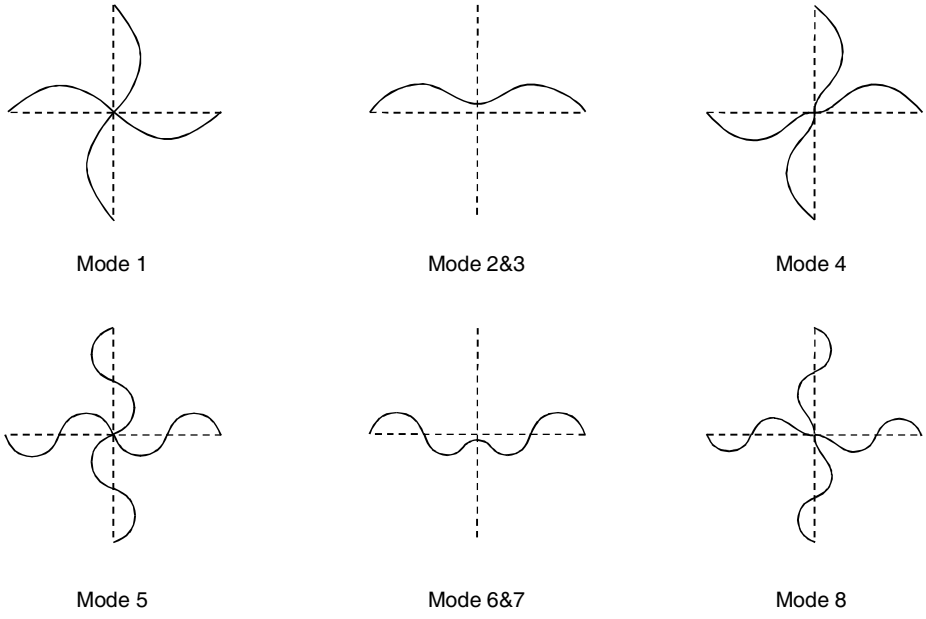

Table 2.3.1.1 Natural frequencies in Hz obtained using beam elements

Mode Number		1	2, 3	4	5	6, 7	8
Reference		*11.336*	*17.709*	*17.709*	*45.345*	*57.390*	*57.390*
Element type	Number of elements						
Beam-2	4 per arm	*11.336*	*17.687*	*17.716*	*45.486*	*57.382*	*57.702*

2) Square Frame

REFERENCE	NAFEMS[1]
ELEMENTS	Beam elements
MODEL FILENAME	Eigen02.mpb

The figure below shows a 2-dimensional square frame model without any fixities. Each side is modeled with four beam elements. Three rigid body modes have been omitted, and results for modes 4 through 11 are shown below.

Figure 2.3.2.1
Free square frame model

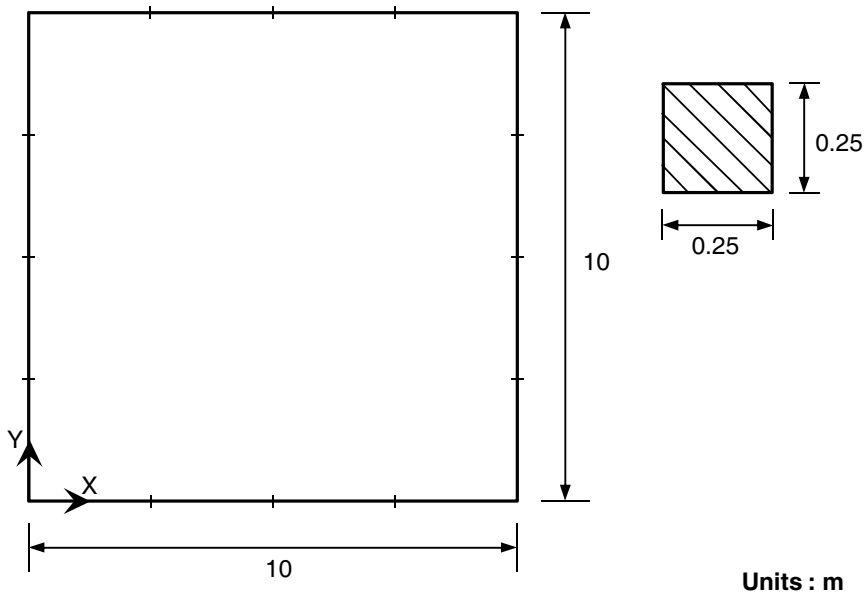

Material data	Elastic modulus	*E = 200 MPa*
	Poisson's ratio	ν *= 0.3*
	Mass density	ρ*= 8000 kg/m*^{3}
Section property	Area, shear area	*A = As = 0.0625 m2*
	Moment of inertia	*Ix =Iy = 0.000326 m4*
Mass option		*Coupled mass*

Figure 2.3.2.2
Vibration mode shapes

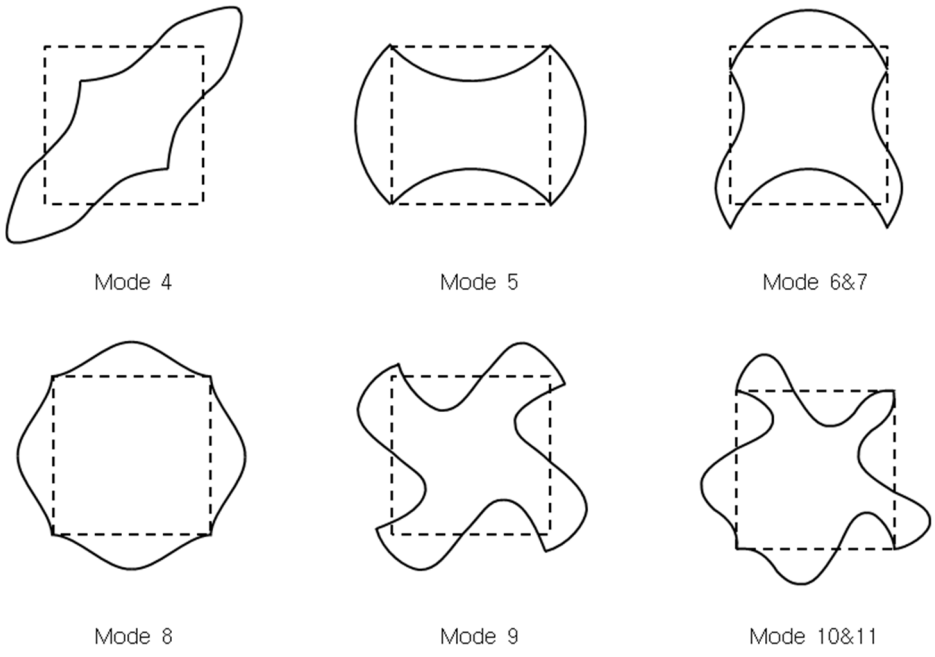

Table 2.3.2.1 Natural frequencies in Hz obtained using beam elements

Mode Number		4	5	6,7	8	9	10,11
Reference		*3.261*	*5.668*	*11.136*	*12.849*	*24.570*	*28.695*
Element type	Number of elements						
Beam-2	4 per arm	*3.262*	*5.666*	*11.135*	*12.802*	*24.628*	*28.720*

3) Cantilever with Off-Center Point Masses

REFERENCE	NAFEMS[2]
ELEMENTS	Beam elements
MODEL FILENAME	Eigen03.mpb

The figure below shows a model with two concentrated masses at some distance from the free end of a cantilever beam.

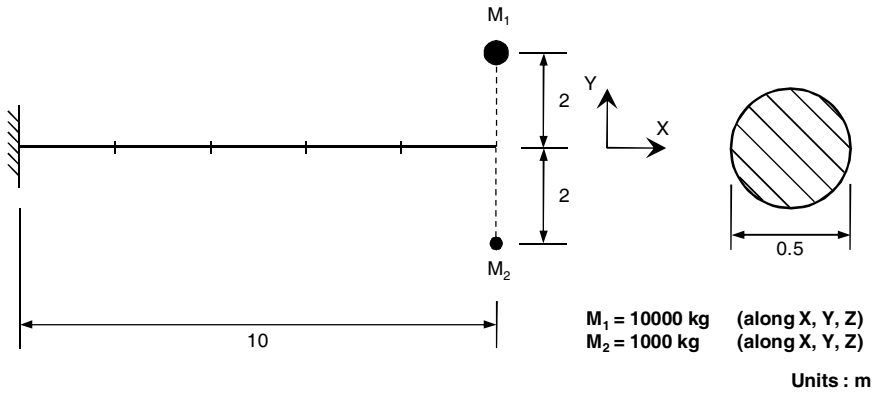

Figure 2.3.3.1 Cantilever with off-center point masses model

Material data	Elastic modulus	$E = 200\ GPa$
	Poisson's ratio	$\nu = 0.3$
	Mass density	$\rho = 8000\ kg/m^3$
Section property	Circular cross-section	$R = 0.25\ m$
Mass option		*Coupled mass*

Figure 2.3.3.2
Vibration mode shapes

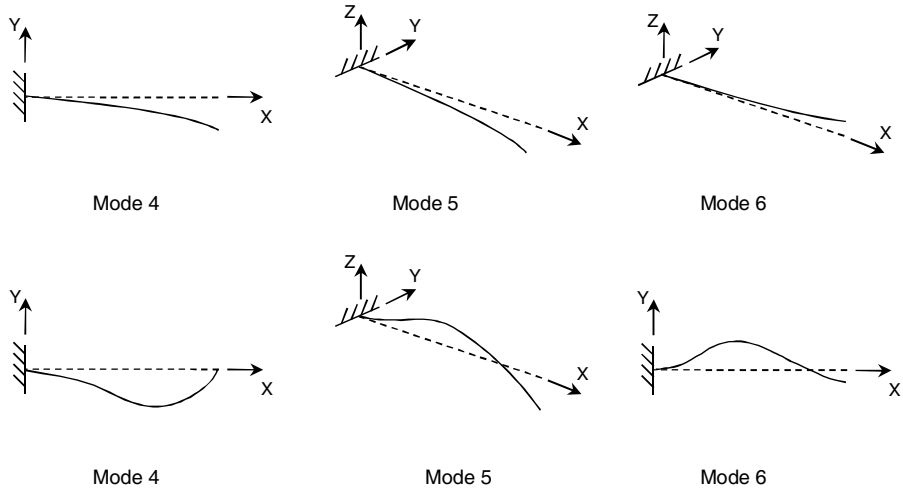

Table 2.3.3.1 Natural frequencies in Hz obtained using beam elements

Mode Number		1	2, 3	4	5	6, 7	8
Reference		*11.336*	*17.709*	*17.709*	*45.345*	*57.390*	*57.390*
Element type	Number of elements						
Beam-2	5	*11.338*	*17.689*	*17.717*	*45.483*	*57.371*	*57.690*

4) Deep Beam

REFERENCE	NAFEMS[2]
ELEMENTS	Beam elements, solid elements
MODEL FILENAME	Eigen04.mpb

The figure below shows a simply-supported deep beam. It must be modeled carefully with consideration of the boundary conditions in order to incorporate three-dimensional mode shapes.

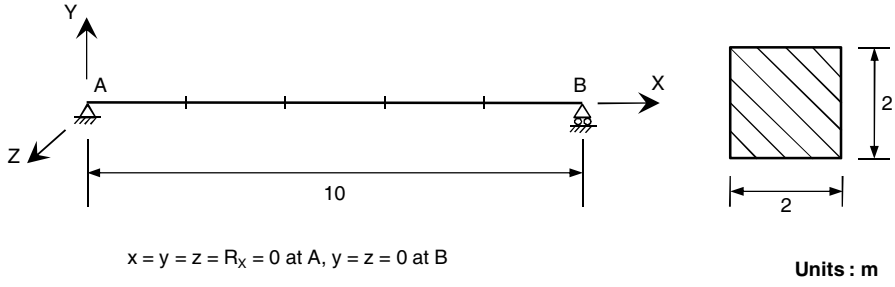

Figure 2.3.4.1
Deep simply-supported beam model

Material data	Elastic modulus	*E = 200 GPa*
	Poisson's ratio	ν *= 0.3*
	Mass density	ρ*= 8000 kg/m*^{3}
Section property	Square cross-section	*2.0 m x 2.0 m*
Mass option		*Coupled mass*

Table 2.3.4.1 Natural frequencies in Hz obtained using beam elements

Mode Number		1, 2	3	4	5, 6	7	8, 9
Reference		*42.649*	*77.542*	*125.00*	*148.31*	*233.10*	*284.55*
Element type	Number of elements						
Beam-2	5	*42.675*	*77.841*	*125.51*	*150.43*	*241.24*	*300.10*

Figure 2.3.4.2
Vibration mode shapes

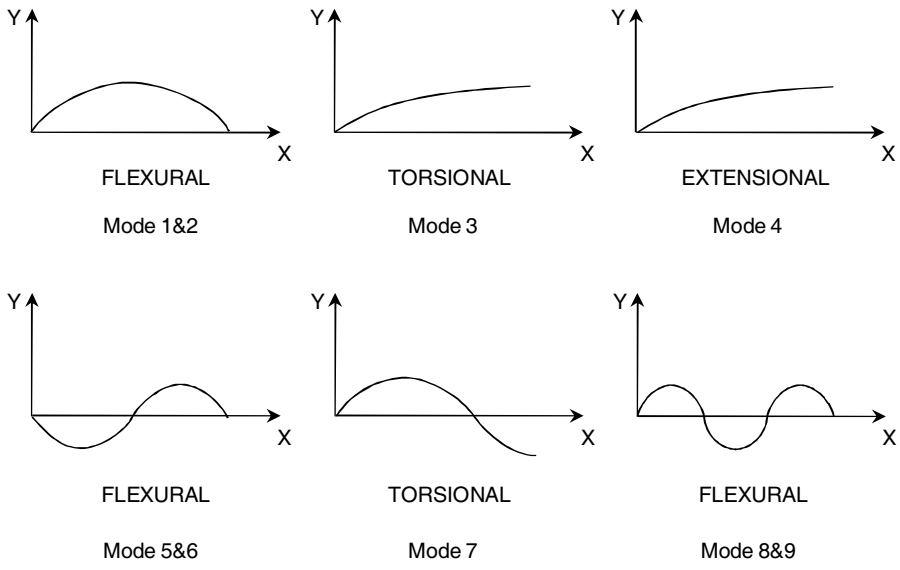

Table 2.3.4.1 Natural frequencies in Hz obtained using solid elements

Mode Number		1	2	3	4	5
Reference		*38.200*	*85.210*	*152.23*	*245.53*	*297.05*
Element type	Number of elements					
TETRA-4	282	*46.381*	*95.982*	*179.77*	*292.81*	*325.68*
PENTA-6	60	*39.317*	*85.659*	*158.54*	*264.38*	*298.68*
HEXA-8	10x1x3	*38.277*	*83.952*	*157.57*	*264.92*	*298.33*

5) Circular Ring

REFERENCE	NAFEMS[1]
ELEMENTS	Beam elements
MODEL FILENAME	Eigen05.mpb

The figure below shows a circular ring with no fixities. Six rigid body modes were omitted, and the results below shows modes 7 through 18.

Figure 2.3.5.1
Circular ring model

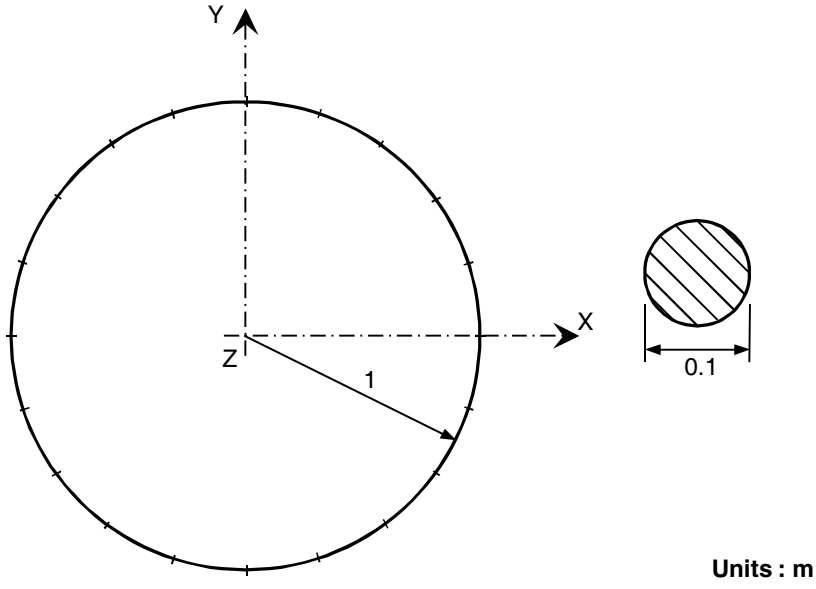

Units : m

Material data	Elastic modulus	$E = 200\ GPa$
	Poisson's ratio	$\nu = 0.3$
	Mass density	$\rho = 8000\ kg/m^3$
Section property	Circular cross-section	$R = 0.05\ m$
Mass option		*Coupled mass*

Figure 2.3.5.2
Mode shapes of vibration

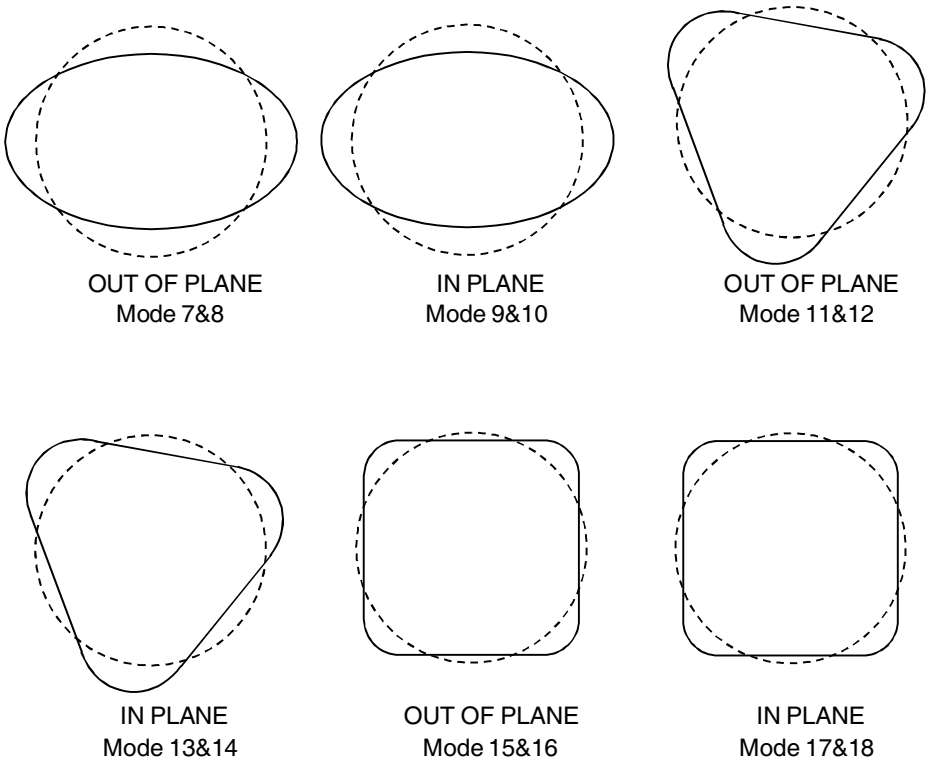

Table 2.3.5.1 Natural frequencies in Hz obtained using beam elements

Mode Number		7, 8	9, 10	11, 12	13, 14	15, 16	17, 18
Reference		*51.849*	*53.382*	148.77	150.99	286.98	289.51
Element type	Number of elements						
Beam-2	20	52.213	53.777	148.93	151.27	285.38	288.19

6) Thin Square Cantilever Plate

REFERENCE	NAFEMS[1]
ELEMENTS	Shell elements, solid elements
MODEL FILENAME	Eigen06.mpb

The figure below shows a square cantilever plate whose left end has been fixed. Using symmetry conditions, only the bottom half has been modeled. Based on the restraint conditions on the symmetry boundary, Case A exhibits only symmetrical mode shapes and Case B exhibits only asymmetrical mode shapes.

Figure 2.3.6.1
Thin square cantilever plate model

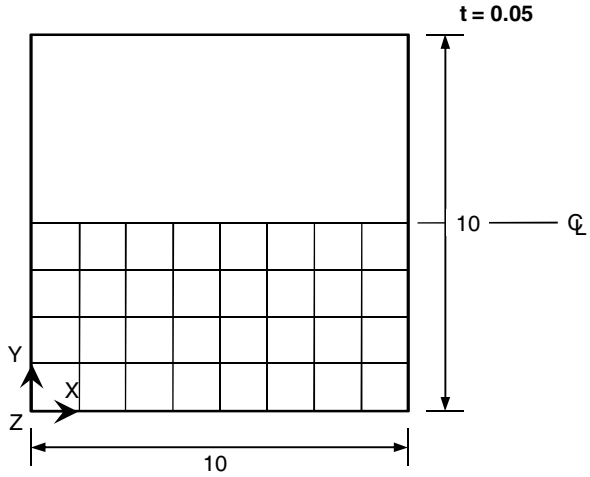

case A $x = y = R_z = 0$ at all nodes,
$z = R_y = R_x = 0$ along y-axis, $R_x = 0$ along y = 5m

case B $x = y = R_z = 0$ at all nodes,
$z = R_y = R_x = 0$ along y-axis

Material data	Elastic modulus	E = 200 GPa
	Poisson's ratio	ν = 0.3
	Mass density	ρ= 8000 kg/m^3
Section property	Thickness	t = 0.05 m
Mass option		Coupled mass

Figure 2.3.6.2
Vibration mode shapes
(Case A)

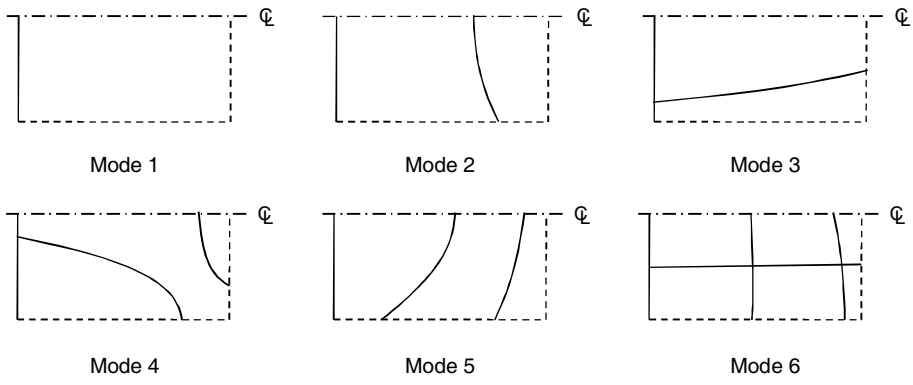

Figure 2.3.6.3
Vibration mode shapes
(Case B)

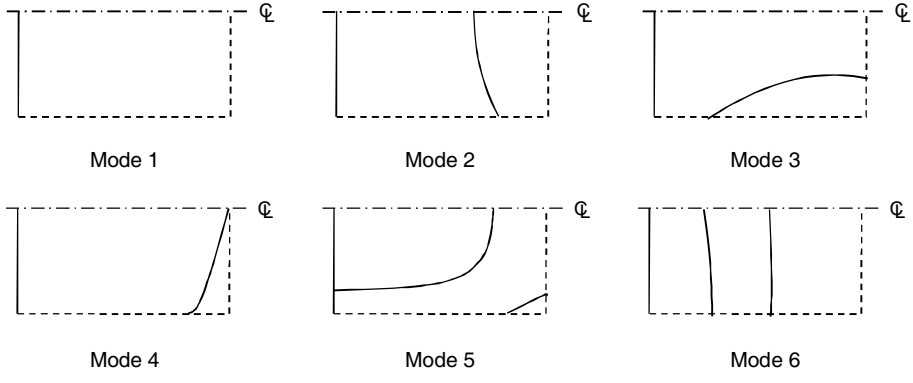

Table 2.3.6.1 Natural frequencies in Hz obtained using shell elements – Case A

Mode Number		1	2	3	4	5	6
Reference		*0.421*	*2.582*	*3.306*	*6.555*	*7.381*	*11.402*
Element type	Number of elements						
TRIA-3	64	*0.418*	*2.623*	*3.362*	*6.931*	*7.963*	*13.160*
QUAD-4	8x4	*0.418*	*2.615*	*3.337*	*6.752*	*7.905*	*12.681*

Table 2.3.6.2 Natural frequencies in Hz obtained using solid elements – Case A

Mode Number		1	2	3	4	5	6
Reference		*0.421*	*2.582*	*3.306*	*6.555*	*7.381*	*11.402*
Element type	Number of elements						
HEXA-8	8x4x1	*0.419*	*2.656*	*3.353*	*6.747*	*8.251*	*12.654*

Table 2.3.6.3 Natural frequencies in Hz obtained using shell elements – Case B

Mode Number		1	2	3	4	5	6
Reference		*1.029*	*3.753*	*7.730*	*8.561*	*N/A*	*N/A*
Element type	Number of elements						
TRIA-3	64	*1.027*	*3.841*	*8.263*	*9.303*	*12.417*	*18.118*
QUAD-4	8x4	*1.026*	*3.807*	*8.220*	*9.194*	*11.974*	*18.004*

Table 2.3.6.4 Natural frequencies in Hz obtained using solid elements – Case B

Mode Number		1	2	3	4	5	6
Reference		*1.029*	*3.753*	*7.730*	*8.561*	*N/A*	*N/A*
Element type	Number of elements						
HEXA-8	8x4x1	*1.029*	*3.840*	*8.356*	*9.416*	*11.977*	*18.248*

7) Thin Square Cantilever Plate – Unbalanced Mesh

REFERENCE	NAFEMS[1]
ELEMENTS	Shell elements
MODEL FILENAME	Eigen07.mpb

The figure below shows a thin square cantilever plate. This model serves to show how the response of the model changes as the mesh becomes unbalanced.

Figure 2.3.7.1
Thin square cantilever plate model

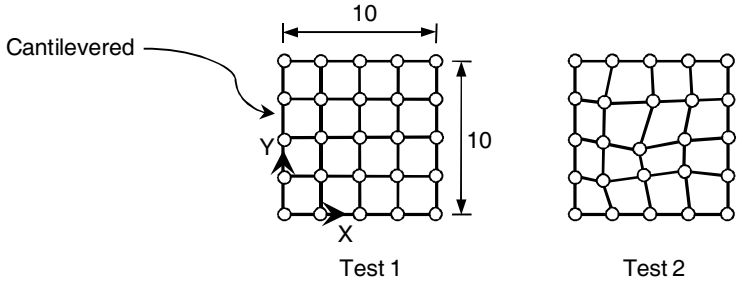

Units : m

Material data	Elastic modulus	$E = 200\ GPa$
	Poisson's ratio	$\nu = 0.3$
	Mass density	$\rho = 8000\ kg/m^3$
Section property	Thickness	$t = 0.05\ m$
Mass option		*Coupled mass*

Table 2.3.7.1 Natural frequencies in Hz obtained using shell elements

Mode Number		1	2	3	4	5	6
Reference		*0.421*	*1.029*	*2.582*	*3.306*	*3.753*	*6.555*
Element type	Mesh						
QUAD-4	Regular	*0.418* *0.417**	*1.044* *1.009**	*2.756* *2.666**	*3.505* *3.465**	*4.199* *3.829**	*7.483* *6.870**
	Distorted	*0.418* *0.417**	*1.043* *1.007**	*2.789* *2.679**	*3.539* *3.485**	*4.192* *3.857**	*7.515* *6.965**

* obtained using shell element formulations with 6-dof per node.

8) Simply-Supported Thick Square Plate

REFERENCE	NAFEMS[1]
ELEMENTS	Shell elements
MODEL FILENAME	Eigen08.mpb

The figure below shows a thick square plate whose four sides are simply-supported. Case A has additional constraints: the model boundaries parallel to the x-axis have rotation restraints about the x-axis and the boundaries parallel to the y-axis have rotation restraints about the y-axis.

Figure 2.3.8.1
Simply-supported thick square plate model

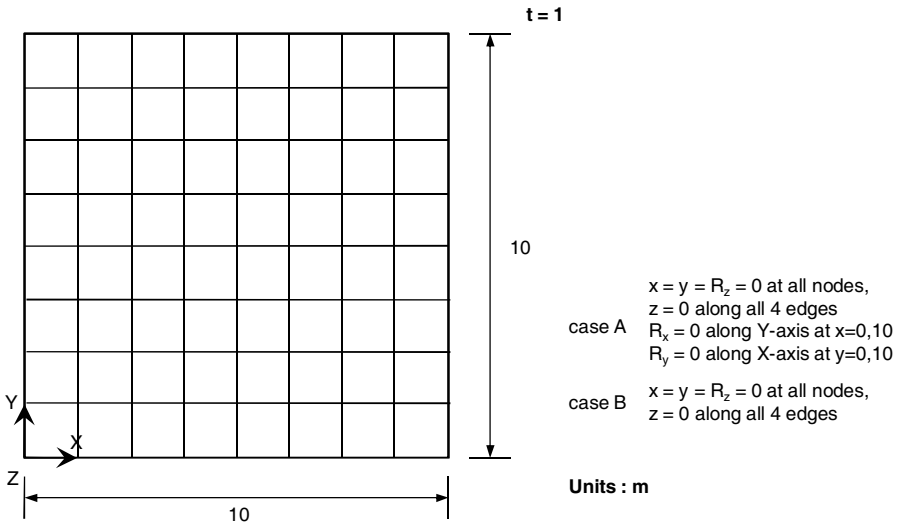

Material data	Elastic modulus	E = 200 GPa
	Poisson's ratio	ν = 0.3
	Mass density	ρ= 8000 kg/m^3
Section property	Thickness	t = 1 m
Mass option		Coupled mass

Figure 2.3.8.2
Vibration mode shapes

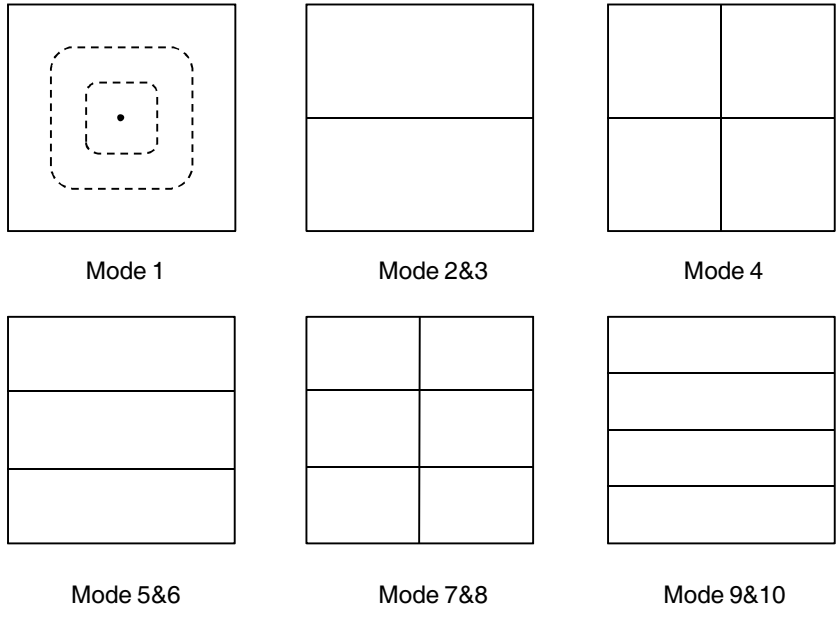

Table 2.3.8.1 Natural frequencies in Hz obtained using shell elements

Mode Number			1	2,3	4	5,6	7,8	9,10
Reference			*45.897*	*109.44*	*167.89*	*204.51*	*256.50*	*336.62*
Element type	Number of elements	*BC type*						
TRIA-3	128	A	*47.386*	*117.76*	*188.58*	*233.57*	*305.04*	*394.14*
		B	*46.215*	*116.00*	*184.46*	*231.42, 231.90*	*299.70*	*392.87*
QUAD-4	8x8	A	*46.493*	*114.46*	*176.33*	*226.93*	*280.64*	*383.73*
		B	*45.128*	*112.60*	*172.20*	*225.22, 225.45*	*276.10*	*382.57*

* QUAD-4 has additional 3by3 mode shape between 8 and 9th modes.

9) Cantilevered Square Membrane

REFERENCE	NAFEMS[1]
ELEMENTS	Shell elements
MODEL FILENAME	Eigen9.mpb

The figure below shows a cantileverd square membrane whose left end has been fixed. Displacement in the z-direction is restrained, and thus the resulting mode shapes are purely in-plane.

Figure 2.3.9.1 Cantiilevered square membrane model

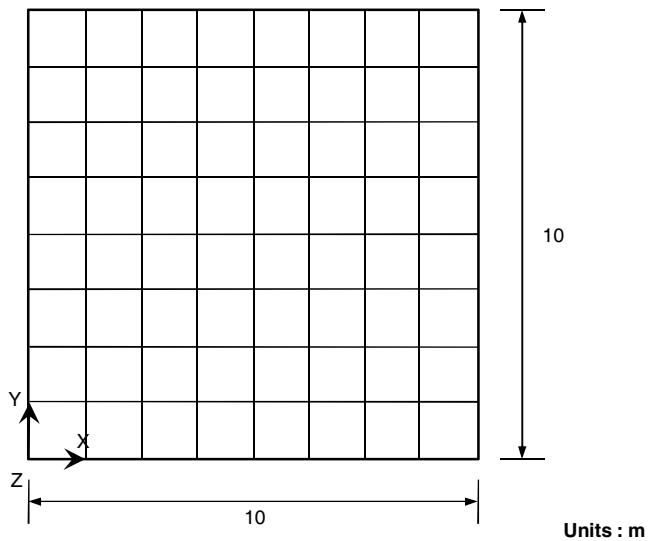

z = 0 at all nodes
x = y = 0 along y-axis

Material data	Elastic modulus	E = 200 GPa
	Poisson's ratio	ν = 0.3
	Mass density	ρ= 8000 kg/m^3
Section property	Thickness	t = 0.05 m
Mass option		Coupled mass

Figure 2.3.9.2
Vibration mode shapes

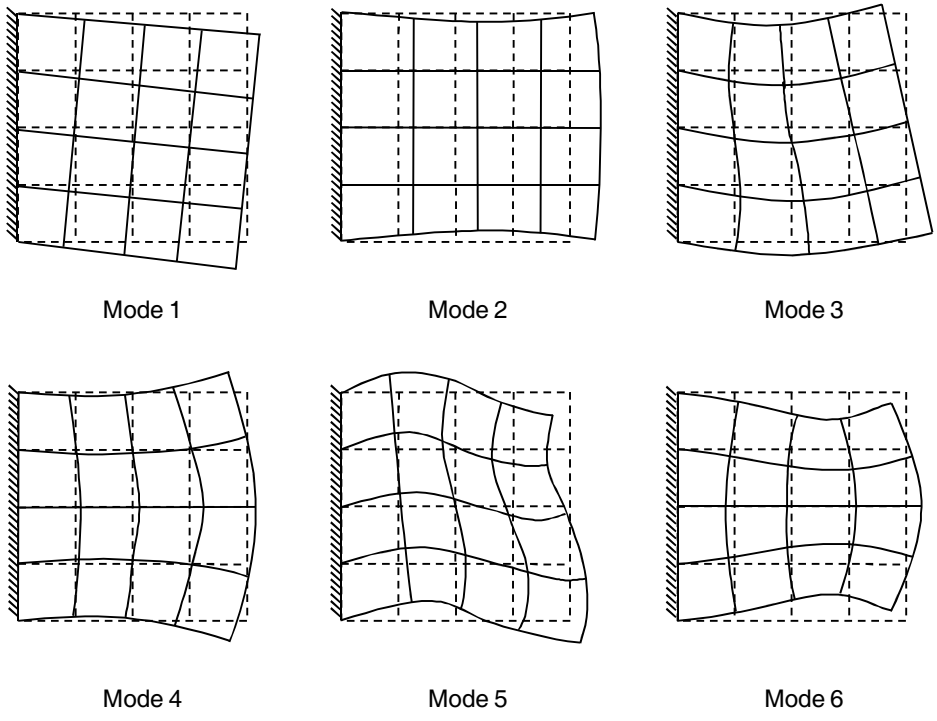

Table 2.3.9.1 Natural frequencies in Hz obtained using shell elements

Mode Number		1	2	3	4	5	6
Reference		*52.404*	*125.69*	*140.78*	*222.54*	*241.41*	*255.74*
Element type	Number of elements						
TRIA-3	128	*53.788*	*126.28*	*144.45*	*234.70*	*249.57*	*263.48*
QUAD-4	8x8	*52.726*	*126.06*	*142.76*	*226.95*	*247.22*	*259.43*

10) Cantilevered Tapered Membrane

REFERENCE	NAFEMS[2]
ELEMENTS	Shell elements
MODEL FILENAME	Eigen10.mpb

The figure below shows a cantilever beam whose cross section is rotated by 90 degrees at its free end. The left end is fixed. There are unit loads exerted in all directions at the right end. The in-plane/out-of-plane motion may be verified through the displacement at the loading point.

Figure 2.3.10.1
Cantilevered tapered membrane model

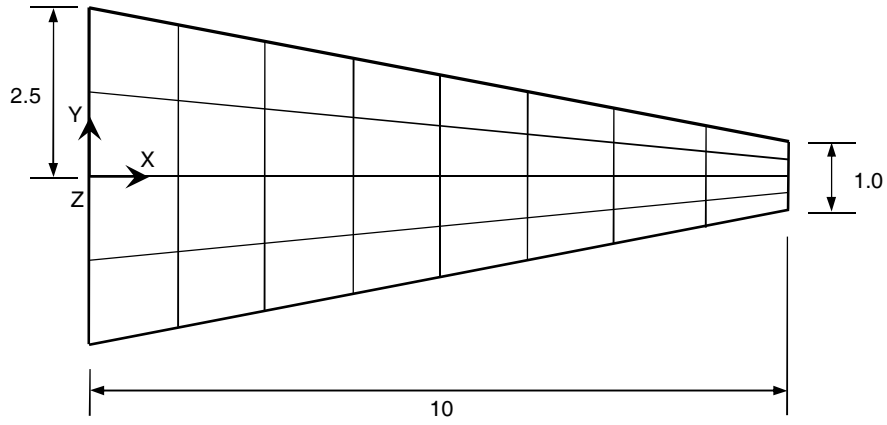

z = 0 at all nodes
x = y = 0 along y-axis

Material data	Elastic modulus	*E = 200 GPa*
	Poisson's ratio	$\nu = 0.3$
	Mass density	$\rho = 8000\ kg/m^3$
Section property	Thickness	*t = 0.05 m*
Mass option		*Coupled mass*

Figure 2.3.10.2
Mode shapes of
vibration

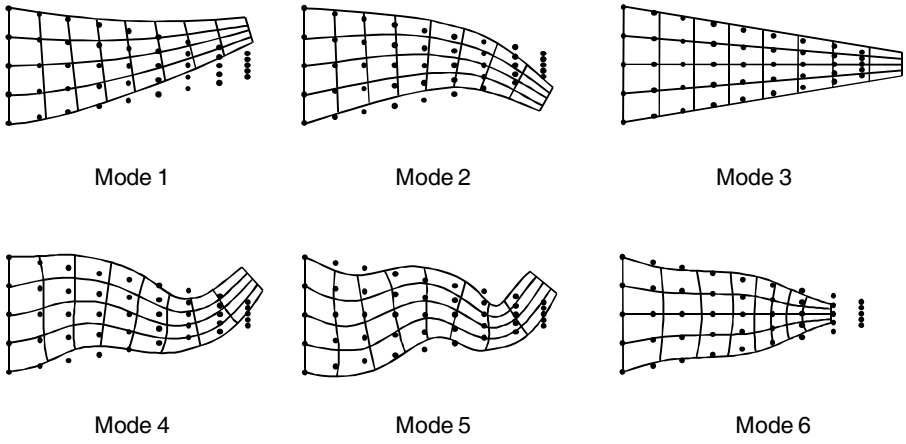

Table 2.3.10.1 Natural frequencies in Hz obtained using shell elements

Mode Number		1	2	3	4	5	6
Reference		*44.623*	*130.03*	*162.70*	*246.05*	*379.90*	*391.44*
Element type	Number of elements						
TRIA-3	256	*45.643* *44.725**	*134.53* *130.60**	*162.92* *162.89**	*258.37* *247.94**	*393.48* *384.41**	*404.95* *393.13**
QUAD-4	16x8	*44.647* *44.628**	*131.04* *130.20**	*162.80* *162.72**	*250.33* *246.82**	*391.54* *382.03**	*393.10* *392.84**

* obtained using shell element formulations with 6-dof per node.

11) Cantilever Beam with Irregular Mesh

REFERENCE	NAFEMS[1]
ELEMENTS	Beam elements
MODEL FILENAME	Eigen11.mpb

The figure below shows a 2-dimensional cantilever beam whose left end is fixed. In the figure, a and b signify the lengths of each beam element. The modal analysis will give different results depending on the ratio of length a to b.

Figure 2.3.11.1
Cantilever beam model

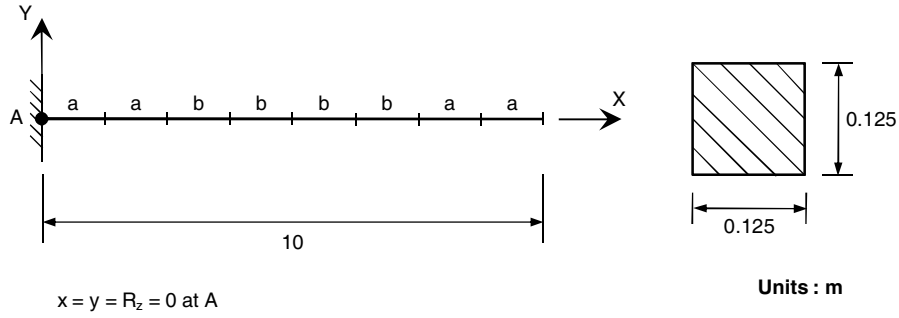

Material data	Elastic modulus Mass density	*E = 200 GPa* *ρ= 8000 kg/m^3*
Section property	Square cross-section	*0.125 m X 0.125 m*
Mass option		*Coupled mass*

Table 2.3.11.1 Natural frequencies in Hz obtained using beam elements

Mode Number		1	2	3	4	5	6
Reference		*1.010*	*6.327*	*17.716*	*34.717*	*57.390*	*85.730*
Element type	Length ratio						
Beam-2	a = b	*1.010*	*6.323*	*17.698*	*34.694*	*57.470*	*86.230*
	a = 10b	*1.010*	*6.327*	*17.796*	*34.873*	*60.626*	*101.694*
	a = 100b	*1.010*	*6.330*	*17.824*	*35.080*	*64.766*	*104.671*

12) Cylindrical Shell with Rigid Diaphgrams

REFERENCE	Soedel[3]
ELEMENTS	Shell elements
MODEL FILENAME	Eigen12.mpb

The figure below shows a cylindrical shell with rigid diaphragms. Only a quarter of the complete shape has been modeled to take advantage of symmetry conditions. Symmetrical boundary conditions are applied, so only symmetrical mode shapes will be produced.

Figure 2.3.12.1
Cylindrical shell model with rigid diaphragms

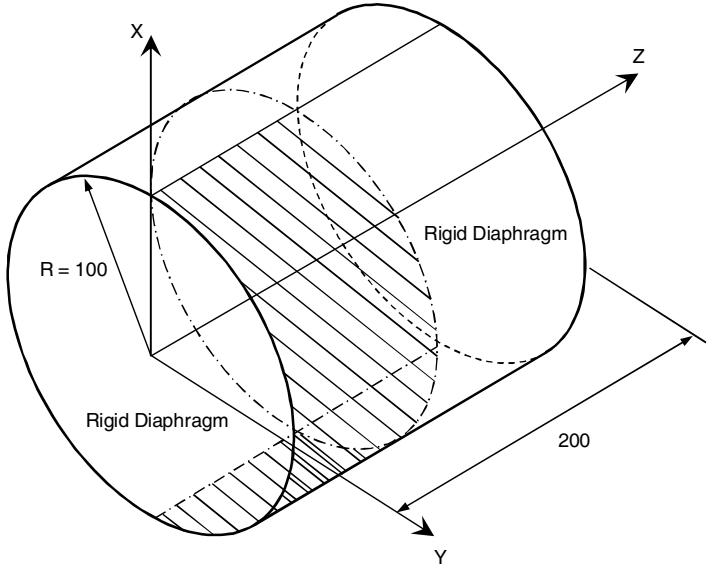

Material data	Elastic modulus	$E = 2.06\times10^{45}$N/mm^2
	Poisson's ratio	$\nu = 0.3$
	Mass density	$\rho = 7.85\times10^{-9}$ kg/mm^3
Section property	Thickness	$t = 2$ mm
Mass option		*Lumped mass*
Element setting	Unique shell normal generation	*Off*

Figure 2.3.12.2
Vibration mode shapes

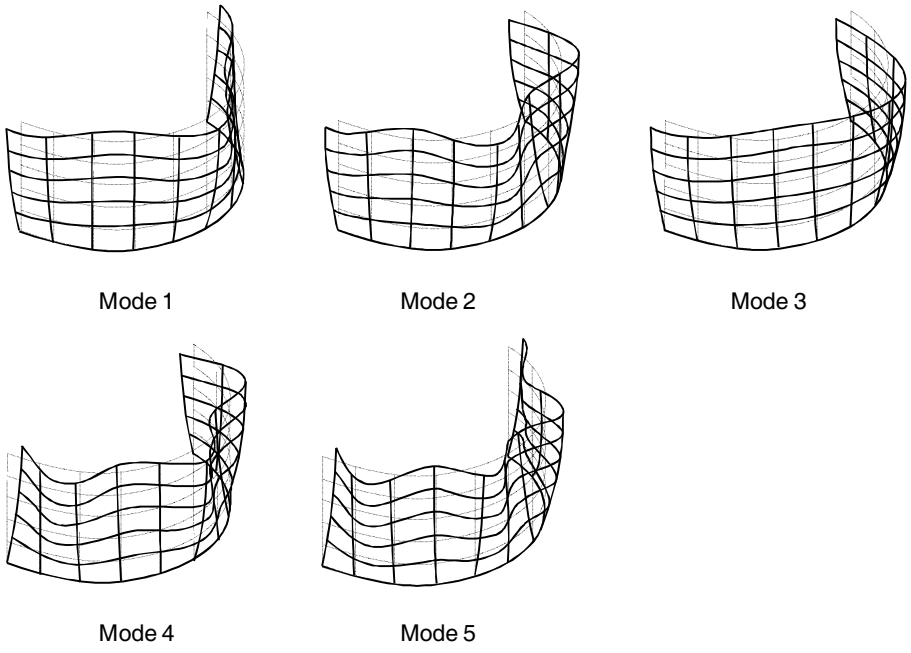

Table 2.3.12.1 Natural frequencies in Hz obtained using shell elements

Mode Number		1	2	3	4	5
Reference		*1342.5*	*1464.8*	*1725.9*	*1892.4*	*2493.1*
Element type	Number of elements					
TRIA-3	400	*1366.0*	*1495.2*	*1745.0*	*1942.0*	*2580.8*
QUAD-4	10x20	*1343.5*	*1470.0*	*1728.8*	*1910.8*	*2535.3*

13) Beam with Elastic Supports

REFERENCE	Timoshenko et al.[4]
ELEMENTS	Beam elements, mass, spring
MODEL FILENAME	Eigen13.mpb

The figure below shows a beam with a lumped mass attachment. The beam is supported by two elastic s prings. To study the effects due to the lumped mass only, the mass of the beam is neglected and only its stiffness is incorporated into the analysis.

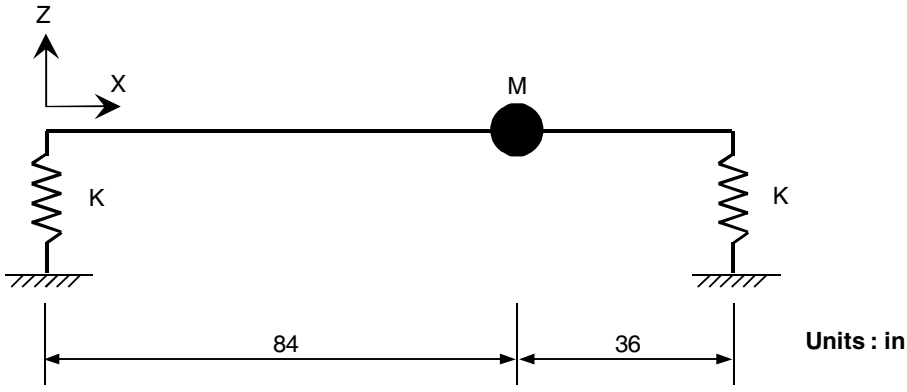

Figure 2.3.13.1 Simple beam with a lumped mass supported on two springs

Material data	Elastic modulus	$E = 3.0 \times 10^7$ *psi*
	Mass	$M = 1000/386$ *lbm*
	Spring constant	$K = 300$ *lbf/in*
Section property	Moment of inertia	$I_x = 1.0$ *in*^{4}

Table 2.3.13.1 Natural frequencies in Hz

Mode Number		1
Reference		*1.875*
Element type	Number of elements	
Beam-2	2	1.875

References

[1] NAFEMS, "Selected Benchmarks for Natural Frequency Analysis", Issue 2, NAFEMS, Glasgow, 1987
[2] NAFEMS, "The Standard NFAFEMS Benchmarks ", Rev.3, NAFEMS, Glasgow, 1990
[3] W. Soedel, “Vibrations of Shells and Plates”, 2nd Edition, Marcel Dekker, New York, 1993
[4] Timoshenko, Young and Weaver, "Vibration Problems in Engineering”, 4th Edition

2.4 Buckling Analysis Examples

1) Column Buckling

REFERENCE	Gere et al[1]
ELEMENTS	Beam elements, shell elements, solid elements
MODEL FILENAME	Buckling01.mpb

The figure below shows a column model whose buckling mode shapes depend on its boundary conditions.

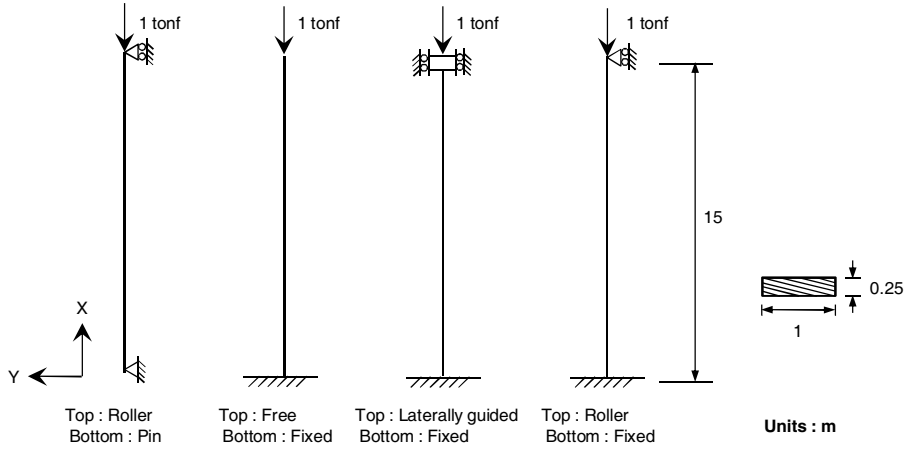

Figure 2.4.1.1
Column model

Material data	Elastic modulus	$E = 10000\ tonf/m^2$
Section property	Rectangular cross-section No shear deformations	*0. 25 m x 1.0 m*

Figure 2.4.1.2
Buckling mode shapes

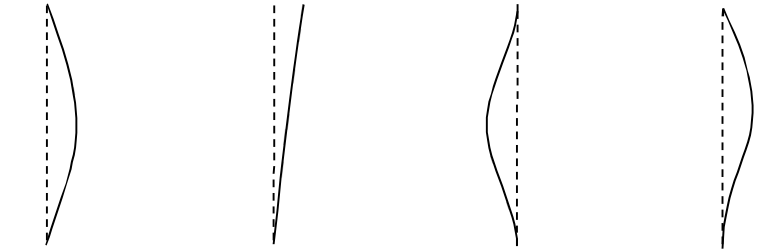

Table 2.4.1.1 Critical loads in tonf obtained using beam elements

Case		1	2	3	4
Reference		*0.5712*	*0.1428*	*2.2846*	*1.1684*
Element type	Number of elements				
Beam-2	15	*0.5714*	*0.1428*	*2.2847*	*1.1685*

Table 2.4.1.2 Critical loads in tonf obtained using shell elements

Case		1	2	3	4
Reference		*0.5712*	*0.1428*	*2.2846*	*1.1684*
Element type	Number of elements				
TRIA-3	30	*0.5741*	*0.1430*	*2.3323*	*1.1812*
QUAD-4	15	*0.5736*	*0.1429*	*2.3245*	*1.1790*

Table 2.4.1.3 Critical loads in tonf obtained using solid elements

Case		1	2	3	4
Reference		*0.5712*	*0.1428*	*2.2846*	*1.1684*
Element type	Number of elements				
HEXA-8	15	*0.5747*	*0.1430*	*2.3421*	*1.1841*

2) Portal Frame

REFERENCE	Timoshenko et al[2]
ELEMENTS	Beam elements
MODEL FILENAME	Buckling02.mpb

The figure below shows a portal frame modeled as a two-dimensional rahmen structural model. There are two concentrated vertical loads applied on the structure. The critical buckling load will change as a function of the number of elements.

Figure 2.4.2.1
Portal Frame Model

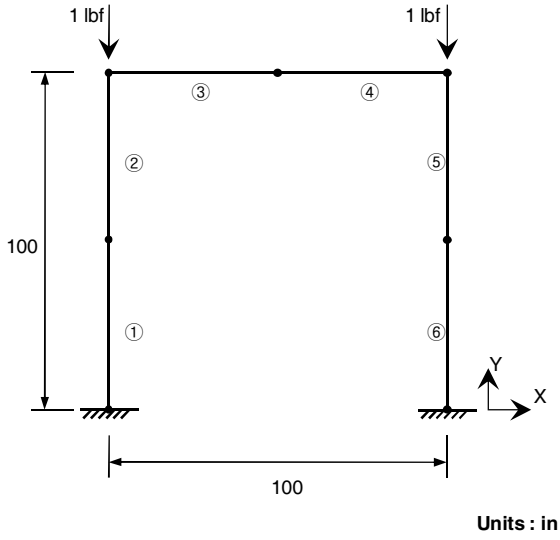

Material data	Elastic modulus	$E = 1 \times 10^6$ *psi*
Section property	Area	$A = 1.0$ *in*^{2}
	Moment of inertia	$I_x = 1.0$ *in*^{4}

Figure 2.4.2.2
Buckling mode shapes

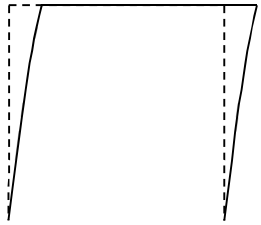

Table 2.4.2.1 Critical loads in tonf obtained using beam elements

Reference		*737.9*
Element type	Number of elements	
Beam-2	2 per member	*739.8*
	4 per member	*737.6*
	8 per member	*737.5*

3) Clamped Square Plate

REFERENCE	Chajes[3]
ELEMENTS	Shell elements, solid elements
MODEL FILENAME	Buckling03.mpb

The figure below shows a clamped square plate subject to in-plane pressure. Using symmetry conditions, only a quarter of the complete shape was modeled.

Figure 2.4.3.1
Clamped square plate model

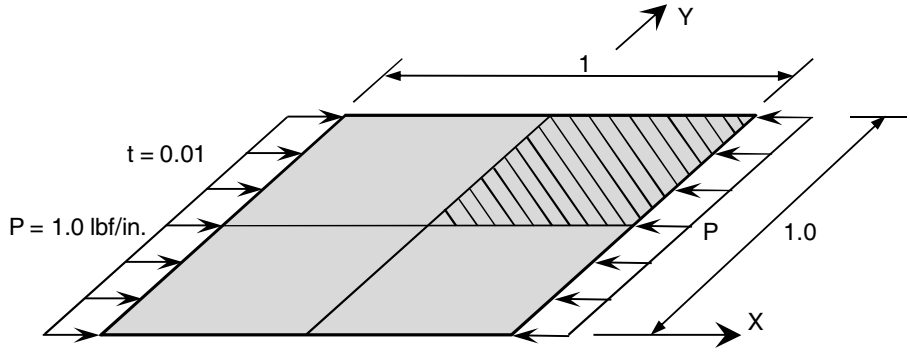

Units : in.

Material data	Elastic modulus	$E = 11.164 \times 10^6$ *psi*
	Poisson's ratio	$\nu = 0.3$
Section property	Thickness	*T = 0.01 in*

Figure 2.4.3.2
Buckling mode shapes

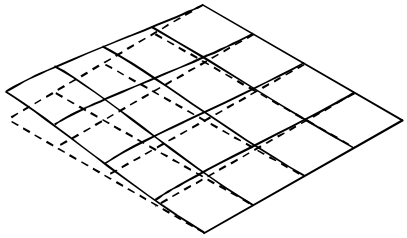

Table 2.4.3.1 Critical loads in lbf obtained using shell elements

Reference		*100.7*
Element type	Number of elements	
TRIA-3	32	*111.7*
QUAD-4	16	*107.3*

Table 2.4.3.2 Critical loads in lbf obtained using solid elements

Reference		*100.7*
Element type	Number of elements	
HEXA-8	16	*98.0*

4) In-Plane Buckling of Square Plate

REFERENCE	Timoshenko et al[2]
ELEMENTS	Shell elements, solid elements
MODEL FILENAME	Buckling04.mpb

The figure below shows a square plate whose out-of-plane motion is simply supported, and the motion of the bottom side is restrained in the in-plane y-axis direction. The centerpoint of the top side (point E) is subject to a concentrated load. In-plane critical buckling loads are computed.

Figure 2.4.4.1
Clamped square plate model

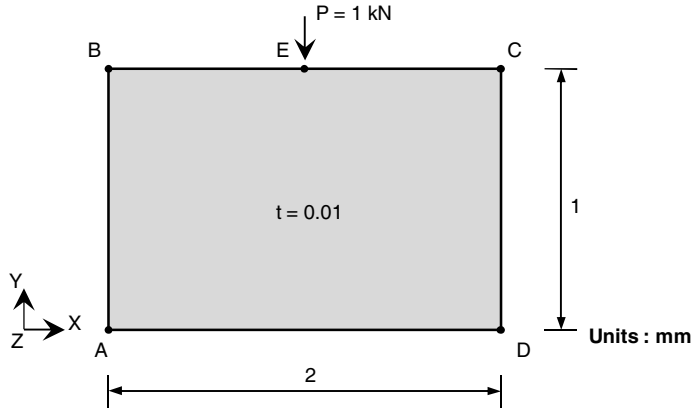

Material data	Elastic modulus	$E = 200\ GPa$
	Poisson's ratio	$\nu = 0.3$
Section property	Thickness	$t = 0.01\ mm$

Table 2.4.4.1 Critical loads in kN obtained using shell elements

Reference		*330*
Element type	Number of elements	
TRIA-3	144	*342*
QUAD-4	72	*327*

Table 2.4.4.2 Critical loads in kN obtained using solid elements

Reference		*330*
Element type	Number of elements	
HEXA-8	72	*298*

5) Axially Compressed Cylinder

REFERENCE	Simo et al.[4]
ELEMENTS	Shell elements, solid elements
MODEL FILENAME	Buckling05.mpb

The figure below shows an axially compressed cylinder whose lateral motion has been restrained. Using symmetry, half of its axial length and a quarter of the circular shape was modeled.

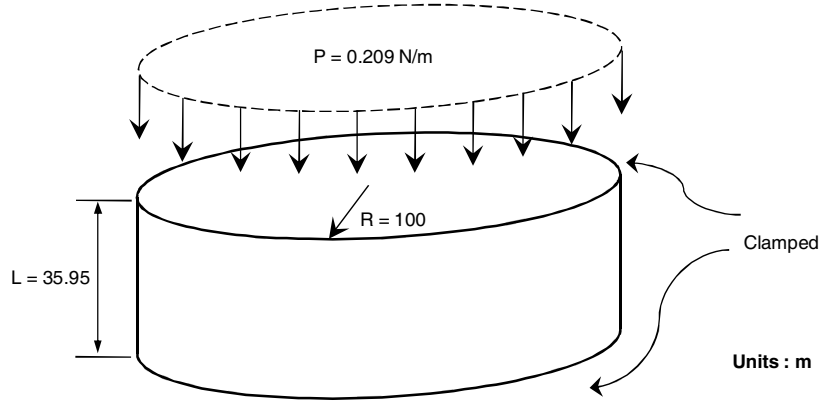

Figure 2.4.5.1
Axially compressed cylinder model

Material data	Elastic modulus	$E = 567\ Pa$
	Poisson's ratio	$\nu = 0.3$
Section property	Thickness	$t = 0.247\ m$

Figure 2.4.5.2
Buckling mode shapes

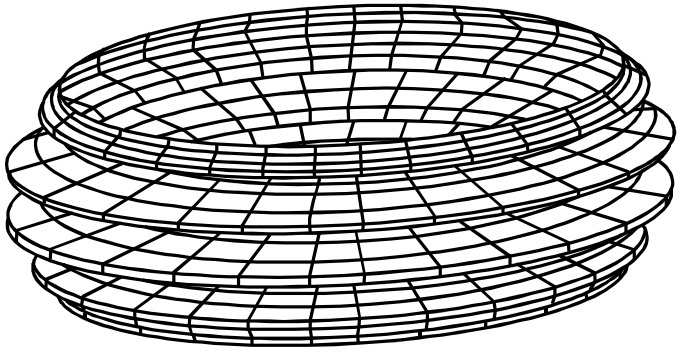

Table 2.4.5.1 Critical load factor obtained using shell elements

Reference		*1.0833*
Element type	Number of elements	
TRIA-3	840	*1.2016**
QUAD-4	420	*1.0734*

* obtained from 10th buckling mode

Table 2.4.5.2 Critical load factor obtained using solid elements

Reference		*1.0833*
Element type	Number of elements	
HEXA-8	420	*1.0631*

6) L-bracket plate

REFERENCE	Simo et al.[4] and Argyris et al.[5]
ELEMENTS	Shell elements, solid elements
MODEL FILENAME	Buckling06.mpb

The figure below shows an L-bracket plate that is subject to in-plane loading. Critical lateral buckling loads occur due to the in-plane moments caused by the loading.

Figure 2.4.6.1
L-bracket plate model

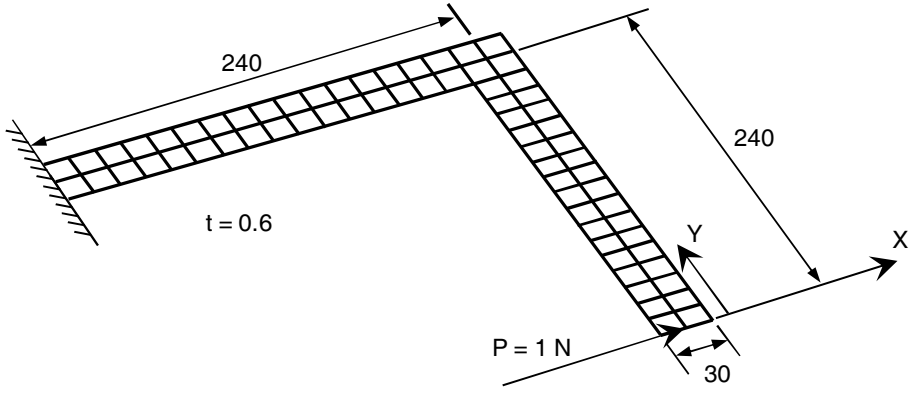

Units : mm

Material data	Elastic modulus	*E = 71.24 GPa*
	Poisson's ratio	ν *= 0.3*
Section property	Thickness	*t = 0.6 mm*

Figure 2.4.6.2
Buckling mode shapes

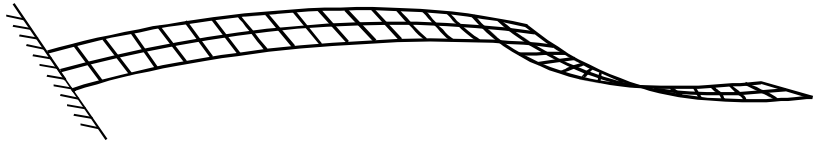

Table 2.4.6.1 Critical loads in N obtained using shell elements

Reference		*1.137 (Simo et al.), 1.155 (Argyris et al.)*
Element type	Number of elements	
TRIA-3	136	*1.187*
QUAD-4	68	*1.199*

Table 2.4.6.2 Critical loads in N obtained using solid elements

Reference		*1.137 (Simo et al.), 1.155 (Argyris et al.)*
Element type	Number of elements	
HEXA-8	68	*1.198*

Reference

1 J.M. Gere and S.P. Timoshenko, “Mechanics of Materials”, 2nd Edition, Thomson Brooks/Cole, California, New York, 1984
2 S.P. Timoshenko and J.M. Gere, “Theory of Elastic Stability”, 2nd Edition, McGraw-Hill, New York, 1961
3 A. Chajes, “Principles of Structural Stability Theory”, Prentice-Hall, Englewood Cliffs, N.J, 1974
4 J.C. Simo, D.D. Fox and M.S. Rifai, “On a Stress Resultant Geometrically Exact Shell Model. Part III: The Computational Aspects of the Nonlinear Theory”, Computer Methods in Applied Mechanics and Engineering, Vol. 79, pp.21-70, 1990
5 J.H. Argyris, H.Balmer, J.St. Doltsinis, P.C. Dunne, M. Haase, M. Kleiber, G.A. Malejannakis, H.P. Malejenek, M. Muller and D.W. Scharpf, “Finite Element Method – Ther natural approach”, Computer Methods in Applied Mechanics and Engineering, VOl. 17/18, pp. 1-106, 1979

Section 3

Effective Mass and Mode Superposition Method

3.1 Effective Mass

When the natural frequency/period and mode shapes have been calculated, other useful numbers like effective mass and mass participation factor may also be computed. The modal participation factor of the i th mode is represented by $\Gamma_{i\alpha}$ and can be determined as follows:

$$\Gamma_{i\alpha} = \frac{1}{m_i}\phi_i^T \mathbf{M}\mathbf{T}_\alpha \ , \quad \alpha = 1,2,3,4,5,6 \quad \text{(no summation)}$$
$$m_i = \phi_i^T \mathbf{M}\phi_i \quad \text{(generalized mass)} \tag{5.3.1}$$

α : Direction of the degree of freedom (1~3 : displacement, 4~6 : rotation)

Here, $\mathbf{T}_\alpha$ represents the size of the rigid body motion in each respective direction, and is set up to maintain the characteristics of each node.

$$\begin{bmatrix} 1 & 0 & 0 & 0 & z-z_0 & y_0-y \\ 0 & 1 & 0 & z_0-z & 0 & x-x_0 \\ 0 & 0 & 1 & y-y_0 & x_0-x & 0 \\ 0 & 0 & 0 & 1 & 0 & 0 \\ 0 & 0 & 0 & 0 & 1 & 0 \\ 0 & 0 & 0 & 0 & 0 & 1 \end{bmatrix} \begin{Bmatrix} e_1 \\ e_2 \\ e_3 \\ e_4 \\ e_5 \\ e_6 \end{Bmatrix}, \quad e_\beta = \delta_{\alpha\beta} \tag{5.3.2}$$

x_0, y_0, z_0 signify the centers of rotation. In midas nGen the centers of rotation are based on the entire model's center of mass (including the mass of restrained nodes).

Effective modal mass is also calculated in each direction, and may be calculated by using all participation factors as shown below:

$$m_{i\alpha}^{eff} = (\Gamma_{i\alpha})^2 m_i \tag{5.3.3}$$

The mode shape for a restrained degree of freedom is always zero. If all the effective modal masses are summed, then the value should be equal to the mass of the entire model excluding the mass of the restrained masses. Thus, even if all modes are calculated, because the masses of the restrained nodes are excluded, the mass participation factor should be slightly less than 100%. Consequently, when calculating the mass participation factor, it is typical to exclude the mass of the restrained nodes from the total mass.

3.2 Modal Superposition Method

In dynamic response analysis, midas nGen offers the ability to apply modal superposition. Modal superposition method solves the linear dynamic equilibrium equation (as shown below) not directly but through a modal equilibrium equation that has reduced the size of the problem through eigenvalue analysis.

$$\mathbf{M}\ddot{\mathbf{u}}(t) + \mathbf{C}\dot{\mathbf{u}}(t) + \mathbf{K}\mathbf{u}(t) = \mathbf{f}(t) \tag{5.3.4}$$

If displacement in space coordinates is written as $\mathbf{u}(t)$, then it may be written as a function of the natural mode shape $\boldsymbol{\Phi}$ and strain functions $\xi(t)$ as follows:

$$\mathbf{u}(t) = \boldsymbol{\Phi}\boldsymbol{\xi}(t), \ \boldsymbol{\Phi} = [\phi_1 \quad \phi_2 \quad \ldots \quad \phi_N] \tag{5.3.5}$$

Using the this, then the dynamic equilibrium equation (Equation 5.3.4) may be expressed in modal coordinates as the following:

$$[\mathbf{\Phi}^T\mathbf{M}\,\mathbf{\Phi}]\ddot{\xi}(t)+[\mathbf{\Phi}^T\mathbf{C}\,\mathbf{\Phi}]\dot{\xi}(t)+[\mathbf{\Phi}^T\mathbf{K}\,\mathbf{\Phi}]\xi(t)=\mathbf{\Phi}^T\mathbf{f}(t) \tag{5.3.6}$$

Typically, when applying modal superposition, higher order modes are neglected and only lower modes are considered in order to constitute the natural mode shape $\mathbf{\Phi}$. Thus, Equation 5.3.6 is considered an approximation of Equation 5.3.4. Thus, if not enough modes are included in the analysis, then the results may not demonstrate the true physical displacements in the model and accuracy may be greatly compromised.

The modal equilibrium equation (Equation 5.3.6) may be expressed as an independent function for each mode, in the case where the modal damping matrix $\mathbf{\Phi}^T\mathbf{C}\mathbf{\Phi}$ is zero:

$$m_i\ddot{\xi}_i(t)+k_i\xi_i(t)=p_i(t) \tag{5.3.7}$$

m_i : ith modal mass
p_i : ith mode loading
k_i : ith modal stiffness
ξ_i : ith mode strain

Likewise, when using modal superposition, the number of unknown variables may be reduced to the number of calculated natural modes. Of course, if each mode may be isolated, then the modal dynamic equilibrium equation may be solved much more efficiently.

Damping

After reducing the size of the modal equilibrium equation (Equation 5.3.6) using natural modes and decoupling the modes with a diagonal damping matrix ($\mathbf{\Phi}^T\mathbf{C}\mathbf{\Phi}$), then the equilibrium equation may be expressed in modal functions like Equation 5.3.7:

$$m_i\ddot{\xi}_i(t) + b_i\dot{\xi}_i(t) + k_i\xi_i(t) = p_i(t) \tag{5.3.8}$$

b_i : i[th] mode damping coefficient

It also may be expressed as the following:

$$\ddot{\xi}_i(t) + 2\zeta_i\omega_i\dot{\xi}_i(t) + \omega_i^2\xi_i(t) = \frac{1}{m_i}p_i(t) \tag{5.3.9}$$

$\zeta_i = b_i/(2m_i\omega_i)$: Mode damping ratio

$\omega_i^2 = k_i/m_i$: Mode frequency

midas nGen offers users the ability to set the value of damping for each mode. In this option, the modal damping value is added to the modal damping matrix $\mathbf{\Phi}^T\mathbf{C}\mathbf{\Phi}$ that has been constructed from mass-proportional damping, stiffness-proportional damping, or other typical damping values. Therefore, decoupling of the modal equilibrium equation can only occur when the modal damping matrix $\mathbf{\Phi}^T\mathbf{C}\mathbf{\Phi}$ is a diagonal matrix. For this to occur, proportional damping coefficients and structural damping must be consistent and/or springs/dampers must not exist in the model. If not, the modal damping matrix will not be a diagonal matrix and computation can only proceed with the coupled modal equilibrium equations.

Enforced Motion

Enforced motion may not be applied directly to the modal equilibrium equation. Midas nGen applies the enforced motion through the following process.

First, the equilibrium equation (Equation 5.3.4) is separated into degrees of freedom that are subject to enforced motion and degrees of freedom that are not.

$$\begin{bmatrix}\mathbf{M}_{11} & \mathbf{M}_{12}\\ \mathbf{M}_{21} & \mathbf{M}_{22}\end{bmatrix}\begin{Bmatrix}\ddot{\mathbf{u}}_1\\ \ddot{\mathbf{u}}_2\end{Bmatrix} + \begin{bmatrix}\mathbf{C}_{11} & \mathbf{C}_{12}\\ \mathbf{C}_{21} & \mathbf{C}_{22}\end{bmatrix}\begin{Bmatrix}\dot{\mathbf{u}}_1\\ \dot{\mathbf{u}}_2\end{Bmatrix} + \begin{bmatrix}\mathbf{K}_{11} & \mathbf{K}_{12}\\ \mathbf{K}_{21} & \mathbf{K}_{22}\end{bmatrix}\begin{Bmatrix}\mathbf{u}_1\\ \mathbf{u}_2\end{Bmatrix} = \begin{Bmatrix}\mathbf{f}_1\\ \mathbf{f}_2\end{Bmatrix} \tag{5.3.10}$$

$\mathbf{u}_1$: Displacement of degree of freedom not subject to enforced motion

$\mathbf{u}_2$: Displacement of degree of freedom subject to enforced motion

$\mathbf{f}_1$: Loading on degree of freedom not subject to enforced motion

$\mathbf{f}_2$: Loading on degree of freedom subject to enforced motion

Displacement $\mathbf{u}_1$ may then be separated into quasi-static displacement $\mathbf{u}_1^{qs}$ and dynamic relative displacement $\mathbf{y}$.

$$\begin{aligned}\mathbf{u}_1 &= \mathbf{u}_1^{qs} + \mathbf{y} \\ \mathbf{u}_1^{qs} &= -\mathbf{K}_{11}^{-1}\mathbf{K}_{12}\mathbf{u}_2\end{aligned} \tag{5.3.11}$$

Rearranging the equation with respect to the dynamic relative displacement $\mathbf{y}$:

$$\mathbf{M}_{11}\ddot{\mathbf{y}} + \mathbf{C}_{11}\dot{\mathbf{y}} + \mathbf{K}_{11}\mathbf{y} = \mathbf{f}_1 + \left(\mathbf{M}_{11}\mathbf{K}_{11}^{-1}\mathbf{K}_{12} - \mathbf{M}_{12}\right)\ddot{\mathbf{u}}_2 \tag{5.3.12}$$

This equation omits the damping term on the right handside. Applying modal superposition, the equation may be expressed as a function of the modal relative displacement x, using $\mathbf{y}(t) = \mathbf{\Phi}_{11}\mathbf{x}(t)$:

$$\begin{gathered}\left[\mathbf{\Phi}_{11}^T\mathbf{M}_{11}\mathbf{\Phi}_{11}\right]\ddot{\mathbf{x}} + \left[\mathbf{\Phi}_{11}^T\mathbf{C}_{11}\mathbf{\Phi}_{11}\right]\dot{\mathbf{x}} + \left[\mathbf{\Phi}_{11}^T\mathbf{K}_{11}\mathbf{\Phi}_{11}\right]\mathbf{x} = \mathbf{\Phi}_{11}^T\left[\mathbf{f}_1 + \left(\mathbf{M}_{11}\mathbf{K}_{11}^{-1}\mathbf{K}_{12} - \mathbf{M}_{12}\right)\ddot{\mathbf{u}}_2\right] \\ \mathbf{u}_1 = \mathbf{u}_1^{qs} + \mathbf{y} = -\mathbf{K}_{11}^{-1}\mathbf{K}_{12}\mathbf{u}_2 + \mathbf{\Phi}_{11}\mathbf{x}\end{gathered} \tag{5.3.13}$$

If $\mathbf{K}_{11}$ is singular due the existence of a rigid-body mode, then mass shifting may be used on the stiffness matrix $\mathbf{K}_{11}$ with mass matrix $\mathbf{M}_{11}$ to remove this singularity.

Residual Vector

Before proceeding with modal superposition, it is important to remain cautious of errors due to higher order modes that are not included in the natural mode shape $\mathbf{\Phi}$, as was previously explained. To reduce these errors, midas nGen uses the residual vector $\mathbf{R}$, which is constructed to be orthogonal to the basic natural modes by using the mass matrix $\mathbf{M}$ and stiffness matrix $\mathbf{K}$.

$$\mathbf{R} = \mathbf{K}^{-1}(\mathbf{I} - \mathbf{M}\mathbf{\Phi}\mathbf{\Phi}^T)\mathbf{F} \tag{5.3.14}$$

Here, $\mathbf{F}$ is typically the loading vector. If there are damping elements, then damping is included. Midas nGen follows the methods proposed by Dickens and other authors[3], and finds augmented mode shapes orthogonal to one another based on the residual vector $\mathbf{R}$. Then, these augmented mode shapes are added to the fundamental mode shape $\mathbf{\Phi}$ and then modal superposition is applied.

[3] J.M. Dickens, J.M. Nakagawa, and M.J. Wittbrodt, "A Critique of Mode Acceleration and Modal Truncation Augmentation Methods for Modal Response Analysis" Computers & Structures, Vol 62, No. 6, 1997, pp. 985-998

Section 4

Dynamic Response Analysis

4.1 Time Integration

In midas nGen, the transient response to the linear equation of motion (such as in Equation 5.3.4) can be computed using direct time integration and mode superposition. Direct time integration for linear problems use the implicit method.

Implicit Direct Time Integration

The implicit direct time integration in midas nGen uses the α method ($\mathrm{HHT}-\alpha$)[1] proposed by Hilber, Hughes, and Taylor. $\mathrm{HHT}-\alpha$ is a generalized Newmark method[2] and has an adjustable, numerical damping effect. Through this, high frequency noise can be eliminated, and, like the Newmark method, has second order accuracy with respect to the timestep. The HHT-α method uses a modified dynamic equilibrium equation as shown below:

$$\mathbf{M}\,\mathbf{a}^{n+1} + (1+\alpha_H)\left[\mathbf{C}\,\mathbf{v}^{n+1} + \mathbf{f}^{\mathrm{int},n+1} - \mathbf{f}^{ext,n+1}\right] - \alpha_H\left[\mathbf{C}\,\mathbf{v}^{n} + \mathbf{f}^{\mathrm{int},n} - \mathbf{f}^{ext,n}\right] = \mathbf{0} \tag{5.4.1}$$

Here, $\mathbf{a}^{n+1}$ and $\mathbf{v}^{n+1}$ signify the acceleration and velocity at the $n+1$ th timestep, respectively. $\alpha_H \in [-1/3, 0]$ is a coefficient that determines the numerical damping effect. Incorporating effects due to non-mechnical strains (e.g. thermal expansion) and internal forces due to prestressing and pore water pressure, the internal force in linear analysis is expressed as the following equation which includes the product of the stiffness matrix and degrees of freedom:

---

[1] H.M Hilber, T.J.R. Hughes, and R.L. Taylor, "Improved Numerical Dissipation for Time Integration Algorithms in Structural Dynamics," Earthquake Engineering and Structural Dynamics, Vol 5, No. 3, 1977, pp. 283-292

[2] .M. Newmark, "A Method of Computation for Structural Dynamics," ASCE Journal of the Engineering Mechanics Division, Vol. 5, No. EM3, 1959, pp. 67-94

$$\mathbf{f}^{\text{int},n+1} = \mathbf{K}\mathbf{u}^{n+1} - \mathbf{f}^{\text{nonmech},n+1} + \mathbf{f}^{\text{int},0} \tag{5.4.2}$$

If the time difference equation of the Newmark method is introduced, the relationship between velocity, displacement, and acceleration at time steps n, $n+1$ may be expressed as shown below:

$$\begin{aligned}
\mathbf{v}^{n+1} &= \mathbf{v}^n + \Delta t\left[\gamma\mathbf{a}^{n+1} + (1-\gamma)\mathbf{a}^n\right] \\
\mathbf{u}^{n+1} &= \mathbf{u}^n + \Delta t\mathbf{v}^n + \frac{1}{2}\Delta t^2\left[2\beta\mathbf{a}^{n+1} + (1-2\beta)\mathbf{a}^n\right]
\end{aligned} \tag{5.4.3}$$

If Equation 5.4.1 (equilibrium equation) is rearranged with Equations 5.4.2 and 5.4.3, then the displacement at time $n+1$ may be written as the unknown variable and the system of simultaneous equations may be written as shown below:

$$\begin{aligned}
&\mathbf{K}^{eff}\mathbf{u}_{n+1} = \mathbf{f}^{eff} \\
&\mathbf{K}^{eff} = \frac{1}{\beta\Delta t^2}\mathbf{M} + \frac{(1+\alpha_H)\gamma}{\beta\Delta t}\mathbf{C} + (1+\alpha_H)\mathbf{K}, \\
&\mathbf{f}^{eff} = -\mathbf{f}^{\text{int},0} + (1+\alpha_H)\left[\mathbf{f}^{ext,n+1} + \mathbf{f}^{nonmech,n+1}\right] - \alpha_H\left[\mathbf{f}^{ext,n} + \mathbf{f}^{nonmech,n}\right] + \\
&\quad \mathbf{M}\left[\frac{1}{\beta\Delta t^2}\mathbf{u}^n + \frac{1}{\beta\Delta t}\mathbf{v}^n + \left(\frac{1}{2\beta} - 1\right)\mathbf{a}^n\right] + \\
&\quad \mathbf{C}\left[\frac{(1+\alpha_H)\gamma}{\beta\Delta t}\mathbf{u}^n + \left\{\frac{(1+\alpha_H)\gamma}{\beta} - 1\right\}\mathbf{v}^n + \Delta t(1+\alpha_H)\left(\frac{\gamma}{2\beta} - 1\right)\mathbf{a}^n\right] + \alpha_H\mathbf{K}\mathbf{u}^n
\end{aligned} \tag{5.4.4}$$

The righthandside $\mathbf{f}^{eff}$ in Equation 5.4.4 is determined by the external force and the calculated displacement, velocity, and acceleration at time step n. If the righthand side has been determined, then the system of simultaneous equations (explained in the previous paragraph) is applied to solve for the displacement at time $n+1$ ($\mathbf{u}_{n+1}$). This displacement may then be substituted into the Newmark difference equation (Equation 5.4.3) to obtain the velocity and acceleration at time $n+1$. The transient response of the structure follows this series of steps to carry out repeated time integration.

The lefthandside of Equation 5.4.4 shows an effective stiffness matrix $\mathbf{K}^{eff}$. If the time step is uniform throughout the analysis, then the decomposed matrix is reused and only the forward backward substitution is repeated, allowing for an efficient analysis scheme.

HHT $-\alpha$ time integration has unconditional stability if $\gamma = (1-2\alpha_H)/2$ and $\beta = (1-\alpha_H)^2/4$. If $\alpha_H = 0$, then the analysis becomes more specialized as the algorithm will resort to using a Newmark method that is based on average acceleration. Midas nGen uses $\alpha_H = -0.05$ as the default value.

Damping Effects

Midas nGen allows for mass-proportional damping and stiffness-proportional damping. As mentioned in Section 5.3.2, there is also modal damping that is only applied in modal superposition. The damping effects incorporated into linear time history analysis is applied to the damping matrix $\mathbf{C}$ as shown below:

$$\mathbf{C} = \alpha_j^e \mathbf{M}_j^e + \beta_j^e \mathbf{K}_j^e + \mathbf{B} \tag{5.4.5}$$

α_j^e : j[th] element mass-proportional damping coefficient

β_j^e : j[th] element stiffness-proportional damping coefficient

$\mathbf{M}_j^e$: j[th] element mass matrix

$\mathbf{K}_j^e$: j[th] element stiffness matrix

$\mathbf{B}$: Damping matrix due to damper elements

Application of Mode Superposition

In order to apply time integration that uses modal superposition, the mass in the modal equilibrium equation (Equation 5.3.6) may be factored to take on a value of 1 and the equation may be rewritten as the following:

$$\ddot{\xi}_i(t) + \overline{C}_{ij}\dot{\xi}_j(t) + \omega_i^2 \xi_i(t) = p_i(t) = p_i(t-\Delta t) + \frac{\Delta p_i}{\Delta t} t$$
$$\overline{C}_{ij} = [\overline{\mathbf{C}}]_{ij} = [\mathbf{\Phi}^T \mathbf{C} \mathbf{\Phi}]_{ij} \tag{5.4.6}$$

Time integration that replies on modal superposition can be divided into the following two cases depending on the coupling state of the modal damping matrix $\overline{C}_{ij}$:

① Uncoupled이 모드마 Uncoupled System

If the modal damping matrix $\overline{C}_{ij}$ is a diagonal matrix and the system becomes decoupled, then the response per mode may be calculated independent of the other modes. The displacement and velocity at each time step may be calculated as a function of the previous time step's displacement and velocity, as shown below. The mode-specific integration coefficients $a^i_{\alpha\beta}$, $b^i_{\alpha\beta}$ may be calculated using the initial conditions (the displacement and velocity at the previous time step) and the particular and homogeneous solutions of Equation 5.4.6.

$$\begin{bmatrix} \xi_i^{n+1} \\ \dot{\xi}_i^{n+1} \end{bmatrix} = \begin{bmatrix} a_{11}^i & a_{12}^i \\ a_{21}^i & a_{22}^i \end{bmatrix} \begin{bmatrix} \xi_i^n \\ \dot{\xi}_i^n \end{bmatrix} + \begin{bmatrix} b_{11}^i & b_{12}^i \\ b_{21}^i & b_{22}^i \end{bmatrix} \begin{bmatrix} p_i^n \\ p_i^{n+1} \end{bmatrix} \tag{5.4.7}$$

② Coupled System

If the modal damping matrix cannot be decoupled, then coupled modes must be considered and unlike the previous system, system response may not be computed on a per-mode basis. In this case, midas nGen decomposes the modal damping matrix into the diagonal component and the off-diagonal component. The damping due to the off-diagonal component is treated as an external load.

$$\overline{\mathbf{C}} = \overline{\mathbf{C}}_{diag} + \overline{\mathbf{C}}_{off} \tag{5.4.8}$$

As such, the modal displacements are independent and the modal velocities remain coupled. Like direct time integration, the following system of equations may be solved without continuous decomposition of the matrix if the time step is uniform throughout the analysis.

$$\begin{bmatrix} \mathbf{I} & \mathbf{B}_{12}\overline{\mathbf{C}}_{off}^{T} \\ 0 & \mathbf{I}+\mathbf{B}_{22}\overline{\mathbf{C}}_{off}^{T} \end{bmatrix} \begin{bmatrix} \boldsymbol{\xi}^{n+1} \\ \dot{\boldsymbol{\xi}}^{n+1} \end{bmatrix} = \begin{bmatrix} \mathbf{A}_{11} & \mathbf{A}_{12} \\ \mathbf{A}_{21} & \mathbf{A}_{22} \end{bmatrix} \begin{bmatrix} \boldsymbol{\xi}^{n} \\ \dot{\boldsymbol{\xi}}^{n} \end{bmatrix} + \begin{bmatrix} \mathbf{B}_{11} & \mathbf{B}_{12} \\ \mathbf{B}_{21} & \mathbf{B}_{22} \end{bmatrix} \begin{bmatrix} \mathbf{p}^{n} - \overline{\mathbf{C}}_{off}^{T}\dot{\boldsymbol{\xi}}^{n} \\ \mathbf{p}^{n+1} \end{bmatrix} \tag{5.4.9}$$

$$\mathbf{A}_{\alpha\beta} = diag(a_{\alpha\beta}^{i}), \quad \mathbf{B}_{\alpha\beta} = diag(b_{\alpha\beta}^{i})$$

Initial Conditions of Modal Superposition

If initial displacement and velocity are given, then the initial displacement ξ_i^0 and initial velocity $\dot{\xi}_i^0$ are defined as follows for all coordinate systems. If all modes are used then equality is satisfied; if only some modes are used, then the following becomes an approximate relationship.

$$\begin{aligned} \xi_i^0 &= \frac{1}{m_i}\phi_i^T \mathbf{M}\mathbf{u}_0 \\ \xi_i^0 &= \frac{1}{m_i}\phi_i^T \mathbf{M}\mathbf{v}_0 \end{aligned} \tag{5.4.10}$$

ϕ_i : i[th] fundamental mode shape

$\mathbf{u}_0$: Initial displacement

$\mathbf{v}_0$: Initial velocity

4.2 Frequency Response Analysis

Frequency response analysis measures the response of an object that vibrates at a certain period. It is most often used in vibration analysis of specialized equipment. In frequency response analysis, all loads are defined in the frequency domain and are expressed as a function of the excitation frequency. Thus, if the angular excitation frequency is ω, then the loading for frequency response analysis may be expressed as a complex harmonic function as shown below:

$$\mathbf{f}(t) = \mathbf{f}(\omega)e^{i\omega t} \tag{5.4.11}$$

Then the response due to that load may be expressed likewise:

$$\mathbf{u}(t) = \mathbf{u}(\omega)e^{i\omega t} \tag{5.4.12}$$

Applying this, the equation of motion is expressed as:

$$\left[-\omega^2\mathbf{M} + i\omega\mathbf{C} + \mathbf{K}\right]\mathbf{u}(\omega) = \mathbf{f}(\omega) \tag{5.4.13}$$

Here, loading and displacement are both expressed as complex numbers. The magnitude of a complex number represents the maximum value within the load or displacement's period of motion, and the phase angle represents the location of that maximum value within the period of motion. The real component of a complex number represents the load or displacement at the start of its periodic motion. The imaginary component is the load or displacement at the quarter-point of the periodic motion and shows how the load or displacement changes as a function of the period of motion. Magnitude, phase angle, real component and imaginary component are defined by the following relationships:

$u = \sqrt{u_r^2 + u_i^2}$: Magnitude

$\theta = \tan^{-1}(u_i / u_r)$: Phase Angle

$u_r = u\cos\theta$: Real Component

$u_i = u\sin\theta$: Imaginary Component

Direct Frequency Response Analysis

If the direct method is used in frequency response analysis, then the solution to the system of simultaneous equations in Equation 5.4.13 will yield the frequency response $\mathbf{u}(\omega)$. Without damping, Equation 5.4.13 becomes an imaginary system of equations, but, with damping, a system of complex equations must be solved. When using the direct method, an accurate result can be reached but the system of equations must be re-solved for all excitation frequencies. Thus, for larger problems or a large number of excitation frequencies, the computation becomes very inefficient.

4.3 Response Spectrum Analysis

Response spectrum analysis measures the effects of base motion (the equal shaking of nodes that have been restrained with boundary conditions), particularly in the response of structures due to earthquake ground motions. This analysis is one of the most common analysis methods in earthquake engineering. This method assumes that the system response is linear and measures only the maximum response (spectral ordinate). Thus, for problems in which the nonlinear behavior dominates or the value and/or consistency of the time step is especially important, then analysis using time integration (Section 4.4.1, Section 7.1) is more appropriate.

The maximum response is determined based on a combination of modes that reflects the modal participation factor of the modal responses that correspond to the pre-defined spectral functions. Here, the simultaneity of the maximum response per mode is not considered and instead the maximum response per mode is calculated using a combination method to arrive at the final response value. Thus, response spectrum analysis may be seen as an approximation of time integration. Consequently, if the spectral function is defined based on a specific acceleration or specific earthquake ground motion, then response spectrum analysis can obtain the approximate maximum value of linear transient analysis (linaer time history analysis) due to that specified acceleration. However, it is more typical to use a design response spectrum (statistical spectrum based on earthquake ground motion records within a specific region or nation) to obtain analytical results for seismic design.

Modal Spectral Ordinate

The dynamic equilibrium equation for response spectrum analysis is the same as Equation 5.3.6, and the maximum response per mode may be expressed using spectral data as shown below:

$$\begin{aligned} \xi_i^{\max} &= \max\left[\xi_i(t)\right] = \Gamma_i S_D\left(\omega_i, \zeta_i\right) \\ \dot{\xi}_i^{\max} &= \max\left[\dot{\xi}_i(t)\right] = \Gamma_i S_V\left(\omega_i, \zeta_i\right) \\ \ddot{\xi}_i^{\max} &= \max\left[\ddot{\xi}_i(t)\right] = \Gamma_i S_A\left(\omega_i, \zeta_i\right) \end{aligned} \tag{5.4.14}$$

$S_D\left(\omega_i, \zeta_i\right)$: Displacement spectral data

$S_V\left(\omega_i, \zeta_i\right)$: Velocity spectral data

$S_A(\omega_i, \zeta_i)$: Acceleration spectral data

Γ_i : i th mode participation factor

If Equation 5.4.14 is substituted in to Equation 5.3.5, then the contribution to maximum displacement, velocity, and acceleration per mode may be expressed using spectral data as shown below:

$$\begin{aligned} u_i^{\max} &= \phi_i \Gamma_i S_D(\omega_i, \zeta_i) = \phi_i \Gamma_i S_A(\omega_i, \zeta_i) / \omega_i^2 \\ v_i^{\max} &= \phi_i \Gamma_i S_V(\omega_i, \zeta_i) = \phi_i \Gamma_i S_A(\omega_i, \zeta_i) / \omega_i \\ a_i^{\max} &= \phi_i \Gamma_i S_A(\omega_i, \zeta_i) \end{aligned} \quad (5.4.15)$$

A single spectral ordinate is defined as the maximum response of that mode with respect to the natural period, and includes effects due to modal damping. The response spectrum due to a specific acceleration record has a large variation in the maximum response at each frequency, and thus may look quite complicated when presented on a graph. In the case of a design response spectrum, it's more typical to present the design criteria as a linear function in logspace, as shown in Figure 5.4.1. Likewise, it is normal to save spectral data in logarithmic scale.

Figure 5.4.1 Sample acceleration spectrum

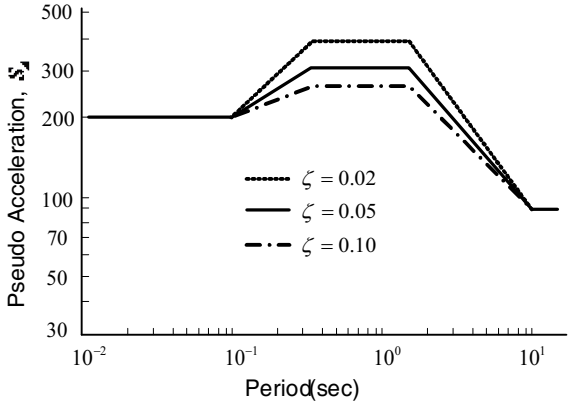

Modal Combination

If the maximum quantity for the i[th] mode is called $R_i^{\max}$ (the quantity may be displacement, stress, internal force, reaction force, etc), then the true maximum value of that quantity might be assumed to be the sum of the modal maxima, but it cannot be guaranteed that the maximum quantities per each mode occur at the same time step. Thus, a simple linear combination does not lead to an accurate maximum value.

$$R_{\max} \neq \sum_{i=1}^{N} R_i^{\max} \tag{5.4.16}$$

Thus, there needs to be a method for approximating the maximum value via modal combination. There are various modal combination methods that incorporate different modal characteristics like damping, but these methods do not yield proper approximate values for all types of models. Thus, it is necessary to be cognizant of the characteristics of the different modal combination methods.

① Summation of the absolute value (ABS)

$$R_{\max} = \sum_{i=1}^{N} \left| R_i^{\max} \right| \tag{5.4.17}$$

This method assumes that each modal response has the same phase, and that the maximum quantity per mode all occur simultaneously. Thus, this method yields the largest value.

② Square root of the summation of the squares (SRSS)

$$R_{\max} = \sqrt{\sum_{i=1}^{N} \left(R_i^{\max} \right)^2} \tag{5.4.18}$$

This method provides a good approximation if the modes are sufficiently decoupled.

③ Naval research laboratory method (NRL)

$$R_{\max} = \left|R_m^{\max}\right| + \sqrt{\sum_{i=1, i\neq m}^{N} \left(R_i^{\max}\right)^2} \tag{5.4.19}$$

This method has separated a single mode (m) from the SRSS method, and this mode possesses the largest quantity across all modes. Similar to the SRSS method, the NRL method is appropriate if the modes are sufficiently decoupled.

The above methods are effective only if the modes are sufficiently decoupled. The U.S. Nuclear Regulatory Commission (NRC)'s regulatory guide 1.92(1976) provies other methods of approximating the maximum quantity even if the modes are not sufficiently decoupled.

④ Ten percent method (TENP)

$$R_{\max} = \sqrt{\sum_{i=1}^{N} \left(R_i^2 + 2\sum_{j=1}^{i-1} \left|R_i R_j\right| \right)} \tag{5.4.20}$$

This method includes the effect due to modes with frequencies that are within 10% of one another. Here, if the two modes' $i, j\ (j < i)$ frequencies satisfy the following relationship, then it can be said that the modes have frequencies that are within 10% of one another.

$$\frac{\omega_i - \omega_j}{\omega_i} \leq 0.1 \tag{5.4.21}$$

⑤ Complete quadratic combination method (CQC)

$$R_{\max} = \sqrt{\sum_{i=1}^{N}\sum_{j=1}^{i} R_i \rho_{ij} R_j} \tag{5.4.22}$$

Here, ρ_{ij} is the cross-correlation coefficient between modes and is defined by the following relationship:

$$\rho_{ij} = \frac{8\sqrt{\zeta_i \zeta_j}(\zeta_i + r_{ij}\zeta_m) r_{ij}^{3/2}}{(1-r_{ij}^2)^2 + 4\zeta_i\zeta_j r_{ij}(1+r_{ij}^2) + 4(\zeta_i^2 + \zeta_j^2) r_{ij}^2} \tag{5.4.23}$$

r_{ij} : Frequency ratio (ω_j / ω_i), $\omega_j < \omega_i$

If $i = j$ in Equation 5.4.23, then regardless of the damping ratio $\rho_{ij} = 1$. If the damping ratio is zero, then $\rho_{ij} = 1$ for all modes and thus the result is the same as the SRSS method. If the damping ratio for the two modes are equal, then the equation may be simplified as shown below:

$$\rho_{ij} = \frac{8\zeta^2(1+r_{ij}) r_{ij}^{3/2}}{(1-r_{ij}^2)^2 + 4\zeta^2 r_{ij}(1+r_{ij})^2} \quad (\zeta_i = \zeta_j = \zeta) \tag{5.4.24}$$

This combination method accurately considers the relationship between the modes, but the calculated result tends to increase proportionally to the square of the number of modes.

Sign of the Result of Modal Combination Methods

The modal combination methods yield results as an absolute value, and as such the response spectrum data is always positive. However, vector results such as reaction force or strain requires an appropriate direction (i.e. sign). Typically, the sign is defined to be the sign of the major mode. The major mode is selected from the modes with the highest mass participation factors and whose direction is most similar to the loading direction specified by the spectrum. Other ways of assigning the

sign is to take the sign of the mode whose value is the absolute maximum, and then, for strain energy, to assign the sign of the mode at which the sum of the element strain energies is the largest.

Modification of Spectrum Data

As shown in Equation 5.4.14, spectrum data is a function of the natural frequency and modal damping. However, the user does not know the frequency before running the analysis, so the spectrum data takes a tabular format with consistent spacing. Thus, an interpolation method is used to read the spectrum data corresponding to a modle's natural frequency or period. It is most common to use linear interpolation on a logarithmic scale as this most accurately captures the relationship of spectral response and frequency. For spectrum data recorded for various damping values, the same interpolation scheme is used for the structure's modal damping ratio.

However, if the spectrum data is created for a single damping ratio, then interpolation is not possible. Thus, there needs to be a modification method for spectra with a single damping ratio. The Japanese Highway Bridge Specifications (2002) provides a correction factor for damping ratios (as shown below):

$$C_D(\zeta)=\frac{1.5}{40\zeta+1}+0.5 \tag{5.4.25}$$

Figure 5.4.2 Correction factor for the damping ratio

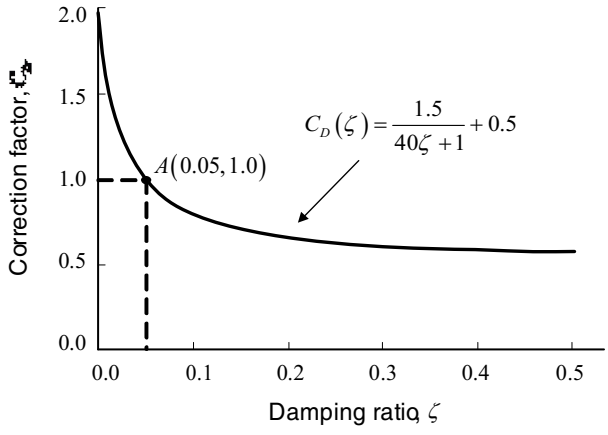

When the damping ratio is 0.05, then $C_D = 1$ (point A). Thus, Equation 5.4.25 is a correction factor for when the damping ratio is 0.05. Equation 5.4.26 shows how the correction factor may be applied for spectra whose damping ratio is not 0.05.

$$\overline{R}_i^{\max} = \frac{C_D(\zeta_i)}{C_D(\zeta_{spectrum})} R_i^{\max} \tag{5.4.26}$$

Selection of Excitation Direction

The excitation direction of an earthquake is not pre-determined, so in seismic design it is typical to design for a combination of excitations in two orthogonal directions. However, even for an earthquake of the same magnitude, the damage to the structure may vary depending on the direction. Midas nGen offers the capability to find the direction in which the most amount of structural damage can be expected. This is given in the global coordinate system and in the x-y plane. Using the z-axis of the GCS as the center and within 0 to 180 degrees, the direction in which the sum of the reactions per mode is maximized or in which the total strain energy is maximized is selected to be the excitation direction or angle.

Figure 5.4.3 Sample graph showing structural response as a function of excitation

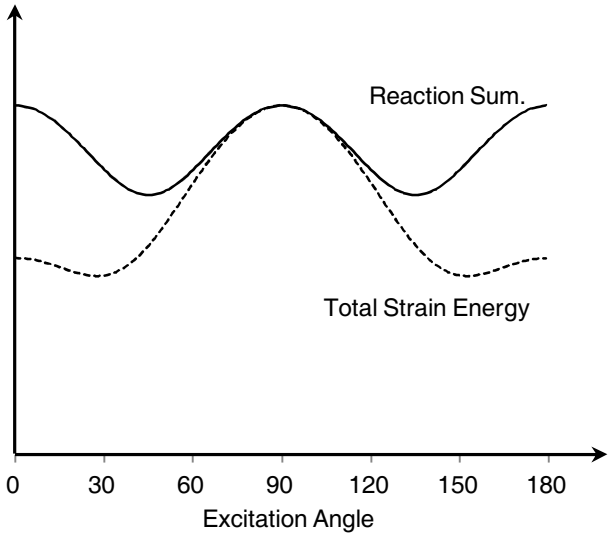

4.4
Linear Dynamic Analysis Examples

1) Simply Supported Deep Beam

REFERENCE	NAFEMS[1]
ELEMENTS	Beam elements, solid elements
MODEL FILENAME	LinearDynamic01.mpb

The figure below shows a simply supported deep beam subject to a distributed load. Time-variant forcing functions are exerted on the structure. The following results show displacement and stress at point A.

Figure 4.4.1.1
Simply supported deep beam model

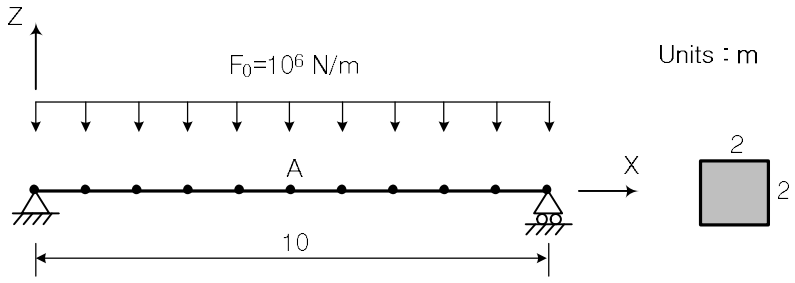

Material data	Elastic modulus	*E = 200 GPa*
	Poisson's ratio	ν *= 0.3*
	Mass density	ρ *= 8000 kg/m^3*
	Mass proportional damping	α *= 5.36 sec^{-1}*
	Stiffness proportional damping	β *= 7.46×10^{-5}sec*
	Modal damping	ξ *= 0.02*
Section property	Squre cross-section	*2 m x 2 m*
Forcing functions	(1) Harmonic	$F = F_0 \sin \omega t$ (where $w = 2\pi f$)
	(2) Periodic	$F = F_0(\sin \omega t - \sin 3\omega t)$ (where $w = 2\pi f$, $f = 20Hz$)
	(3) Transient	$F = F_0$, $t > 0$

** Rayleigh damping coefficients, α and β are chosen to give 0.02 damping in the dominant first mode.*

Table 4.4.1.1 Peak responses and frequency of beam subjected to harmonic load

		Peak u_Z^A [*mm*]		Peak σ^A [*MPa*]		Peak Frequency [*Hz*]	
Reference		*13.45*		*241.9*		*42.65*	
Element type	Number of elements	*Direct*	*Modal*	*Direct*	*Modal*	*Direct*	*Modal*
BEAM-2	10	*13.51*	*13.51*	*244.4*	*244.3*	*42.60*	*42.60*
HEXA-8	10	*13.09*	*13.09*	*236.5*	*236.5*	*43.40*	*43.40*
PENTA-6	10×4	*12.22*	*12.23*	*235.2*	*235.5*	*44.75*	*44.75*

Table 4.4.1.2 Peak responses of beam subjected to periodic forcing function

		Peak u_Z^A [*mm*]		Peak σ^A [*MPa*]	
Reference		*0.951*		*17.1*	
Element type	Number of elements	*Direct*	*Modal*	*Direct*	*Modal*
BEAM-2	10	*0.955*	*0.955*	*17.5*	*17.4*
HEXA-8	10	*0.962*	*0.962*	*17.5*	*17.3*
PENTA-6	10x4	*0.964*	*0.965*	*17.3*	*18.1*

Table 4.4.1.3 Peak responses of beam subjected to transient step load

		Peak u_Z^A [*mm*]		Peak time [*sec*]		Peak σ^A [*MPa*]		Static u_Z^A [*mm*]	
Reference		*1.043*		*0.0117*		*18.76*		*0.538*	
Element type	Number of elements	*Direct*	*Modal*	*Direct*	*Modal*	*Direct*	*Modal*	*Direct*	*Modal*
BEAM-2	10	*1.044*	*1.043*	*0.0117*	*0.0116*	*18.51*	*18.51*	*0.537*	*0.537*
HEXA-8	10	*1.012*	*1.1012*	*0.0116*	*0.0116*	*18.03*	*18.03*	*0.521*	*0.521*
PENTA-6	10x4	*0.946*	*0.945*	*0.0112*	*0.0112*	*17.40*	*17.31*	*0.487*	*0.487*

2) Simply Supported Thin Plate

REFERENCE	NAFEMS[1]
ELEMENTS	Shell elements
MODEL FILENAME	LinearDynamic02.mpb

The figure below shows a simply supported thin square plate model that is subject to a vertical distributed pressure load. Time-variant forcing functions are applied to the structure. The following results show the displacement and stress at point A.

Figure 4.4.2.1
Simply supported thin plate model

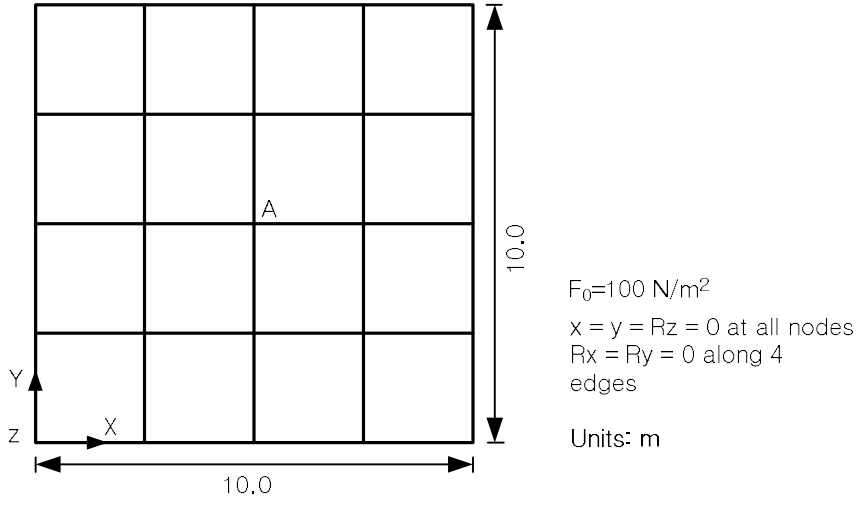

Material data	Elastic modulus	E = 200 GPa
	Poisson's ratio	ν = 0.3
	Mass density	ρ = 8000 kg/m^3
	Mass proportional damping	α = 0.229 sec^{-1}
	Stiffness proportional damping	β = 1.339x10^{-3} sec
	Modal damping	ξ = 0.02
Section property	Thickness	t = 0.05 m
Forcing functions	(1) Harmonic	$F = F_0 \sin \omega t$ (where $w = 2\pi f$)
	(2) Periodic	$F = F_0(\sin \omega t - \sin 3\omega t)$ (where $w = 2\pi f$, $f = 1.2Hz$)
	(3) Transient	$F = F_0$, $t > 0$

* Rayleigh damping coefficients, α and β are chosen to give 0.02 damping in the dominant first mode.

Table 4.4.2.1 Peak responses and frequency of thin plate subjected to harmonic load

		Peak u_Z^A [*mm*]		Peak σ^A [*MPa*]		Peak Frequency [*Hz*]	
Reference		*45.42*		*30.03*		*2.377*	
Element type	Number of elements	*Direct*	*Modal*	*Direct*	*Modal*	*Direct*	*Modal*
QUAD-4	8×8	*45.12*	*45.15*	*31.68*	*31.70*	*2.415*	*2.415*
TRIA-3	128	*43.59*	*43.63*	*30.38*	*30.41*	*2.455*	*2.455*

Table 4.4.2.2 Peak responses of thin plate subjected to periodic forcing function

		Peak u_Z^A [*mm*]		Peak σ^A [*MPa*]	
Reference		*2.863*		*2.018*	
Element type	Number of elements	*Direct*	*Modal*	*Direct*	*Modal*
QUAD-4	8×8	*2.913*	*2.914*	*2.073*	*2.075*
TRIA-3	128	*2.883*	*2.884*	*2.037*	*2.039*

Table 4.4.2.3 Peak responses of thin plate subjected to transient step load

		Peak u_Z^A [*mm*]		Peak time [*sec*]		Peak σ^A [*MPa*]		Static u_Z^A [*mm*]	
Reference		*3.523*		*0.210*		*2.484*		*1.817*	
Element type	Number of elements	*Direct*	*Modal*	*Direct*	*Modal*	*Direct*	*Modal*	*Direct*	*Modal*
QUAD-4	8×8	*3.474*	*3.487*	*0.210*	*0.212*	*2.382*	*2.435*	*1.770*	*1.770*
TRIA-3	128	*3.355*	*3.368*	*0.206*	*0.206*	*2.282*	*2.325*	*1.709*	*1.709*

3) Simply Supported Thick Square Plate

REFERENCE	NAFEMS[1]
ELEMENTS	Shell elements, solid elements
MODEL FILENAME	LinearDynamic03.mpb

The figure below shows a simply supported thick square plate model that is subject to a vertical distributed pressure load. Time-variant forcing functions are applied to the structure. The following results show the displacement and stress at point A.

Figure 4.4.3.1
Simply supported thick plate model

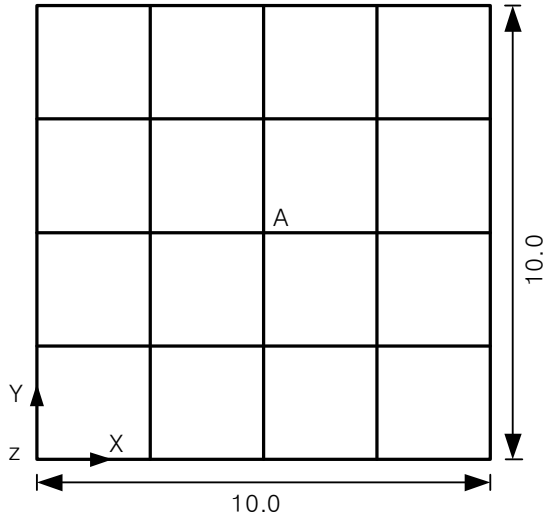

$F_0=10^6$ N/m^2

x = y = Rz = 0 at all nodes
Rx = Ry = 0 along 4 edges

Units: m

Material data	Elastic modulus	E = 200 GPa
	Poisson's ratio	ν = 0.3
	Mass density	ρ = 8000 kg/m^3
	Mass proportional damping	α = 5.772 sec^{-1}
	Stiffness proportional damping	β = 6.929x10^{-5} sec
	Modal damping	ξ = 0.02
Section property	Thickness	t = 1 m
Forcing functions	(1) Harmonic	$F = F_0 \sin \omega t$ (where $w = 2\pi f$)
	(2) Periodic	$F = F_0(\sin \omega t - \sin 3\omega t)$ (where $w = 2\pi f$, $f = 1.2Hz$)
	(3) Transient	$F = F_0$, $t > 0$

* Rayleigh damping coefficients, α and β are chosen to give 0.02 damping in the dominant first mode.

Table 4.4.3.1 Peak responses and frequency of thick plate subjected to harmonic loads

		Peak u_Z^A [*mm*]		Peak σ^A [*MPa*]		Peak Frequency [*Hz*]	
Reference		*58.33*		*800.8*		*45.90*	
Element type	Number of elements	*Direct*	*Modal*	*Direct*	*Modal*	*Direct*	*Modal*
QUAD-4	8×8	*60.00*	*60.00*	*809.7*	*809.7*	*46.50*	*46.50*
TRIA-3	128	*57.77*	*57.80*	*773.7*	*774.1*	*47.35*	*47.35*
HEXA-8	96	*59.15*	*59.16*	*777.2*	*777.3*	*46.80*	*46.80*

Table 4.4.3.2 Peak responses of thick plate subjected to periodic forcing function

		Peak u_Z^A [*mm*]		Peak σ^A [*MPa*]	
Reference		*4.929*		*67.67*	
Element type	Number of elements	*Direct*	*Modal*	*Direct*	*Modal*
QUAD-4	8×8	*5.300*	*5.303*	*72.53*	*72.59*
TRIA-3	128	*5.428*	*5.431*	*73.54*	*73.60*
HEXA-8	96	*5.341*	*5.344*	*70.96*	*71.01*

Table 4.4.3.3 Peak responses of thick plate subjected to transient step load

		Peak u_Z^A [*mm*]		Peak time [*sec*]		Peak σ^A [*MPa*]		Static u_Z^A [*mm*]	
Reference		*4.524*		*0.0108*		*62.11*		*2.333*	
Element type	Number of elements	*Direct*	*Modal*	*Direct*	*Modal*	*Direct*	*Modal*	*Direct*	*Modal*
QUAD-4	8×8	*4.565*	*4.545*	*0.0107*	*0.0105*	*59.03*	*59.58*	*2.339*	*2.339*
TRIA-3	128	*4.398*	*4.380*	*0.0106*	*0.0105*	*56.11*	*56.07*	*2.253*	*2.253*
HEXA-8	96	*4.505*	*4.489*	*0.0108*	*0.0109*	*56.66*	*57.05*	*2.310*	*2.310*

4) Response Spectrum Analysis of a Simply Supported Beam

REFERENCE	Biggs, J.M.[2]
ELEMENTS	Beam elements, shell elements, solid elements
MODEL FILENAME	LinearDynamic04.mpb

The figure below shows a simply supported beam with a rectangular cross section. Response spectrum analysis yield displacement, moment, and stress results as shown below.

Figure 4.4.4.1
Simply supported beam model

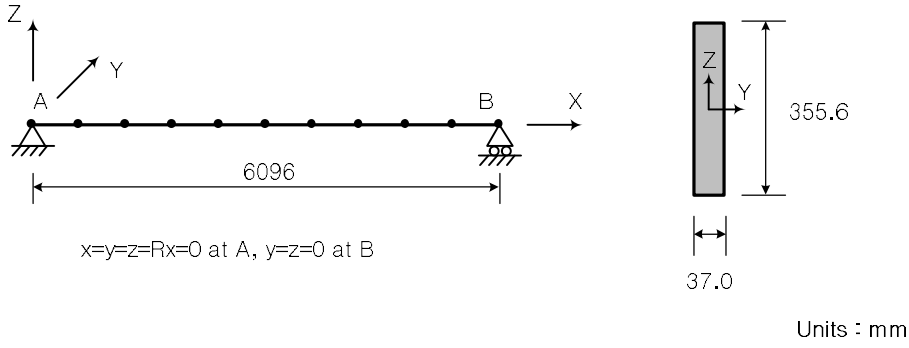

Material data	Elasitic modulus Mass density	$E = 206.8\ GPa$ $\rho = 1.0473 \times 10^5\ kg/m^3$
Section property	Rectangular cross-section	$37.0\ mm \times 37.0\ mm$
Mass option		*Lumped mass*

Table 4.4.4.1 Response spectra definition (unit: m)

Frequency [*Hz*]		*5.000*	*6.000*	*6.098*	*7.000*	*8.000*
Period [*sec*]		*0.2000*	*0.1667*	*0.1640*	*0.1429*	*0.1250*
Type (scale factor)	Displacement(1.0)	*0.0199*	*0.0115*	*0.0110*	*0.0072*	*0.0056*
	Velocity(1.0)	*0.6248*	*0.4339*	*0.4201*	*0.3188*	*0.2837*
	Acceleration(0.5)	*39.258*	*32.716*	*32.190*	*28.042*	*28.521*

Table 4.4.4.2 Response spectrum analysis results obtained using beam elements

Result at mid-span		Displacement [*mm*]	Stress [*MPa*]	Moment x10^5 [*Nm*]
Reference		*14.2*	*140.4*	*1.095*
Element type	Spectra type			
BEAM-2	Displacement	*14.2*	*138.4*	*1.079*
	Velocity	*14.1*	*138.1*	*1.077*
	Acceleration	*14.1*	*138.1*	*1.077*

Table 4.4.4.3 Response spectrum analysis results obtained using shell elements

Result at mid-span		Displacement [*mm*]	Stress [*MPa*]
Reference		*14.2*	*140.4*
Element type	Spectra type		
QUAD-4	Displacement	*13.8*	*132.4*
	Velocity	*13.7*	*132.0*
	Acceleration	*13.7*	*132.0*
TRIA-3	Displacement	*13.9*	*134.6*
	Velocity	*13.9*	*134.2*
	Acceleration	*13.9*	*134.2*

Table 4.4.4.4 Response spectrum analysis results obtained using solid elements

Result at mid-span		Displacement [*mm*]	Stress [*MPa*]
Reference		*14.2*	*140.4*
Element type	Spectra type		
HEXA-8	Displacement	*13.7*	*132.3*
	Velocity	*13.7*	*131.9*
	Acceleration	*13.7*	*131.9*

5) Comparison of Linear Dynamic Analysis of a Truss Structure

REFERENCE	Chopra, A.K.[3]
ELEMENTS	Truss elements, shell elements, solid elements
MODEL FILENAME	LinearDynamic05.mpb

The figure below shows a truss structure that is only subject to axial forces. There is either acceleration applied at point A or force applied at point D. The results below illustrate differences between the various linear dynamic analyses.

Figure 4.4.5.1
Simply supported beam model

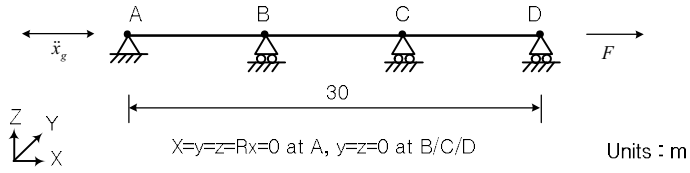

Material data	Elastic modulus Mass density	*E = 5 Pa* *ρ= 1/90 kg/m^3*
Section property	Cross-section Area	*A = 2.0 m^2*
Analysis condition	Modal transient with tip load Modal transient with base acceleration Modal frequency with tip load Response spectrum	*F = 10 N, 10% damping* *x_R =1.0m/sec^2,10% damping* *F = 10 N, 10% damping* *displacement spectra, 2% damping*

Figure 4.4.5.2
Displacement response spectra

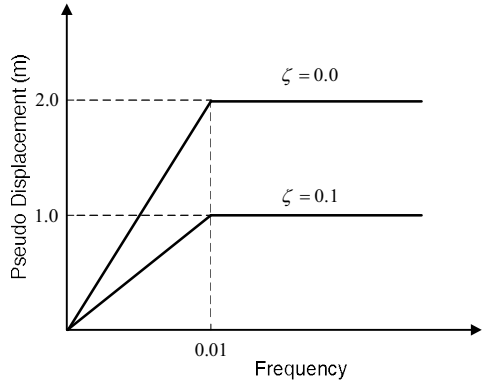

Table 4.4.5.1 Displacement and acceleration at point D using modal transient analysis with tip load

Result type	*Displacement* [*m*]			*Acceleration* [*m/sec*^{2}]		
Time step [*sec*]	*0.1*	*0.2*	*0.3*	*0.1*	*0.2*	*0.3*
Reference	*0.4387*	*1.686*	*3.598*	*81.42*	*66.71*	*48.06*
Element type						
TRUSS-2	*0.4387*	*1.686*	*3.598*	*81.42*	*66.71*	*48.06*
QUAD-4	*0.4387*	*1.686*	*3.598*	*81.42*	*66.71*	*48.06*
HEXA-8	*0.4387*	*1.686*	*3.598*	*81.42*	*66.71*	*48.06*

Table 4.4.5.2 Total displacement at point D using modal transient analysis with base acceleration

Result type	*Displacement* [*m*]		
Time step [*sec*]	*0.1*	*0.2*	*0.3*
Reference	*0.244x10^{-4}*	*1.965x10^{-4}*	*6.692x10^{-4}*
Element type			

TRUSS-2	$0.244x10^{-4}$	$1.965x10^{-4}$	$6.692x10^{-4}$
QUAD-4	$0.244x10^{-4}$	$1.965x10^{-4}$	$6.692x10^{-4}$
HEXA-8	$0.244x10^{-4}$	$1.965x10^{-4}$	$6.692x10^{-4}$

Table 4.4.5.3 Stress of element 1 and reaction force at point A using modal frequency analysis with tip load

Result type	*Displacement* [*m*]			*Acceleration* [*m/sec*^{2}]		
Time step [*sec*]	*0.01*	*0.175*	*0.477*	*0.01*	*0.175*	*0.477*
Reference	*2.51*	*15.50*	*3.988*	*5.019*	*31.00*	*7.977*
Element type						
TRUSS-2	*2.51*	*15.49*	*3.993*	*5.019*	*30.97*	*7.987*
QUAD-4	*2.51*	*15.49*	*3.993*	*5.019*	*30.97*	*7.987*
HEXA-8	*2.51*	*15.49*	*3.993*	*5.019*	*30.97*	*7.987*

Table4.4.5.4 Peak displacement at point D using response spectrum analysis with 2% modal damping ratio

Result type	*Displacement* [*m*]				
Combination method	ABS	SRSS	TENP	NRL	CQC
Reference	*2.902*	*2.248*	*2.248*	*2.767*	*2.246*
Element type	*2.902*	*2.248*	*2.248*	*2.767*	*2.246*
TRUSS-2	*2.902*	*2.248*	*2.248*	*2.767*	*2.246*
QUAD-4	*2.902*	*2.248*	*2.248*	*2.767*	*2.246*
HEXA-8	*2.902*	*2.248*	*2.248*	*2.767*	*2.246*

6) Column Subject to Earthquake Loads

REFERENCE	Hilber, H.M. et al[4], Hurty, W.C. et al[5]
ELEMENTS	Truss elements, shell elements, solid elements
MODEL FILENAME	LinearDynamic06.mpb

To simulate earthquake loading, an acceleration time history is exerted to the fixed end of the column shown below. The reference value is the maximum value in the time history analysis. The results below compare the different combination methods for response spectrum analysis. The results also illustrate the effect of baseline correction on the acceleration time history.

Figure 4.4.6.1
Column model

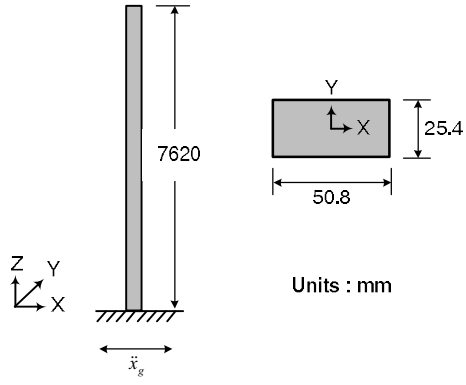

Material data	Elastic modulus Mass density	*E = 206.8 GPa* ρ*= 7780 kg/m*^{3}
Section property	Rectangular cross-section	*50.8 mm x 25.4 mm*

Figure 4.4.6.2
El Centro N-S
acceleration history

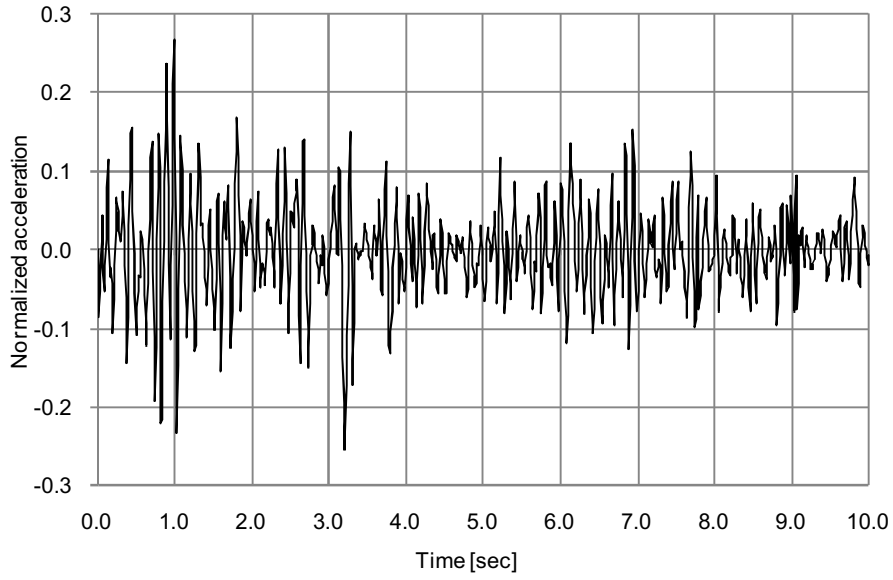

Figure 4.4.6.3
Displacement spectra
for the period range
0.03~10 sec

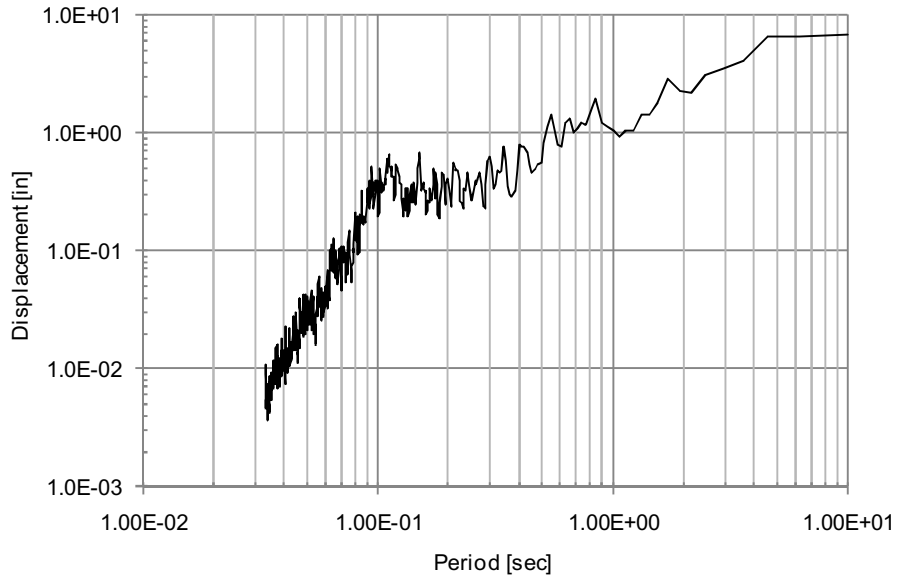

Figure 4.4.6.4
Velocity spectra for the period range 0.03~10 sec

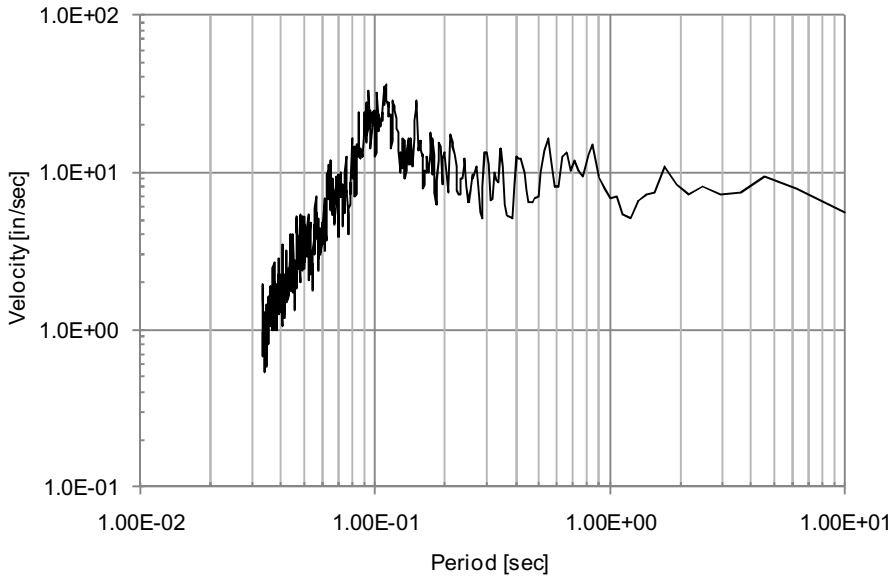

Figure 4.4.6.5
Absolute displacement of the cantilever's tip with and without baseline correction

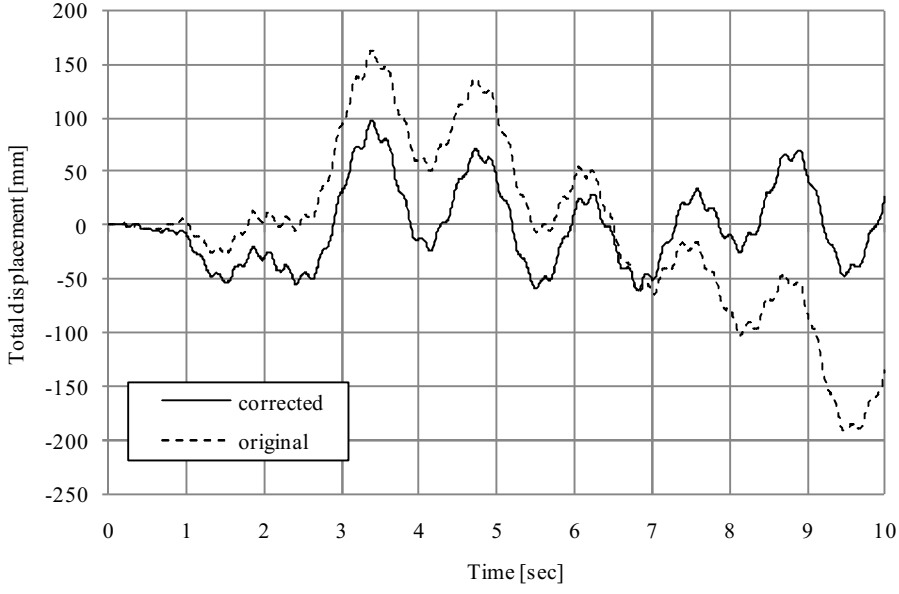

Figure 4.4.6.6
Base displacement with and without baseline correction

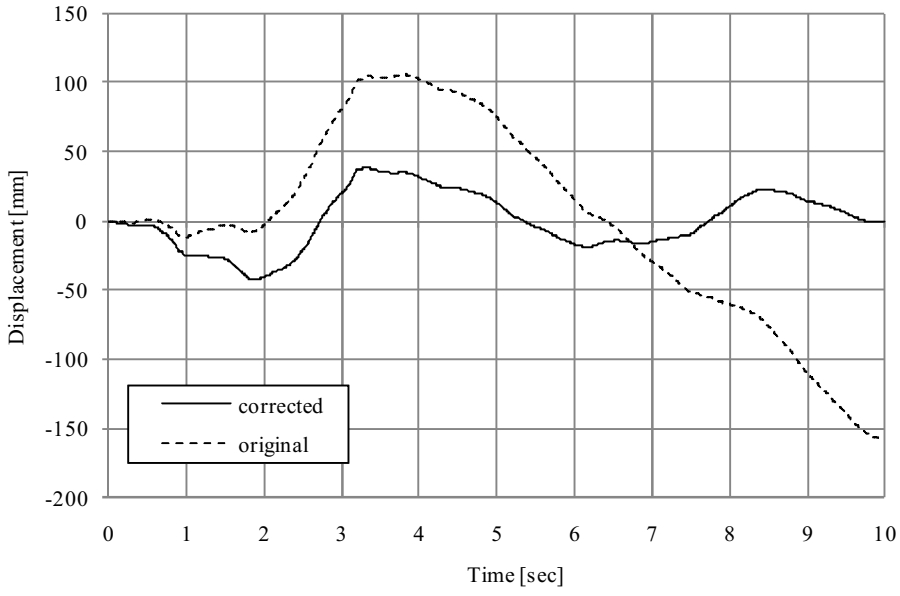

Table 4.4.6.1 Maximum displacement and velocity at the top of the column provided by transient analysis (relative to base)

Result type		Displacement [*mm*]	Velocity [*m/sec*]
Reference		*59.2*	*0.508*
Analysis type	Number of elements		
Direct transient	10	*58.9*	*0.439*
	20	*58.9*	*0.438*
	50	*58.9*	*0.438*
Modal transient	10	*59.2*	*0.512*
	20	*59.1*	*0.515*

	50	*59.1*	*0.516*

Table 4.4.6.2 Maximum displacement and velocity at the top of the column provided by response spectrum analysis (relative to base)

Result type			Displacement [*mm*]	Velocity [*m/sec*]
Reference			*59.2*	*0.508*
Number of elements	Spectrum type	Combination method		
10	Displacement	ABS	*67.2*	*0.639*
		SRSS	*57.0*	*0.392*
	Velocity	ABS	*70.8*	*0.640*
		SRSS	*61.0*	*0.395*
20	Displacement	ABS	*67.2*	*0.638*
		SRSS	*57.0*	*0.392*
	Velocity	ABS	*70.8*	*0.639*
		SRSS	*61.0*	*0.395*
50	Displacement	ABS	*67.2*	*0.638*
		SRSS	*57.0*	*0.392*
	Velocity	ABS	*70.8*	*0.639*
		SRSS	*61.0*	*0.395*

7) Frequency Response Analysis using Residual Modes

REFERENCE	Dickens et al[6]
ELEMENTS	Elastic link elements, mass elements
MODEL FILENAME	LinearDynamic07.mpb

The figure below shows a mass-spring system whose frequency response analysis will illustrate the effects of using residual modes on result accuracy. There are four degrees of freedom, and the reference value is the result produced with all four modes. This reference is used to judge the improvement of accuracy when considering residual modes.

Figure 4.4.7.1
Spring-mass system

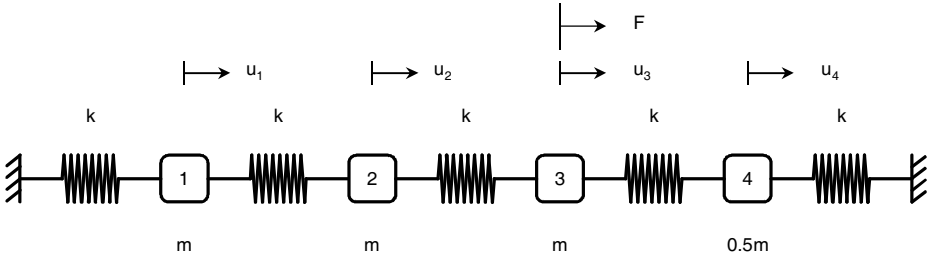

Material data	Lumped mass	$m = 1.0\ kg$
	Link stiffness	$k = 10000\ N/m$
	Modal damping	$\xi = 0.02$

Figure 4.4.7.2
Displacement amplitude response for DOF 3

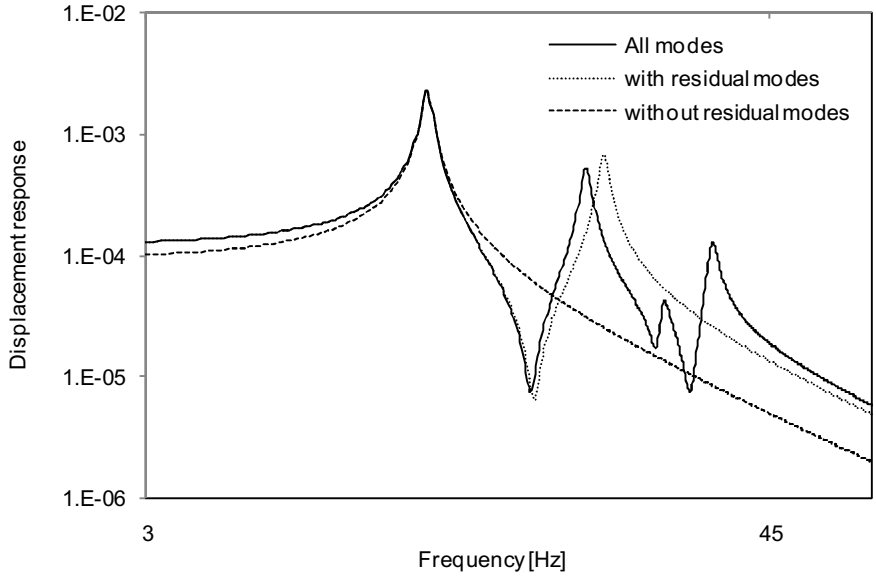

Figure 4.4.7.3
Acceleration amplitude response for DOF 1

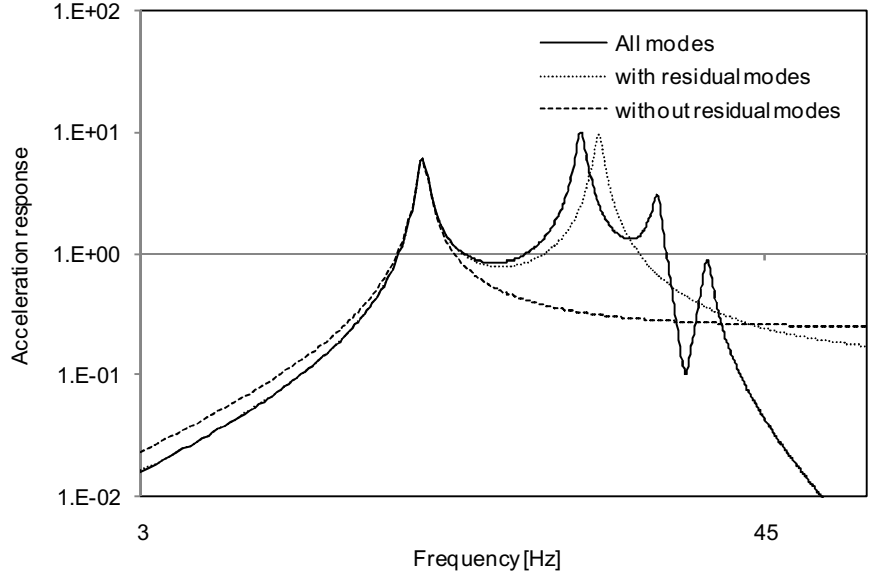

Table 4.4.7.1 Displacement and percentage error at 3 Hz

	DOF 1	*DOF 2*	*DOF 3*	*DOF 4*
Reference	*4.52E-05*	*8.89E-05*	*1.29E-04*	*6.53E-05*
All Modes	*4.52E-05*	*8.89E-05*	*1.29E-04*	*6.53E-05*
% error	*0.0%*	*0.0%*	*0.0%*	*0.0%*
with residual modes	*4.54E-05*	*8.89E-05*	*1.29E-04*	*6.51E-05*
% error	*0.3%*	*0.0%*	*0.0%*	*-0.3%*
without residual modes	*6.60E-05*	*1.05E-04*	*1.01E-04*	*5.65E-05*
% error	*31.5%*	*15.5%*	*-27.5%*	*-15.5%*

Table 4.4.7.2 Acceleration and percentage error at 3 Hz

	DOF 1	*DOF 2*	*DOF 3*	*DOF 4*
Reference	*1.61E-02*	*3.16E-02*	*4.60E-02*	*2.32E-02*
All Modes	*1.61E-02*	*3.16E-02*	*4.60E-02*	*2.32E-02*
% error	*0.0%*	*0.0%*	*0.0%*	*0.0%*
with residual modes	*1.61E-02*	*3.16E-02*	*4.60E-02*	*2.31E-02*
% error	*0.3%*	*0.0%*	*0.0%*	*-0.3%*
without residual modes	*2.35E-02*	*3.74E-02*	*3.61E-02*	*2.01E-02*
% error	*31.5%*	*15.5%*	*-27.5%*	*-15.5%*

8) Steady State Response of a Plate

REFERENCE	Thomson[7]
ELEMENTS	Shell elements
MODEL FILENAME	LinearDynamic08.mpb

The figure below shows a 2-dimensional plate model whose left end is restrained and the right end is subject to an in-plane pressure. Two techniques for frequency response analysis—direct method and modal method—are used and both results are shown below to confirm consistency.

Figure 4.4.8.1
2D steady state dynamics model

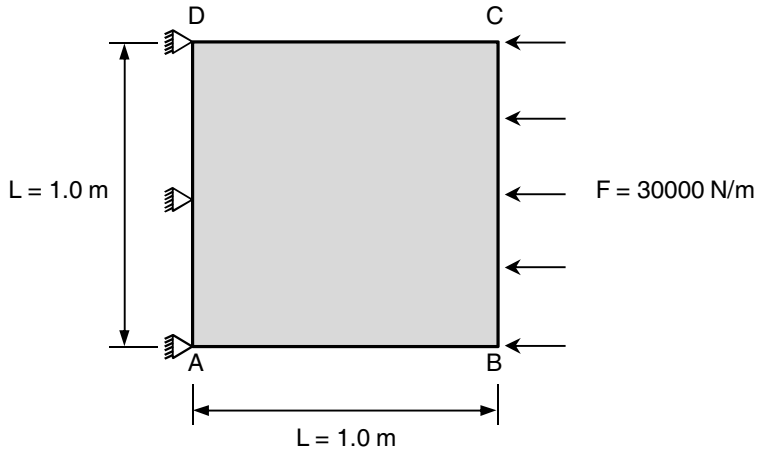

Material data	Elastic modulus	$E = 2.0\times10^{7}$ *Pa*
	Poisson's ratio	$\nu = 0.0$
	Mass Density	$\rho = 8000$ *kg/m*^{3}
	Mass proportional damping	$\alpha = 5.36$ *sec*$^{-1}$
	Stiffness proportional damping	$\beta = 7.46\times10^{-5}$ *sec*
Section property	Thickness	*t = 1m*

Table 4.4.8.1 Preak displacement and stress at resonant frequency

		Peak u [*mm*]		Peak σ [*MPa*]		Frequency [*Hz*]	
Reference		*16.94*		*0.478*		*12.16*	
Element type	Number of elements	*Direct*	*Modal*	*Direct*	*Modal*	*Direct*	*Modal*
QUAD-4	2×2	*16.94*	*16.94*	*0.478*	*0.478*	*12.16*	*12.16*
TRIA-3	2×(2×2)	*17.56*	*17.56*	*0.476*	*0.467*	*12.07*	*12.07*

9) Tower with a Lumped Mass

REFERENCE	Paz[8]
ELEMENTS	Bar elements
MODEL FILENAME	LinearDynamic09.mpb

The figure below shows a tower model with a lumped mass at the top. The tower element is modeled with a simplified beam with an effective stiffness, and the top weight was modeled with a lumped mass. The tower's time-variant lateral displacement results are shown below.

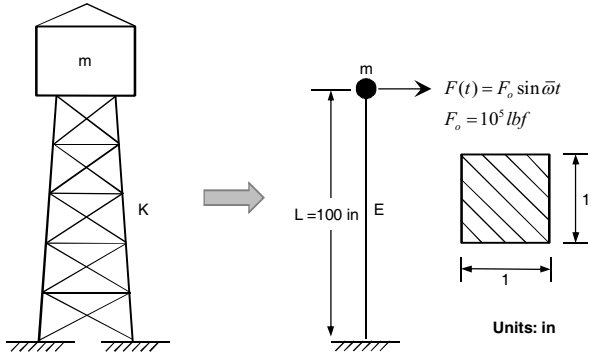

Figure 4.4.9.1
A tower model subjected to sinusoidal force

Model data	Spring constant Mass	$K = 2.0 \times 10^7$ *Pa* *m = 100 lbm*
Equivalent material data	Elastic modulus Poisson's ratio	$E = 2.0 \times 10^6$ *psi* $\nu = 0.3$
Section property	Square cross-section	$A = 1.0\ In^2$
Mass option		*Coupled mass*

Table 4.4.9.1 Horizontal displacement at t=0.1, 0.2 and 0.3 seconds

Time		0.1	0.2	0.3
Reference		1.6076	-3.1865	4.7420
Method	Direct	1.6079	-3.1843	4.6982
	Modal	1.6082	-3.1848	4.6992

Table 4.4.9.2 Horizontal velocity at t=0.1, 0.2 and 0.3 seconds

Time		0.1	0.2	0.3
Reference		2.9379	-11.6917	26.0822
Method	Direct	3.3498	-13.3339	29.7521
	Modal	3.3439	-13.3084	29.6941

Table 4.4.9.3 Horizontal acceleration at t=0.1, 0.2 and 0.3 seconds

Time		0.1	0.2	0.3
Reference		-1466.51	2907.53	-4298.04
Method	Direct	-1447.58	2867.97	-4231.91
	Modal	-1449.45	2870.58	-4235.68

References

1 NAFEMS, "Selected Benchmarks for Forced Vibration", Ref. R0016, NAFEMS, Glasgow, 1993

2 Biggs, J.M. “Introduction to Structural Dynamics”, McGraw-Hill, Inc., New York, 1964

3 Chopra, A.K., Dynamics of Structures: Theory and Applications to Earthquake Engineering, Prentice-Hall, Englewood Cliffs, N.J., 1995

4 Hilber, H.M., Hughes T.J.R. and Taylor R.L., “Improved Numerical Dissipation of Time Integration Algorithms in Structural Dynamics”, Earthquate Engineering and Structural Dynamics, Vol. 5, pp. 283-292, 1977

5 Hurty, W.C. and Rubinstein M.F., “Dynamics of Structures”, Prentice-Hall, Englewood Cliffs, N.J., 1964

6 Dickens, J.M., Nakagawa and Wittbrodt, M.J., “A Critique of Mode Acceleration and Modal Trucation Augmentation Methods for Modal Response Analysis,” Computers & Structures, Vol. 62, pp.985-998, 1997

7 Thomson, W.T., “Theory of Vibration with Application”, 4th Edition, Prentice-Hall, Englewood Cliffs, N.J., 1993

8 Paz, M., “Structural Dynamics: Theory and Computation”, 4th Edition, Chapman & Hall, International Thomson Publishing, 1997

Section 5 Nonlinear Finite Element Method

5.1 Nonlinear Method

Nonlinear finite element method incorporates geometric nonlinearities of an element or material. In midas nGen, the nonlinear method is used to consider nonlinear elastic properties or P-Delta effects. Figure 5.5.1 shows how the incremental solution of the linear iterative calculations approach the correct solution with nonlinear FEM.

Figure 5.5.1 Convergence of the incremental solution and finite element method

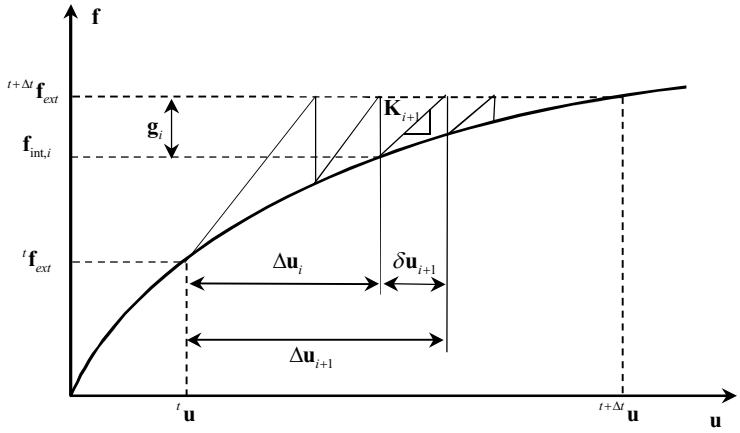

Here, $^{t}\mathbf{f}_{ext}$ and $^{t+\Delta t}\mathbf{f}_{ext}$ refer to the external force at time t and $t+\Delta t$, respectively. The incremental solution between time t and time $t+\Delta t$ may be expressed by the following relationship:

$$^{t+\Delta t}\mathbf{u} = {}^{t}\mathbf{u} + \Delta\mathbf{u} \tag{5.5.1}$$

$\Delta\mathbf{u}$: Incremental solution that occurs within time increment

If iterative calculations are conducted within the time increment Δt to exhibit nonlinear behavior, then the accumulation of the incremental solutions are shown below:

$$\Delta \mathbf{u} = \sum_{i=1}^{n} \delta \mathbf{u}_i \qquad \text{or} \qquad \Delta \mathbf{u}_{i+1} = \Delta \mathbf{u}_i + \delta \mathbf{u}_{i+1} \tag{5.5.2}$$

$\Delta \mathbf{u}_i$: accumulated incremental solutions that have occurred up to the i th iterative calculation

$\delta \mathbf{u}_{i+1}$: incremental solution that occurs at the $i+1$ th iterative calculation

$\delta \mathbf{u}_{i+1}$ is calculated using the tangential stiffness matrix $\mathbf{K}_{i+1}$ and linear finite element methods, as shown below:

$$\delta \mathbf{u}_{i+1} = \mathbf{K}_{i+1}^{-1} \mathbf{g}_i \tag{5.5.3}$$

$\mathbf{g}_i$: Residual/unbalanced force

Residual/unbalanced force $\mathbf{g}_i$ is the difference between external force ${}^{t+\Delta t}\mathbf{f}_{ext}$ and internal force $\mathbf{f}_{int,i}$, as shown below:

$$\mathbf{g}_i = {}^{t+\Delta t}\mathbf{f}_{ext} - \mathbf{f}_{int,i} \tag{5.5.4}$$

Equations 5.5.2 through 5.5.4 are repeated until the user-specified convergence criteria have been satisfied. Convergence criteria may be based on axial force, displacement, energy, or other variable property.

Line Search

To improve the effcency of the basic iterative method explained above, midas nGen offers line search capabilities. The fundamental principle of line search inserts a scalar η in Equation 5.5.3 (where the incremental solution $\delta \mathbf{u}_{i+1}$ is added to the accumulated solution) to improve accuracy. In such a case, the accumulated incremental solution is then calculated as follows:

$$\Delta \mathbf{u}_{i+1} = \Delta \mathbf{u}_i + \eta \delta \mathbf{u}_{i+1} \tag{5.5.5}$$

If the $\Delta \mathbf{u}_{i+1}$ calculated from the above equation is assumed to satisfy equilibrium conditions, then the principle of stationary total potential energy may be used. Consequently, the line search problem boils down to finding the value of η at which the differential value of potential energy becomes zero.

$$s(\eta) = \delta \mathbf{u}_{i+1}{}^T \mathbf{g}(\eta) = 0 \tag{5.5.6}$$

Figure 5.5.2 Conceptual diagram of the line search algorithm

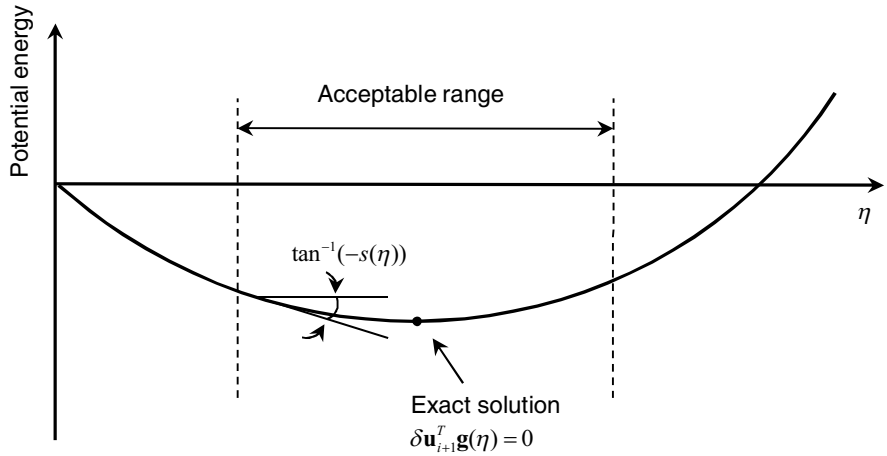

If the differential value of energy $s(\eta)$ is assumed to be a linear function of η, the value of η that satisfies Equation 5.5.6 is as shown below:

$$\eta = \frac{-s(\eta = 0)}{s(\eta = 1) - s(\eta = 0)} \tag{5.5.7}$$

Here, the gradient at which η is zero or one may be expressed as shown below:

$$s(\eta = 0) = \delta \mathbf{u}_{i+1}{}^{T} \mathbf{g}_{i}$$
$$s(\eta = 1) = \delta \mathbf{u}_{i+1}{}^{T} \mathbf{g}_{i+1} \quad (5.5.8)$$

In actuality, the assumptions required for the line search algorithm are not completely satisfied. Thus, the $s(\eta)$ calculated using Equation 5.5.7 is typically not equal to zero. Midas nGen allows the user to set a value on the ratio $s(\eta_j) / s(\eta = 0)$, and when the calculated value falls below the user-specified value, then the iterations will stop.

Initial Stiffness Method, Newton Raphson Method, Modified Newton Raphson Method

In nonlinear analysis, iterative methods can be categorized depending on the calculation point of the tangential stiffness. The methods are initial stiffness method, Newton Raphson Method, and Modified Newton Raphson Method. In the initial stiffness method, the tangential stiffness calculated at the beginning of the analysis is maintained throughout. In the Newton Raphson Method, the tangential stiffness is re-calculated at every iteration. In the Modified Newton Raphson Method, the tangential stiffness is calculated at the time of external force application or when a change occurs in the model. The calculation of the tangential stiffness matrix and matrix decomposition requires a lot of computational time, so using the Modified Newton Raphson method can lead to a much faster processing speed compared to the Newton Raphson method (if there are no problems in reaching convergence). Midas nGen does not explicitly differentiate the initial stiffness method from the Newotn Raphson method. Simply setting the procotol for stiffness recalculation can help utilize effects of all iterative methods.

Automatic Stiffness Update

The degree of nonlinearity, the smoothness of the convergent solution, and other factors of the model/problem will decide how to best define the point of tangential stiffness update. For nonlinear problems that will use the nonlinear finite element method, midas nGen provides an automated

tangential stiffness update that comprehensively judges the problem's characteristics—for example, convergence characteristics and divergence possibilities for an iterative solution—and arrives at a decision for setting the calculation point/time for a stiffness update. Generally, if the problem satisfies the following conditions, then the tangential stiffness is updated automatically.

► If the expected number of iterations for a convergent solution exceeds the user-specified maximum number of iterations

► If the solution is expected to diverge

Convergence Criteria

In iterative methods, the convergence or divergence of a solution is determined based on the force norm, displacement norm, and energy norm.

$$\text{Force norm ratio} = \frac{\sqrt{\mathbf{g}_i^T \mathbf{g}_i}}{\sqrt{\Delta\mathbf{f}_{\text{int},i}^T \Delta\mathbf{f}_{\text{int},i}}} \tag{5.5.9}$$

$$\text{Displacement norm ratio} = \frac{\sqrt{\delta\mathbf{u}_i^T \delta\mathbf{u}_i}}{\sqrt{\Delta\mathbf{u}_i^T \Delta\mathbf{u}_i}} \tag{5.5.10}$$

$$\text{Energy magnitude ratio} = \left| \frac{\delta\mathbf{u}_i^T \mathbf{g}_i}{\Delta\mathbf{u}_i^T \Delta\mathbf{f}_{\text{int},i}} \right| \tag{5.5.11}$$

For a typical nonlinear system, all convergence norms decrease simultaneously and reach convergence. In particular, the force norm is a measure of unbalanced equilibrium and is an excellent indicator of whether or not the nonlinear equation is satisfied. In contrast, the displacement norm represents the size of the incremental solution. When using penalty methods or solving problems in which the local stiffness is very large, it is not appropriate to use the displacement norm as the sole convergence criteria.

Midas nGen uses one or multiple of these criteria to compare to the user-specified allowable values and determine whether the solution will reach convergence.

Determining Divergence or Load Bisection

The divergence of a solution is an important criterion in the automated stiffness matrix update method, and is based on the divergence rate E_i.

$$E_i = \frac{\delta \mathbf{u}_i^T \mathbf{g}_i}{\delta \mathbf{u}_i^T \mathbf{g}_{i-1}} \tag{5.5.12}$$

If the absolute value of the divergence rate is greater than 1 ($|E_i| \geq 1$), then the solution to the nonlinear analysis has a risk of divergence. When this occurs, there are additional steps taken in the stiffness matrix update, such as the load bisection method.

The load bisection method is applied when the solution diverges, or if the number of iterations exceeds the user-specified maximum number of iterations. It may also be applied if the increment required for the current load step is too large. The method divides the basic load step into two and restarts the iterative process. Thus, it is a flexible way to tackle inappropriately-sized load increments. In midas nGen, if a problem requires load bisection, the load bisection method is applied automatically and repeatedly until the maximum bisection level has been reached.

Automated Time Increment Control

To improve the efficiency of nonlinear analysis methods, midas nGen offers the capability to automatically update the time increment size based on the convergence of the nonlinear analysis solution. The default time step and maximum time step is specified by the user. If the automated control capability is applied, the time step size is reduced based on the number of iterations required for convergence after the previous iteration.

$$\Delta t^{i+1} = n_s \ \Delta t^i \qquad (1 \leq n_s \leq n_{s,\max}) \tag{5.5.13}$$

Here, the increment control coefficient n_s is limited to the domain of natural numbers. This way, the nonlinear analysis solution should still be found close to the user's intended time step or load step size,

if possible. The increment control coefficient represents the initial increment size. Its minimum value is 1, and the user may specify the maximum value $n_{s,\max}$.

Quasi-Newton Method

Quasi-Newton method is a generalized secant method and is a type of nonlinear analysis method. It recalculates the stiffness matrix only when there is a loading increment in the nonlinear finite element method, which is a distinct advantage of the Newton method, and paves the way towards convergence with the least number of errors. Thus, there is no unnecessary computational time spent on recalculating the stiffness matrix during the iterations. The quasi-Newton method allows for efficient computation using decomposed stiffness matrices, and improves upon convergence and overall performance.

Midas nGen specifically uses the Broyden-Fletcher-Goldfarb-Shanno method[6]. The BFGS update procedure for the stiffness matrix in the context of nonlinear finite element analysis is shown below:

$$\mathbf{K}_j^{-1} = \mathbf{\Gamma}_j^T \mathbf{K}_{j-1}^{-1} \mathbf{\Gamma}_j + z_j \boldsymbol{\delta}_j \boldsymbol{\delta}_j^T \tag{5.5.14}$$

Here, j is the BFGS update index, and matrix $\mathbf{\Gamma}_j$ and scalar z_j are calculated as follows:

$$\begin{aligned} \mathbf{\Gamma}_j &= \mathbf{I} - z_j \boldsymbol{\gamma}_j \boldsymbol{\delta}_j^T \\ z_j &= \frac{1}{\boldsymbol{\delta}_j^T \boldsymbol{\gamma}_j} \end{aligned} \tag{5.5.15}$$

Then, the quasi-Newton vectors $\boldsymbol{\delta}_j$ and $\boldsymbol{\gamma}_j$ are the difference between the incremental solution $\delta\mathbf{u}_i$ after incorporating the line search coefficient η and the unbalanced equilibrium in the iterations, as shown below:

[6] Matthies, H. and Strang, G., "The solution of nonlinear finite element equations," International Journal for Numerical Methods in Engineering, Vol. 14, Issue 11, pp. 1613-1626, 1979

$$\boldsymbol{\delta}_j = \Delta\mathbf{u}_i - \Delta\mathbf{u}_{i-1} = \eta\delta\mathbf{u}_i$$
$$\boldsymbol{\gamma}_j = \mathbf{g}_i - \mathbf{g}_{i-1} \tag{5.5.16}$$

In the iterative calculations, the i th incremental solution is calculated using the unbalanced equilibrium and the j th BFGS-updated stiffness matrix and unbalanced equilibrium:

$$\delta\mathbf{u}^i = \mathbf{K}_j^{-1}\mathbf{g}^{i-1} = \boldsymbol{\Gamma}_j^T\mathbf{K}_{j-1}^{-1}\boldsymbol{\Gamma}_j\mathbf{g}^{i-1} - z_j\boldsymbol{\delta}_j\boldsymbol{\delta}_j^T\mathbf{g}^{i-1} \tag{5.5.17}$$

The inverse stiffness matrix is not actually modified through the BFGS update procedure, and the incremental solution is determined through the recursive method. Thus, the initial stiffness matrix (before the BFGS update has been applied) is maintained in its decomposed form. The incremental solution can instead be calculated through simple vector arithmetic and recursive iterations. For such calculations, the quasi-Newton vector is saved, and this vector is deleted when the incremental solution has converged and the stiffness matrix has been reconstructed.

Arc-Length Method

Figure 5.5.3 shows various load-displacement paths with unstable equilibrium. When conducting static nonlinear analyses in these cases, it is impossible to progress the analysis of the unstable static equilibrium beyond the limit point (when using the typical load-controlled nonlinear method). Thus, the typical nonlinear method cannot converge to a solution once it passes the limit point. If the displacement controlled method is used instead, the domain of solvable problems becomes larger. However, the displacement controlled method is atypical and it is impossible to predict phenomena like snap-back behavior. In such cases, the arc-length method may be used. Even in the case of unstable equilibrium, the arc-length method can successfully predict the equilibrium load path.

Figure 5.5.3 Various unstable equilibrium paths

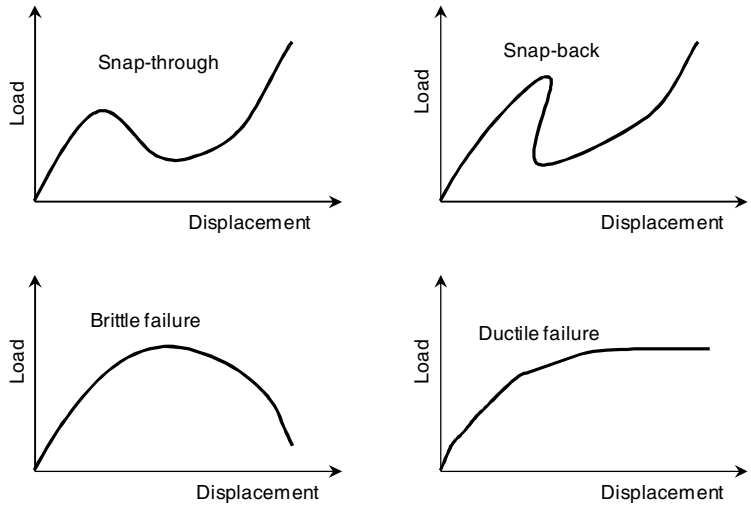

The arc-length method assumes that the external force is proportional to the independent scalar loading parameter λ . Consequently, the arc-length method intrinsically increases the number of degrees of freedom by one in a finite element problem. However, the algorithm ensures that the parameter λ , along with the accumulated incremental solution, satisfies the arc-length constraint. Thus, the final number of degrees of freedom is maintained. The unbalanced equilibrium equation with the loading parameter may be expressed as follows:

$$\mathbf{g}_i(\mathbf{u}_i, \lambda_i) = \lambda_i \mathbf{f}_{ext} - \mathbf{f}_{int,i} \tag{5.5.18}$$

Here, if the condition that unbalanced equilibrium that occurs at the $i+1$ th iteration becomes zero with the incremental solution $\delta\mathbf{u}_{i+1}$ and the incremental load parameter $\delta\lambda_{i+1}$ becomes linearized, then the relationship between the incremental solution and incremental loading parameter can be expressed as shown below:

$$\delta\mathbf{u}_{i+1} = \mathbf{K}_{i+1}^{-1} (\mathbf{g}_i + \delta\lambda_{i+1} \mathbf{f}_{ext}) \tag{5.5.19}$$

Using this, then the $i+1$ th iterative calculation yields the incremental solution as shown below:

$$\Delta \mathbf{u}_{i+1} = \Delta \mathbf{u}_i + \delta \bar{\mathbf{u}} + \delta \lambda_{i+1} \mathbf{u}_T \tag{5.5.20}$$

$\delta \bar{\mathbf{u}} = \mathbf{K}_{i+1}^{-1} \mathbf{g}_i$: Incremental solution due to unbalanced equilibrium

$\mathbf{u}_T = \mathbf{K}_{i+1}^{-1} \mathbf{f}_{ext}$: Displacement due to the total load

Midas nGen uses the Cirsfield, Riks, or Modified Riks arc-length method, and the Crisfield method[7] uses the following basic restraint condition:

$$\Delta \mathbf{u}_{i+1}^T \Delta \mathbf{u}_{i+1} = \Delta l^2 \tag{5.5.21}$$

Δl : Arc-length

Using the above equation, the incremental loading parameter $\delta \lambda_{i+1}$ can be calculated. Substituting this, the $i+1^{\text{th}}$ iterative solution can be calculated. Like typical nonlinear solution methods, this procedure is repeated until the user-specified convergence criteria has been satisfied, and the converge criteria is the same as that of the typical nonlinear method. Thus, internal force, displacement, or change in energy are used as the convergence condition.

When using the arc-length method, the load increment cannot be decided by the user and is instead decided by the arc-length restraint condition. Thus, it may be difficult to achieve an accurate solution based on the desired loading criteria. As a aresult, the arc-length method should be applied specifically to problems in which unstable equilibrium is involved and there are no additional benefits for solving typical nonlinear problems.

[7] Crisfield, M.A., "An arc-length method including line searches and accelerations," International Journal for Numerical Methods in Engineering, Vol. 19, Issue 9, pp 1269-1289, 1983

Section 6 P-Delta Effect

6.1 Consideration of P-Delta

In cases where the structure is subject to both lateral and axial forces, the P-Delta effect is a consideration of second order structural motion. To solve for this second order motion, it utilizes the numerical solution method applied to buckling problems. First, the static analysis for the given loading criteria is completed. Then, the geometric stiffness matrix is constructed based on the element stresses. The modified stiffness matrix is used in iterative calculations that are repeated until the given conditions are satisfied. The static equilibrium equation used in the iterations is shown below:

$$\mathbf{K}\mathbf{u} + \mathbf{K}_g\mathbf{u} = \mathbf{f} \tag{5.6.1}$$

$\mathbf{K}$: Stiffness matrix

$\mathbf{K}_g$: Geometric stiffness matrix based on axial stress

$\mathbf{u}$: Displacement

$\mathbf{f}$: Loading vector

Definition of the P-Delta Effect

When a structure experience moment and shear force due to an external force, the tension increases the lateral stiffness and the compression decreases the stiffness.

Figure 5.6.1 shows a structure subject to both tensile and lateral force. In the case where the P-Delta effect is not considered, the moment at the top is zero. From top to bottom, the moment follows the linear relationship $M=VL$. In reality, displacement occurs due to the lateral force, and the lateral displacement reduces the moment due to tension. Similarly, in cases where the structure is subject to both compression and lateral force, the moment increases and the resulting effect can be likeend to a reduced lateral stiffness.

Figure 5.6.1 P-Delta Effect

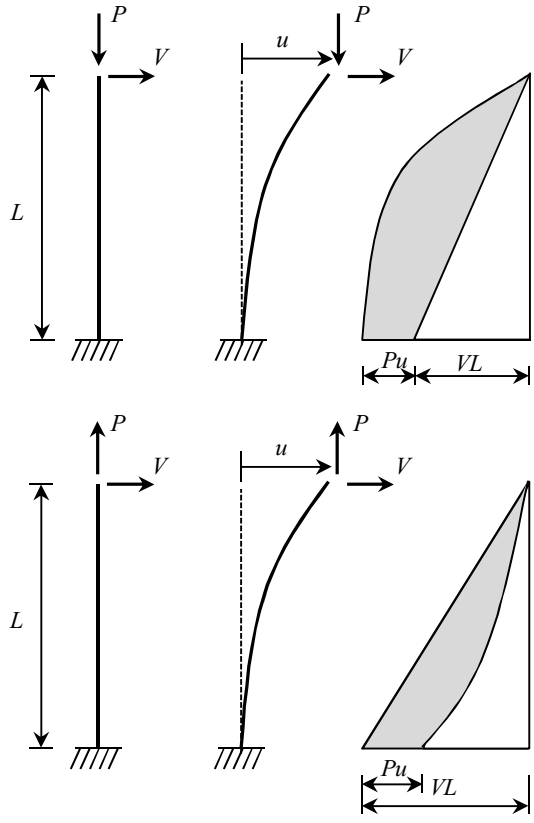

6.2 P-Delta Verification Examples

1) Cantilever Column

REFERENCE	Livesley, R. K., and Chandler[1]
ELEMENTS	Bar elements
MODEL FILENAME	PDelta01.mpb

The figure below shows a cantilever column model. This example serves to verify the P-Delta effect and how that may change as a result of the loading criteria and the boundary conditions.

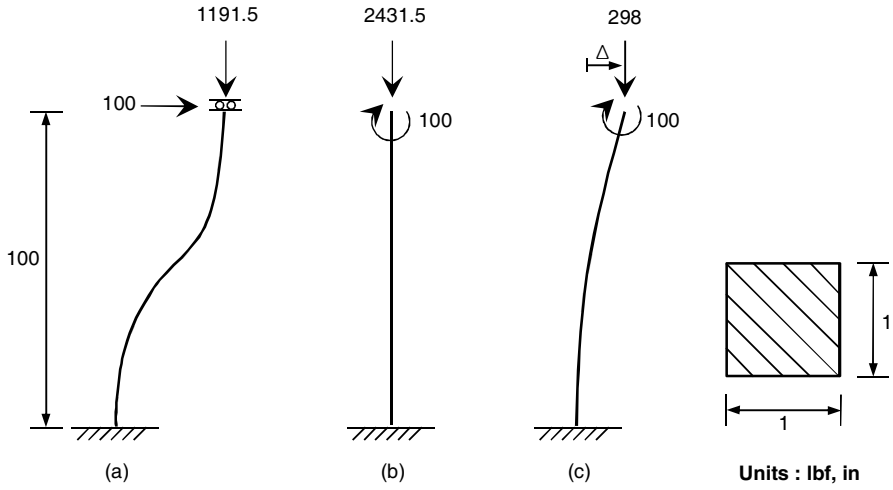

Figure 6.2.1.1 Structural geometry and analysis models (a) Pure sway, (b) No sway, (c) No shear

Material data	Elastic modulus	$E = 2.9x10^7$ *psi*
	Poisson's ratio	$\nu = 0.0$

Table 6.2.1.1 Comparison of pure sway model result

Result	Reference	midas nGen
Lateral displacement at the top	*6.849*	*6.820*
Bending moment at the bottom	*9084.0*	*9062.8*

Table 6.2.1.2 Comparison of no sway model result

Result	Reference	midas nGen
Lateral displacement at the top	*0.420*	*0.420*
Bending moment at the bottom	*-102.0*	*-101.2*
Shear force at the bottom	*-202*	*-201*
Rotational displacement at the top	*0.00170*	*0.00168*

Table 6.2.1.3 Comparison of no shear model result

Result	Reference	midas nGen
Lateral displacement at the top	*0.00752*	*0.00751*
Bending moment at the bottom	*225.2*	*225.1*

2) 2-Dimensional Portal Frame

REFERENCE	Livesley, R. K., and Chandler[1]
ELEMENTS	Bar elements
MODEL FILENAME	PDelta02.mpb

The figure bellow shows a 2-dimensional portal frame. This example serves to verify how the P-Delta effect changes as a result of the load location.

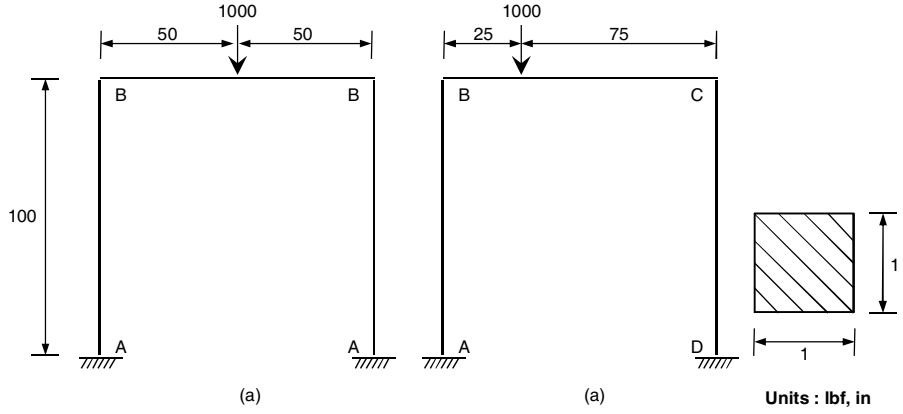

Figure 6.2.2.1
Structural geometry and analysis models
(a) Symmetric load case, (b) Eccentric load case

Material data	Elastic modulus	$E = 2.9x10^7$ *psi*
	Poisson's ratio	$\nu = 0.0$

Table 6.2.2.1 Comparison of symmetric load case result

Result	P-Delta effect analysis		Conventional analysis	
	Reference	midas nGen	Reference	midas nGen
Rotation at B	*0.09192*	*0.09179*	*0.08620*	*0.08621*
Moment at A	*4606.6*	*4588.9*	*4166.7*	*4166.5*
Moment at B	*8254.0*	*8260.3*	*8333.3*	*8333.2*
Shear force at A	*128.6*	*128.5*	*125.0*	*125.0*

Table 6.2.2.2 Comparison of eccentric load case result

Result	P-Delta effect analysis		Conventional analysis	
	Reference	midas nGen	Reference	midas nGen
Lateral displacement at B	*1.893*	*1.893*	*1.385*	*1.385*
Rotation at B	*0.1013*	*0.1014*	*0.0924*	*0.0924*
Rotation at C	*0.0367*	*0.0367*	*0.0369*	*0.0370*
Moment at A	*2544.9*	*2551.2*	*2455.4*	*2455.6*
Moment at B	*6088.6*	*6183.4*	*6919.6*	*6919.2*
Moment at C	*6153.0*	*6125.0*	*5580.4*	*5580.7*
Moment at D	*4456.9*	*4503.5*	*3794.6*	*3794.1*
Shear force at A	*101.4*	*101.6*	*93.75*	*93.75*

References

[1] Livesley, R. K., and Chandler, D. B., “Stability Functions for Structural Frameworks”, Manchester University Press, UK, 1956.

Section 7

Nonlinear Dynamic Response Analysis

Midas nGen offers the ability to conduct nonlinear time history analysis that incorporates nonlinear elastic properties and the analysis is based on implicit time integration.

7.1 Implicit Time Integration

When computing the static equilibrium equation in nonlinear time history analysis, $\mathrm{HHT}-\alpha$ method is used to conduct implicit time integration, which is also used in linear time history analysis. A modified form of the equilibrium eqation, shown below, is used:

$$\frac{\partial}{\partial t}\left(\mathbf{M}\mathbf{v}^{n+1}\right)+(1+\alpha_H)\left[\mathbf{C}\mathbf{v}^{n+1}+\mathbf{f}^{\mathrm{int},n+1}-\mathbf{f}^{ext,n+1}\right]-\alpha_H\left[\mathbf{C}\mathbf{v}^{n}+\mathbf{f}^{\mathrm{int},n}-\mathbf{f}^{ext,n}\right]=\mathbf{0} \tag{5.7.1}$$

In nonlinear time history analysis, the rotation of the mass matrix (due to the geometric nonlinearities) is incorporated. The rotationa linertia of the mass matrix is calculated at every iteration based on each node's limited rotation, and the analysis incorporates the inertia due to the change in the mass matrix.

Nonlinear time history analysis uses the nonlinear finie element method discussed in Section 5.5, and solves for a convergent solution at each time step. The unbalanced equilibrium equation is expressed as shown below, based on Equation 5.7.1:

$$\mathbf{g}_{n+1} = \frac{\partial}{\partial t}\left(\mathbf{M}^{n+1}\mathbf{v}^{n+1}\right) + (1+\alpha_H)\left[\mathbf{C}^{n+1}\mathbf{v}^{n+1} + \mathbf{f}^{\text{int},n+1} - \mathbf{f}^{ext,n+1}\right] - \alpha_H\left[\mathbf{C}^{n+1}\mathbf{v}^{n} + \mathbf{f}^{\text{int},n} - \mathbf{f}^{ext,n}\right] \quad (5.7.2)$$

The tangential stiffness matrix can be expressed by applying the temporal difference equation from the Newmark method (Equation 5.4.3) to the velocity and acceleration due to unbalanced equilibrium. It may be solved with respect to the unknown variable of the displacement degree of freedom and can be expressed as shown below:

$$\mathbf{A} = \frac{1}{\beta\Delta t^2}\mathbf{M}^{n+1} + \frac{\gamma}{\beta\Delta t}\dot{\mathbf{M}}^{n+1} + \frac{(1+\alpha_H)\gamma}{\beta\Delta t}\mathbf{C}^{n+1} + (1+\alpha_H)\frac{\partial \mathbf{f}^{\text{int},n+1}}{\partial \mathbf{u}} - (1+\alpha_H)\frac{\partial \mathbf{f}^{ext,n+1}}{\partial \mathbf{u}} \quad (5.7.3)$$

Like linear tiem history analysis, $\alpha_H = -0.05$ is the default value. Furthermore, to ensure unconditional stability, the following values are used: $\gamma = (1-2\alpha_H)/2$, $\beta = (1-\alpha_H)^2/4$

Angular Velocity and Angular Acceleration

When considering geometric nonlinearities in nonlinear time history analysis, the angular velocity and angular acceleration must be updated to reflect the effects due to the rotation of the body axis system. If ϕ represents the axis about which rotation occurs, then the Newmark difference equation in the body axis coordinate system is as follows:

$$\boldsymbol{\omega}_\phi^{n+1} = \boldsymbol{\omega}_\phi^{n} + \Delta t\left[\gamma\boldsymbol{\alpha}_\phi^{n+1} + (1-\gamma)\boldsymbol{\alpha}_\phi^{n}\right] \quad (5.7.4)$$

$\boldsymbol{\omega}_\phi$, $\boldsymbol{\alpha}_\phi$: Angular Velocity and Angular Acceleration with respect to ϕ

Using the vector $\mathbf{e}_\phi$ (orthogonal to the body axis), the above expression can be modified to be expressed with respect to the global coordinate system:

$$\boldsymbol{\omega}^{n+1} = \Delta t\gamma\boldsymbol{\alpha}^{n+1} + \left(\mathbf{e}_\phi^{n+1}\mathbf{e}_\phi^{n}\right)\left[\boldsymbol{\omega}^{n} + \Delta t(1-\gamma)\boldsymbol{\alpha}^{n}\right] \quad (5.7.5)$$

The product of the basal vector in Equation 5.7.5 is the same as the incremental rotation matrix that is computed with the equation below:

$$\Delta \mathbf{C} = \exp(\Delta \hat{\theta}) \tag{5.7.6}$$

$\Delta \hat{\theta}$: Skew Symmetric matrix due to incremental rotation

Using the incremental rotation matrix, the rotation increment may be expressed with the Newmark method as shown below:

$$\Delta \boldsymbol{\theta} = \Delta t^2 \beta \boldsymbol{\alpha}^{n+1} + \Delta \mathbf{C} \left[\Delta t \boldsymbol{\omega}^n + \Delta t^2 \left(\frac{1}{2} - \beta \right) \boldsymbol{\alpha}^n \right] \tag{5.7.7}$$

Equation 5.7.7 may be rearranged with respect to the angular velocity and angular acceleration, and then substituted into Equation 5.7.5. The result equations, shown below, update the angular velocity and angular acceleration:

$$\begin{aligned} \boldsymbol{\omega}^{n+1} &= \frac{\gamma}{\Delta t \beta} \Delta \boldsymbol{\theta} + \Delta \mathbf{C} \left[\left(1 - \frac{\gamma}{\beta} \right) \boldsymbol{\omega}^n + \Delta t \left(1 - \frac{\gamma}{2\beta} \right) \boldsymbol{\alpha}^n \right] \\ \boldsymbol{\alpha}^{n+1} &= \frac{1}{\Delta t^2 \beta} \Delta \boldsymbol{\theta} + \Delta \mathbf{C} \left[\frac{1}{\Delta t \beta} \boldsymbol{\omega}^n + \left(1 - \frac{1}{2\beta} \right) \boldsymbol{\alpha}^n \right] \end{aligned} \tag{5.7.8}$$

Damping Effect

Like in linear time history analysis, nonlinear time history analysis incorporates mass-proportional and stiffness-proportional damping. In this case, the stiffness matrix is composed similar to Equation 5.4.5. In nonlinear time history analysis, the mass matrix used in the construction of the damping matrix is the mass matrix that incorporates the rotation effects discussed previously, and the stiffness matrix exclusively includes the stiffness matrix composed of material nonlinearities.

$$\mathbf{C} = \alpha_j^e \mathbf{M}_j^e + \beta_j^e \mathbf{K}_{mat,j}^e + \mathbf{B} \tag{5.7.9}$$

$\mathbf{K}_{mat}$: Stiffness matrix due to material nonlinearities

Section 8

Moving Crane Analysis

8.1 Moving Crane Analysis

Midas nGen offers the ability to conduct moving crane analysis. This capability outputs the analysis results of a crane girder, and is used to reflect the the reaction at the supports due to the static crane moving load when the structure is being constructed. The principal capabilities are as follows:

• Computation of the impact due to sagging, internal force, support reactions
• Computation of maximum/minimum displacement, internal force, and support reactions due to the computed impact and crane load

Dynamic analysis for structures computes the response due to loads caused by a moving crane. Thus, the analysis incorporates the crane movement and calculates maximum and minimum values. The results are output as moving analysis results.

The moving analysis in midas nGen does not analyze the impact on the entire structure, but models the selected craine girder and calculates the girder's axial force, displacement of the nodes within the span, and the support reactions. The analysis of crane load on the entire structure is incorporated by transforming the support reactions into nodal loads.

The results are output after being categorized based on the location of the lifting load or the existence of the load. A typical crane moves by using two crane girders as rails and the lifting load acts between the two crane girders. The loading locations based on the crane's moving direction are estimated with respect to the crane girder's nodes, and thus the number of nodes must be appropriately defined. The lifting load between the two girders must experience the maximum value, and thus the software considers the location that is as close as possible to each of the crane girders. Furthermore, for proper

combination with earthquake loads, the situation in which lifting loads do not occur is also considered. Midas nGen will also create loads to reflect effects due to the lateral movement of the lifting load or crane's operation status. The results of the moving crane analysis can be categorized into the following six types.

- Max. Crane Load(Max)

  The maximum value that occurs as a result of the lifting load located closest to the selected girder

- Max. Crane Load(Min)

The minimum value that occurs as a result of the lifting load located closest to the selected girder
- Min. Crane Load(Max)

The maximum value that occurs as a result of the lifting load located closest to the opposite girder
- Min. Crane Load(Min)

  The minimum value that occurs as a result of the lifting load located closest to the opposite girder

- Empty Crane Load(Max)

  In a situation in which there is no lifting load, the maximum reaction that occurs as a result of the trolley being located closest to the selected girder

- Empty Crane Load(Min)

  In a situation in which there is no lifting load, the maximum reaction that occurs as a result of the trolley being located closest to the opposite girder

An outline of the analysis procedure for moving cranes is shown below.

1. Unit loads are exerted on the selected crane girder's nodes, and the impact analysis is completed.
2. Using the inputs to the moving crane analysis and impact analysis results, the moving analysis is conducted using possible crane locations. Maximum and minimum values are computed and the nodal displacements, girder forces, and support reactions are also calculated. Other components that occur simultaneously with the girder's internal force and support reactions may be computed for structural design purposes.

3. Using the support reactions, the crane static loads are computed and then the analysis of the entire structure can continue.

8.2 Crane Movement Simulation

In mdas Plant, the crane load is simulated as a concentrated load that is repeated at equal distances, as shown in Figure 8.2.1. Vertical loads are decided based on the self weight of the crane, trolley, hoist, and maximum lifting load. Horizontal or longitudinal forces are computed as a proportion of the vertical loads. Horizontal loads represent the loads that occur due to horizontal movement of the trolley, and the operational loads are loads that occur when the crane begins or stops moving. Operational loads do not apply to all wheels on the crane, but only on the wheels that are in the direction of operation.

The vertical loads are always assumed to be in the direction of gravity and thus are in the z-axis direction of the global coordinate system. Horizontal loads are orthogonal to the crane's moving direction, and the longitudinal loads are set in the direction of the crane's movement. Horizontal and longitudinal loads may be defined in either positive or negative directions. The following seven load combinations are used to calculate internal forces and reactions.

1. Vertical Load
2. Vertical Load + Horizontal Load (Left orthogonal direction to the crane's movement)
3. Vertical Load + Horizontal Load (Right orthogonal direction to the crane's movement)
4. Vertical Load + Tractive Force (In the direction of the crane's movement)
5. Vertical Load + Tractive Force (Opposite to the direction of the crane's movement)
6. Vertical Load + Braking Force (In the direction of the crane's movement)
7. Vertical Load + Braking Force (Opposite to the direction of the crane's movement)

Figure 8.2.1 Simulation of Crane Loads

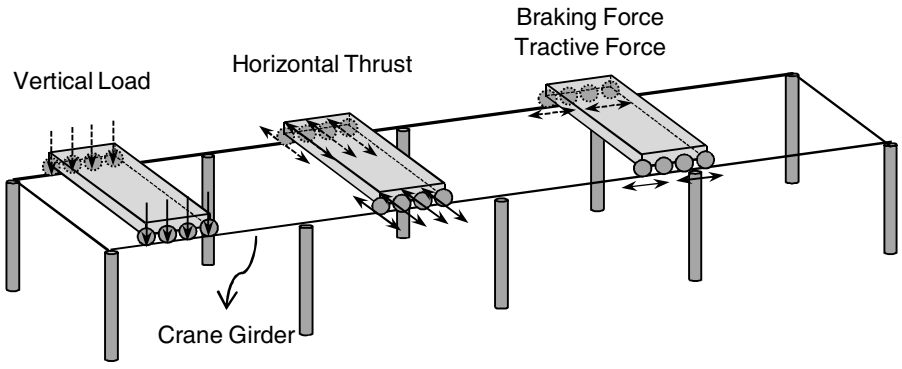

The results from moving crane analysis can be categorized into max. crane and min. crane. The cases in which the lift force (including the hoist) is closest to and furthest from the crane girder of interest are separated, and the crane girder's displacement, reaction, and internal force are calculated. The closest distance result is called Max. Crane and the furthest distance result is called Min. Crane. Thus, the vertical load for Max. Crane and Min. Crane are applied differently. The horizontal loads are applied independently of the location of the lift force, and have the same values for all cases. Bracking and tractive forces are defined as a proportion of the vertical load. The inputs that define crane loads are shown below, and the Max. Crane and Min. Crane can be calculated simply based on the vertical load.

Crane Information

Capacity (A)	Lifting Load
Crane total weight (B)	Crane Self Weight
Trolly & Hoist weight (C)	Weight of the trolley and hoist
Crane span (D)	Distance between the crane girders
Hook approach (E)	Smallest distance between the lifting load and crane girder
Number of wheel (N)	Number of wheels on the crane

Factor of horizontal load(F)	Ratio of the horizontal load to the vertical load

Crane Wheel Load

Max. Crane Vertical Load	$\frac{1}{N}\left(\frac{A}{2}+\frac{(B+C)(D-E)}{D}\right)$
Min. Crane Vertical Load	$\frac{1}{N}\left(\frac{A}{2}+\frac{(B+C)E}{D}\right)$
Horizontal Load	$\frac{1}{N}\left(\frac{A+B+C}{2}\right)\times F$

8.3 Impact Line Analysis and Moving Analysis Results

The impact analysis in midas nGen expresses the results of unit loads exerted on crane girders. Results that are located between the unit load locations are linearly interpolated, and thus a more accurate impact line can be calculated with additional unit loads. To calculate the impact, the unit loads are applied in three directions in order to reflect the vertical, horizontal, and longitudinal loads of the crane. These directions are the x- and y-axes of the element coordinate system, along with the z-axis of the global coordinate system.

The results for actual crane loads are calculated from the product of the size of the crane load and the value of the impact line at the crane location. Figure 8.3.1 shows the calculation for the simply supported girder's impact line for midpoint shear force and maximum value. Using the impact line from exerting unit loads, the impact values at the moving crane's locations are multiplied by the actual crane load to obtain the maximum value result. In the case below, the maximum value of 125 is obtained by multiplying the crane load of 100 and the impact at the location of the crane's wheels.

Figure 8.3.1 Load location and result computation of crane analysis

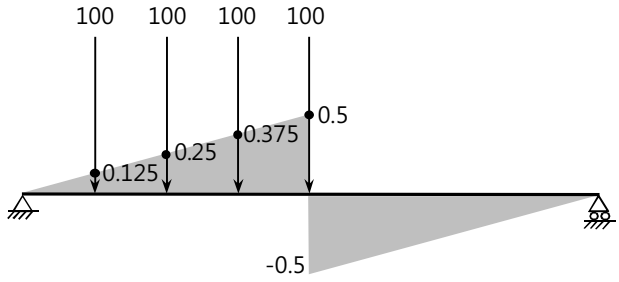

Shear force = 100 x (0.125 + 0.25 + 0.375 + 0.5)
= 125

8.4
Moving Crane
Analysis Examples

1) Moving Crane Analysis

ELEMENTS	Beam elements
MODEL FILENAME	Crane_01.mpb

Figure 8.4.1 shows a typical crane girder structure. The supports of a crane are modeled with column elements. These supports are transformed into simple supports in analysis. Important aspects in crane girder design include sagging, shear, and moment at the span's midpoint (point B), along with the reaction at the support at point A. These results are compared with the exact solution. The crane atop the crane girders are assumed to have the concentrated loads shown in the bottom right figure within Figure 8.4.1. Table 8.4.1 shows the exact solution (through numerical methods) and the results of the moving crane analysis. Excluding displacement, all results are the same. In the case of displacement, there is a small difference of 1.5%, and this is due to the assumption that the impact inbetween the loading locations are linearly interpolated. If the number of elements between the spans are increased, then the number of impact lines increase and thus a more accurate result may be obtained. The results shown in Table 8.4.1 uses a model with 8 elements per span.

Figure 8.4.1 Crane girder structure with crane loads

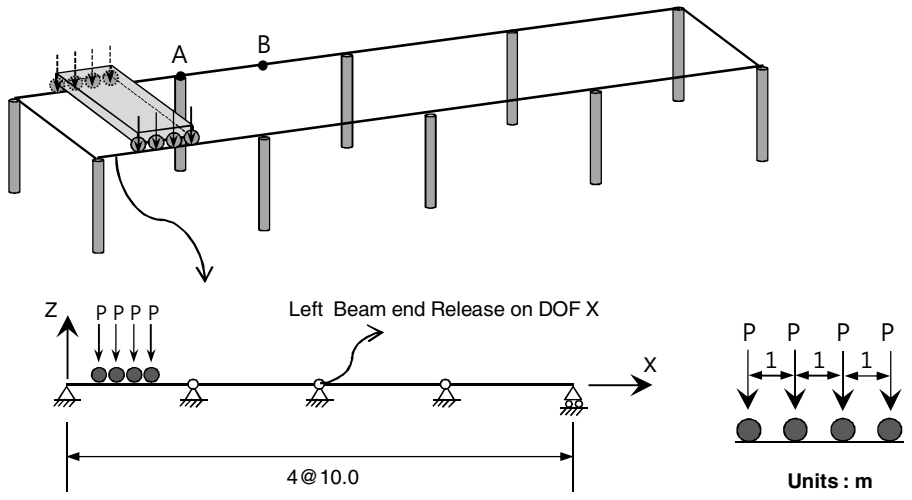
A
B
Z
P P P P
Left Beam end Release on DOF X
X
4@10.0
P P P P
1 1 1
Units : m

Material data	Elastic modulus	$E = 205GPa$
	Poisson's ratio	$\nu = 0.3$
Section property	Area	$A = 3886\ mm^2$
	Shear Area	$A_s = 1882\ mm^2$
	Moment of Inertia	$I_x = 23591960\ mm^4$
Crane	Capacity(A)	*100 kN*
	Crane total weight(B)	*100 kN*
	Trolly & hoist weight(C)	*10 kN*
	Crane span (D)	*10 m*
	Hook approach(E)	*1 m*
	Number of wheel(N)	*4*
	Factor of horizontal load	*0.1*
Wheel load	*Max. crane vertical*	*37.25 kN*
	Min. crane vertical	*15.25 kN*
	Horizontal	*2.625*

Table 8.4.1 Results of crane moving load analysis at point A and B

Max. Crane Case	Crane moving analysis	Exact
Vertical reaction at point A(kN)	*134.1*	*134.1*
Horizontal reaction at point A(kN)	*9.45*	*9.45*
Displacement at point B (mm)	*0.591*	*0.60*
Moment at point B(kN-m)	*298*	*298*
Shear at point B(kN)	*52.15*	*52.15*
Min. Crane Case	Crane moving analysis	Exact
Vertical reaction at point A(kN)	*54.9*	*54.9*
Horizontal reaction at point A(kN)	*9.45*	*9.45*
Displacement at point B (mm)	*0.242*	*0.246*
Moment at point B(kN-m)	*122*	*122*
Shear at point B(kN)	*21.35*	*21.35*

Section 1 Loads

1.1 Types of Structural Loads

Structural loads that may be applied in midas nGen can be broadly categorized into force, gravitational force, displacement, and temperature load. The categories are described in Table 6.1.1.

Table 6.1.1 Loads that can be applied in Midas nGen

Type	Applicable Nodes/Elements
Nodal force/moment	Nodes
Pressure load	2-dimensional elements, 3-dimensional elements
Beam load	Beam elements
Gravity	All elements with nonzero mass
Specified displacement/velocity/acceleration	Nodes
Temperature load	Nodes, 1-dimensional elements, 2-dimensional elements, 3-dimensional elements

Nodal force/moment

Nodal force/moment is the most basic type of load. The user may specify up to three force components and three moment components per node. The directions may be defined based on an arbitrary coordinate system.

Pressure load

Pressure loads are distributed loads exerted on an element's face or edge. Face pressure loads are applicable to 2-dimensional or 3-dimensional loads. Edge pressure loads may be applied to 2-dimensional elements. The load direction can be the axial direction of an arbitrary coordinate system, or the orthogonal direction. Figure 6.1.1 shows how the pressure load be applied to various elements.

Figure 6.1.1 Pressure loads on various surfaces and elements

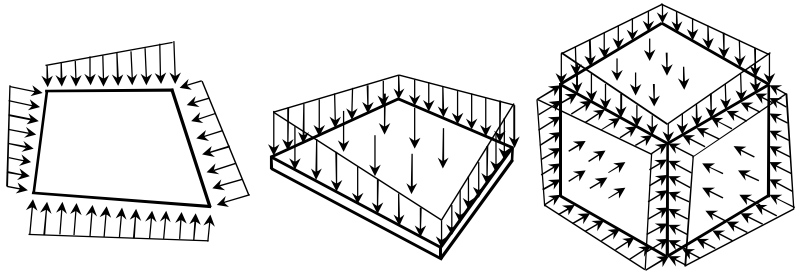

pressure on edge

pressure on surface

Self Weight due to Gravity

Gravity can be used to model a structure's self-weight or inertial force. It may be applied to any elements with mass. In particular, for truss and beam elements, gravity is considered to be a distributed force.

Specified Displacement/Velocity/Acceleration

Specified displacement may be applied to a specific node, and this load is used when the final location of a node is known. Specified displacement is categorized as a load as it causes strain in the structure, but also causes a restraint condition.

Assume that all degrees of freedom for a given problem are contained in the vector $\mathbf{u}_A$. Then, it may be separated into degrees of freedom with specified displacements and degrees of freedom without such displacements, as shown below:

$$\mathbf{u}_A = \begin{Bmatrix} \mathbf{u}_F \\ \mathbf{u}_S \end{Bmatrix} \tag{6.1.1}$$

$\mathbf{u}_F$: Degrees of freedom without specified displacements

$\mathbf{u}_S$: Degrees of freedom with specified displacements

Similarly, the stiffness matrix may be decomposed as follows:

$$\mathbf{K}_{AA}\mathbf{u}_A = \begin{bmatrix} \mathbf{K}_{FF} & \mathbf{K}_{FS} \\ \mathbf{K}_{SF} & \mathbf{K}_{SS} \end{bmatrix} \begin{Bmatrix} \mathbf{u}_F \\ \mathbf{u}_S \end{Bmatrix} = \mathbf{f}_A = \begin{Bmatrix} \mathbf{f}_F \\ \mathbf{f}_S \end{Bmatrix} \tag{6.1.2}$$

In the above equation, $\mathbf{u}_S$ is a defined, known quantity, and the second term in the stiffness equation does not represent a real quantity. Using $\mathbf{u}_S$, the first term may be rearranged and can yield loading due to the specified displacement, as shown below:

$$\mathbf{K}_{FF}\mathbf{u}_F = \mathbf{f}_F - \mathbf{K}_{FS}\mathbf{u}_S \tag{6.1.3}$$

In dynamic analysis, specified velocity and acceleration may be exerted on the structure. Specified velocity and acceleration are connected to time integration and may be transformed as a specified displacement. This transformed displacement condition will be integrated into the analysis using the equations shown above.

Temperature Load

Temperature load can be expressed as ΔT which represents the difference between the final and initial temperatures. The thermal expansion coefficient $\boldsymbol{\alpha}(T_m)$ is a function of the material temperature T_m, and the strain can be expressed as $\boldsymbol{\varepsilon} = \boldsymbol{\alpha}(T_m)\Delta T$. Thus, the initial and final temperatures must be defined for each structural member. Table 6.1.2 shows how temperatures may be applied to different nodes and element types.

Table 6.1.2 Temperature loads that may be applied to different elements

Types	Applicable Types
Nodal temperature	Nodes
Element temperature	Truss, beam, shell, and solid elements

1.2 Definition of Static and Dynamic Loads

Static Load

In midas nGen, static loads are used in linear/nonlinear static analyses, and may be defined according to the aforementioned load types. Loads are added differently for linear and nonlinear analyses.

▸ Linear static analysis

Linear static analysis is executed in a single step and incorporates all loads. The static load is the total load.

▸ Nonlinear static analysis

The load added to the analysis is proportional to the load scale $0 \le \lambda_I \le 1$. In nonlinear analysis, the total loading vector is defined as follows:

$$\mathbf{f}_{ext}(\lambda_I) = (1-\lambda_I)\,\mathbf{f}_{int,0} + \lambda_I \sum_j \mathbf{f}_{ext}^j \tag{6.1.5}$$

Here, $\mathbf{f}_{ext}^j$ represents the external vector due to the j^{th} load. $\mathbf{f}_{int,0}$ represents the internal force at the starting point of nonlinear analysis, and is calculated as a sum of the element internal forces at the initial point ($\mathbf{f}_{int}^e$).

$$\mathbf{f}_{int,0} = \sum_e \mathbf{f}_{int}^e(\boldsymbol{\sigma}_0, \mathbf{u}_0, \cdots) \tag{6.1.6}$$

If the loading scale is $\lambda_0 = 0$, then the total external force becomes in equilibrium with the initial internal forces. If the loading scale is $\lambda_I = 1$, which is in the final stage of the analysis, then the total external force becomes the sum of the load combinations.

Dynamic Loads

In midas nGen, dynamic, time-variant loads may be applied in linear or nonlinear time history analysis. In time history analysis, the total load vector is a function of time t as shown below:

$$\mathbf{f}_{ext}(t) = \sum_j T_j(t)\,\mathbf{f}_{ext}^j \tag{6.1.7}$$

Here, $T_j(t)$ is the j^{th} loading scale. Typically, this can be defined using tabular data, or it may be defined by coefficients of a specific function (Equation 6.1.8).

$$T_j(t) = (A + C\,t)e^{-D\,t}\sin(2\pi\,f\,t + \overline{P}) \tag{6.1.8}$$

Section 2

Boundary/Restraint Conditions

Restraint conditions can be divided into single-point constraints and multi-point constraints. Single-point constraints are applied to a single node, and multi-point constraints define specific relationships between various nodal degrees of freedom.

2.1 Single-Point Constraints

Single-point constraint restrains directional components of a specific node and effectively removes the corresponding degree of freedom. Single-point constraints are typically applied to nodes that do not experience displacement or for enforcing symmetry conditions.

Single-point constraints may also be used to remove degrees of freedom that should not be incorporated into the analysis. This method essentially removes singularities in a stiffness matrix, and it is important to properly set up the direction of the restraint condition. For example, the figure below shows degrees of freedom located at where the two elements meet. Other than a degree of freedom in the axial direction, the other degrees of freedom should not be reflected in the analysis. Thus, all other directions must be restrained and the corresponding singularities should be removed from the stiffness matrix. However, if the coordinate system is defined as an x-y coordinate system as shown in the figure, then an appropriate restrain direction cannot be defined. This brings about the need for a new nodal displacement coordinate system that is based on the axial direction of the element and the vector orthogonal to that axial direction (vector $\mathbf{n}$). Then, the direction of vector $\mathbf{n}$ is restrained and an appropriate restraint condition for analysis has been defined.

Figure 6.2.1 Example of using the nodal displacement coordinate system

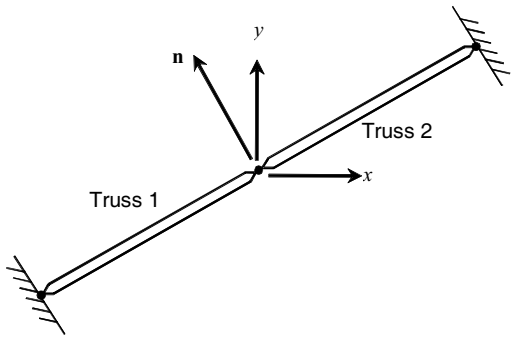

2.2 Multi-Point Constraints

Multi-point constraints apply restraint conditions by defining linear relationships between various nodal degrees of freedom. The typical form is shown below:

$$R_j u_j = 0 \tag{6.2.1}$$

R_j : Coefficient of linear relationship

u_j : Constrained degrees of freedom

If there are multiple multi-point constraints, then the relationships may be expressed as matrices, as shown below:

$$\mathbf{R}_M \mathbf{u}_M = \mathbf{0} \tag{6.2.2}$$

To apply a solution of simultaneous equations to multi-point constraints, the DOF's ($\mathbf{u}_M$) must be categorized into independent and dependent DOF's. When solving the system of equations, the dependent DOF's will be eliminated. First, the degrees of freedom subject to multi-point constraints are categorized into independent DOF's $\mathbf{u}_I$ and dependent DOF's $\mathbf{u}_D$.

$$\mathbf{u}_M = \begin{Bmatrix} \mathbf{u}_I \\ \mathbf{u}_D \end{Bmatrix}, \quad \mathbf{R}_M = \begin{bmatrix} \mathbf{R}_I & \mathbf{R}_D \end{bmatrix} \tag{6.2.3}$$

Using the equation above, Equation 6.2.2 may be expressed as shown below:

$$\mathbf{R}_I\mathbf{u}_I + \mathbf{R}_D\mathbf{u}_D = \mathbf{0} \tag{6.2.4}$$

In this equation, if the inverse of $\mathbf{R}_D$ exists, the relationship between independent and dependent DOF's may be written as follows:

$$\mathbf{u}_D = -\mathbf{R}_D^{-1}\mathbf{R}_I\mathbf{u}_I = \mathbf{G}\mathbf{u}_I \tag{6.2.5}$$

Using this equation to the system of equations for the entire model, the dependent DOF's $\mathbf{u}_D$ may be eliminated.
Multi-point constraints may be applied for a wide variety of modeling situations, and some examples are given below.

► Modeling of relative movement between two nodes
► Modeling of sliding or hinge joints
► When the number of degrees of freedom per node join different elements
► Application of decomposed loads
► When applying restraint conditions in directions that do not match with the displacement coordinate system of that node

Restraints of degrees of freedom in rigid body/interpolation elements are categorized as a type of multi-point constraint. In reality, it is more convenient to use rigid body/interpolation elements rather than multi-point constraints to represent the motion exhibited by these elements.

2.3 Automatic Single-Point Constraint

Midas nGen offers an automatic single-point constraint capability, which automatically finds singularities in the stiffness matrix and applies the appropriate restraint condition to remove this singularity. If this capability is used, then the 3x3 stiffness matrix based on the nodal displacement or rotation is analyzed. The restraint condition is created in the direction where stiffness is nearly zero.

As in Figure 6.2.1, if the automatic single-point constraint is to be used in the truss element model, a restraint condition in the direction of vector $\mathbf{n}$ (where there is no stiffness) is created automatically. As previously explained, it is important to have defined a nodal displacement coordinate system that includes the element axial direction and the vector $\mathbf{n}$ orthogonal to the axial direction.

2.4 Binding Force Calculation

Degrees of freedom are constrained according to various constraint conditions applied to them. When an analytical solution has been reached, the binding force due to the single or multi-point constraint may be calculated following the procedure outlined below.

Single-point constraint binding forces $\mathbf{f}_S$ and multi-point constraint binding forces $\mathbf{f}_M$ must satisfy the following equilibrium condition:

$$\mathbf{f}_{\text{int}} = \mathbf{f}_{ext} + \mathbf{f}_S + \mathbf{f}_M \tag{6.2.6}$$

$\mathbf{f}_{ext}$: External loading vector

$\mathbf{f}_{\text{int}}$: Internal force vector ($\int_\Omega \mathbf{B}^T \boldsymbol{\sigma} d\Omega$)

If the above equation is separated into the independent DOF's ($_I$) and the dependent DOF's ($_D$) and assume that single-point and multi-point constraints may not be applied to the same derees of freedom, then the equation may be rearranged as:

$$\begin{Bmatrix} \mathbf{f}_{\text{int},I} \\ \mathbf{f}_{\text{int},D} \end{Bmatrix} = \begin{Bmatrix} \mathbf{f}_{ext,I} \\ \mathbf{f}_{ext,D} \end{Bmatrix} + \begin{Bmatrix} \mathbf{f}_{S,I} \\ \mathbf{0} \end{Bmatrix} + \begin{Bmatrix} \mathbf{f}_{M,I} \\ \mathbf{f}_{M,D} \end{Bmatrix} \tag{6.2.7}$$

Consequently, binding force $\mathbf{f}_{M,D}$ of dependent DOF's may be expressed as:

$$\mathbf{f}_{M,D} = \mathbf{f}_{\text{int},D} - \mathbf{f}_{ext,D} \tag{6.2.8}$$

Likewise, binding force $\mathbf{f}_{M,I}$ due to independent DOF's satisfies the following relationship when Equation 6.2.5 is used:

$$\mathbf{f}_{M,I} = -\mathbf{G}^T \mathbf{f}_{M,D} \tag{6.2.9}$$

Following this procedure, once the multi-point constraint binding forces are calculated the single-point binding forces $\mathbf{f}_{S,I}$ may be calculated using Equation 6.2.7.

2.5 Singularity Error

When a singularity occurs in the stiffness matrix, a unique solution does not exist and indicates an error in the finite element model. Singularity errors may be classified into single node singularity errors (which may be found through a single node) and mechanism singularity errors (which can be found through the model stiffness).

Single Node Singularity Error

Single node singularity errors occur when elements are used without a clear understanding of the element characteristics. For example, singularity errors may occur if elements without a directional stiffness (truss or solid elements) are used or if the stiffness direction of a spring element is only defined in a singular direction. To solve such problems, single node constraints must be suitably used to remove singularity errors. Single node singularity errors may be discovered for a single node displacement without decomposing the stiffness matrix, so the automatic single node constraint capability may be used to remove the singularity error.

Mechanism Singularity Error

Mechanism singularity errors occur as a result of connection between two or more nodes. More specifically, the error occur often due to improper constraint conditions.

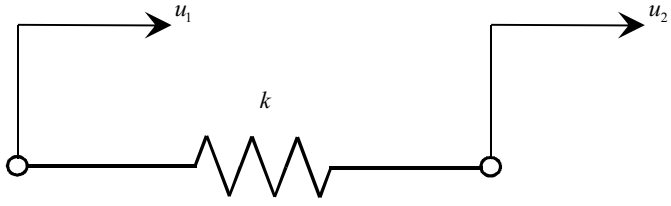

Figure 6.2.2 Elastic connection without constraints

As an example, equilibrium of the above system may be expressed as shown below:

$$\begin{bmatrix} k & -k \\ -k & k \end{bmatrix} \begin{Bmatrix} u_1 \\ u_2 \end{Bmatrix} = \begin{Bmatrix} p_1 \\ p_2 \end{Bmatrix} \tag{6.2.10}$$

The inverse of the above stiffness matrix does not exist, and when the load is $P_1 = -P_2$, many solutions exist. One of the eigenvalues of the stiffness matrix is zero, and the corresponding eigenvectors represent motion of the structure that causes zero strain energy. In typical structures, when no constraints are enforced, six eigenvalues of zero value are output and this represents rigid−body motion. Due to the zero eigenvalues, no unique solution exists and thus we have a mechanism singularity error.

The existence of a mechanism singularity error may be discovered through decomposition of the stiffness matrix. When the stiffness matrix is decomposed and one of the diagonal terms is close to zero, it is considered to have a singularity error. When a singularity error occurs in the matrix decomposition process, the program stops or calculations proceed by adding a small stiffness to the zero diagonal term. This latter method brings about the same effect as adding a spring element to the finite element model.